1994A&AS..108...79R

ASTRONOMY & ASTROPHYSICS
SUPPLEMENT SERIES

Astron. Astrophys. Suppl. Ser. **108,** 79-141 (1994)

Samples of ultra-steep spectrum radio sources*

H.J.A. Röttgering[1,2,3], M. Lacy[2,4], G.K. Miley[1], K.C. Chambers[5] and R. Saunders[2]

[1] Leiden Observatory, P.O. Box 9513, 2300 RA, Leiden, The Netherlands
[2] Mullard Radio Astronomy Observatory, Cavendish Laboratory, Madingley Road, Cambridge, CB3 0HE, U.K.
[3] Institute of Astronomy, Madingley Road, Cambridge, CB3 0HA, U.K.
[4] Dept. of Astrophysics, Keble Road, Oxford, OX1 3RH, U.K.
[5] Institute for Astronomy, University of Hawaii, 2680 Woodlawn Drive, Honolulu, HI 96822, U.S.A.

Received January 21; accepted May 17, 1994

Abstract. — Radio sources with ultra-steep spectra (USS) have been found to be excellent tracers of galaxies at redshifts $z \gtrsim 2$. In order to obtain a large sample of $z \gtrsim 2$ galaxies, we have defined several new flux-limited samples of USS radio sources. These samples are selected at a range of frequencies from 38 MHz to 408 MHz and are fainter by a factor of three than the previously well-studied 4C samples of USS sources. We find that complete samples of radio sources with angular diameters $\lesssim 1$ arcmin selected at 38 MHz contain relatively fewer USS sources than samples of small radio sources selected at higher ($\gtrsim 150$ MHz) frequencies. This is interpreted as due to flattening of the spectra of distant USS sources at frequencies < 100 MHz. As a preliminary to optical imaging and spectroscopy, snapshot observations of sources from these samples have been made with the VLA at 1.5 arcsec resolution. We present the positions, flux densities and radio structures for a total number of 605 sources derived from these observations. Our VLA images indicate that samples of USS sources selected at 38 MHz contain a smaller proportion of small sources and a larger proportion of diffuse sources than USS sources selected at higher ($\gtrsim 150$ MHz) frequencies. This is consistent with the samples of 38 MHz - selected USS sources containing a larger fraction of relatively nearby radio sources, perhaps in clusters of galaxies.

Key words: astronomical data bases: surveys — galaxies: active — radio continuum: galaxies

1. Introduction

Radio galaxies have long been important for studying cosmology. Due to their luminous radio continuum and optical line emission they are relatively easy to find at cosmologically interesting distances. During the last decade, the highest redshift at which radio galaxies have been detected has been pushed from $z < 2$ to almost 4, corresponding to the epoch when some models of cosmological structure formation predict galaxy formation should be occurring (e.g. Efstathiou & Rees 1988). A better understanding of radio sources and especially their evolution is therefore highly relevant to the question of when and how galaxies form. The objectives of studying distant radio galaxies are to obtain information about i) the intrinsic nature of individual objects, ii) the environment of the high-z sources and iii) the geometry of the Universe.

One of the most successful methods of finding distant galaxies has been to concentrate on samples of radio sources with ultra-steep radio spectra (USS, spectral index $\alpha \lesssim -1.0$)*. The basis of this method was the discovery that the fraction of sources found to have counterparts on the Palomar Sky Survey is a strong function of spectral index, with almost no identifications being found for the steepest spectrum sources (e.g. Tielens et al. 1979; Blumenthal & Miley 1979). By observing a sample of radio sources with ultra-steep spectra from the 4C catalogue, Chambers, Miley & van Breugel discovered eight $z > 2$ galaxies among which there are two at $z = 3.8$ (see reviews by Chambers & Miley 1989 and Miley & Chambers 1989). Other groups have also used this technique to find high redshift galaxies (e.g. McCarthy et al. 1991a; 1991b and Rawlings et al. 1990).

The 4C sample covered less than a third of the sky and included only the brightest radio sources (i.e. $S_{178} \gtrsim 4$ Jy). Detection of even more distant radio galaxies should be feasible, since the expected radio emission and $\lesssim$ emission

*The source list is also available electronically via ftp 130.79.128.5 at the CDS (Strasbourg)

*Throughout this paper we define the spectral index α using the convention $S \sim \nu^{\alpha}$, where S is the flux density at frequency ν. $\alpha_{\nu_h}^{\nu_l}$ is the two-point spectral index between a low frequency flux density at ν_l MHz and a high frequency flux density at ν_h MHz.

© European Southern Observatory • Provided by the NASA Astrophysics Data System

1994A&AS..108...79R

are sufficiently luminous to be observable up to a redshift of 6, beyond which the Ly α emission would be shifted into the near-infrared.

Because of their uniqueness as spatially extended probes of the early Universe, we instigated a project to apply this search technique to larger and fainter samples of radio sources. To obtain a large sample of $z \gtrsim 2$ radio galaxies, we instigated a project that consisted of the following steps:

1. *Selection of Samples.* The production of a compendium of candidate ultra-steep spectrum (USS) sources from various radio catalogues.
2. *Radio Imaging.* Observations of the candidate USS sources from the compendium were made with the VLA to obtain accurate radio positions, flux densities and structures. The refined positional and structural information were essential for optical identification work.
3. *Initial Optical Identification.* Using the Guide Star Catalogue (GSC) image processing system at the Space Telescope Science Institute, Baltimore, a small percentage ($\sim$ 10 per cent) of USS radio sources was identified with bright objects. These are not expected to be located at extreme distances and were rejected as candidates for very distant galaxies.
4. *R-band CCD-imaging.* Deep CCD imaging to a limiting magnitude $R \lesssim 24$ with 2-m class telescopes was next carried out. This permitted us to optically identify the majority of the radio sources, to study the structures of the underlying galaxies and to obtain some information about their environments.
5. *Spectroscopy.* Spectroscopic observations of the optical objects were then made with $3-4$ m class telescopes. Since the luminosity of the optical line emission is usually large and can exceed 10^{44} erg s^{-1}, redshifts can often be determined in exposures of about an hour.
6. *Detailed Studies.* The possibilities for follow-up studies for samples of high-z radio galaxies are numerous. For example, mapping of the optical continuum emission at several wavelengths gives information about possible stellar populations and/or scattering media, while spectroscopy and narrow-band imaging of the line emission provides a unique tool for investigating the internal kinematics and physical conditions within the emitting gas.

In this paper we present the results from the first two steps in the programme outlined above. First, we review some results from previous studies of USS radio samples. After discussing the radio catalogues that were available to us, we consider the definition of several samples of USS sources or candidate USS sources. We then describe VLA observations of sources from these samples and present some statistical results on their morphologies. Subsequent papers will deal with the CCD imaging, spectroscopy and follow-up observations of sources in these samples.

We assume a Hubble constant of $H_0 = 75$ km s^{-1} Mpc^{-1} and a density parameter $\Omega_0 = 1$.

2. Ultra-steep spectrum radio sources

2.1. *Classes of USS sources*

In order to optimise our samples for distant galaxy searches, it is important to consider the various other objects that are known to possess ultra-steep radio spectra. Besides distant radio galaxies, there are at least four different classes of USS radio sources. These are radio halos, head-tail galaxies, pulsars and "fading" or "dying" radio sources in which the active nucleus no longer supplies the lobes with energetic electrons. In this section we shall briefly discuss each of these four classes of radio sources.

2.1.1. Radio halos

A radio halo is defined as a diffuse radio source centrally located in a cluster and not identified with an individual galaxy. This is a rare and poorly understood phenomenon. It is rare since, despite extensive searches for radio halos (Jaffe & Rudnick 1979; Hanish 1982; Andernach et al. 1986), only about ten are known. It is poorly understood since there is currently no accepted model for the halo origin. The radio properties of these halos can be summarised as follows (see e.g. Hanisch 1987; Sarazin 1986). They have i) ultra-steep spectra ($\alpha \leq -1.2$), ii) moderate radio luminosities ($P_{1400\ \mathrm{MHz}} \sim 4-10\ 10^{31}$ erg s^{-1} Hz^{-1}) and iii) large projected linear sizes ($0.5-1.3$ Mpc).

2.1.2. Head-tail galaxies

The strongly bent radio structures of these sources are thought to be caused by the motion of the galaxy through the intra-cluster medium (e.g. Miley et al. 1972; O'Dea & Owen 1985a; 1985b), but bulk motion of the synchrotron-emitting plasma may also be important in some cases (Liu et al. 1989). The spectral index of such sources is often observed to steepen with distance from the galaxy nuclei and the tails can have very steep spectra ($\alpha \lesssim -2.0$).

2.1.3. Radio pulsars

Pulsars have spectral indices ranging from $\alpha \sim -0.7$ down to $\alpha \lesssim -3$ with a mean of $\alpha \sim -1.6$ (e.g. Sieber 1973; Malofeev & Malov 1980). Since pulsars are mainly located in the galactic plane (e.g. Taylor et al. 1993) and since our samples of extragalactic radio sources will be defined outside the galactic plane, the samples should not contain a significant number of pulsars. A characteristic angular size of $<< 1$ arcsec further distinguishes pulsars from the majority of extragalactic radio sources which have a median angular size of $\gtrsim 10$ arcsec for flux densities $\gtrsim 100$ mJy at 1412 MHz (Windhorst et al. 1990).

© European Southern Observatory • Provided by the NASA Astrophysics Data System

1994A&AS..108...79R

2.1.4. Fading radio sources

If the lobes of a radio source that is associated with an active nucleus of a galaxy are no longer supplied with energetic electrons, the radio spectrum steepens due to radiation losses and expansion losses (unless confined by dense cluster gas) and eventually fades away. These fading radio sources are rare observationally. Out of a complete sample of 337 sources selected at 327 MHz, Oort (1987) finds one candidate "fader".

2.2. *Frequency-dependence of USS source populations*

A correlation between the radio spectral index and the luminosity of radio sources has been noted by many authors (Heeschen 1960; Veron et al. 1972; Macleod & Doherty 1972; Bridle et al. 1972; Laing & Peacock 1980) and is the basis of our search technique for distant galaxies. This correlation is most clearly seen in the 4C samples of radio sources studied by Conway et al. (1977) and Tielens et al. (1979). In these samples it was found that the fraction of radio sources that could be identified with objects in the Palomar Sky Survey was a strong function of spectral index (Blumenthal & Miley 1979). For the sources with the steepest radio spectra almost no identifications were found. Also the angular size of the radio sources was shown to change as a function of spectral index. The median angular size decreased by a factor 1.5 between $\alpha = -0.7$ and $\alpha = -1.2$. Both these correlations suggested that the 4C sources with the steepest spectra tend to be located at the highest redshifts. Since in flux limited catalogues, redshift is directly related to luminosity, the USS sources should also be the most luminous. Subsequent work showed that the USS sources were indeed very distant. Optical spectroscopy of 32 sources from this 4C sample resulted in the discovery of 16 galaxies with a redshift $z > 0.5$ of which 8 had $z > 2$ including 4C41.17 at $z = 3.8$ (Chambers & Miley 1989; Chambers et al. 1990).

However, there is, in samples of USS sources, a striking variation of radio sources with selection frequency (Blumenthal & Miley 1979). An important study of a sample of USS sources selected at 38 MHz examined 29 sources with $\alpha_{178}^{38} < -1.2$ (Baldwin & Scott 1973; Slingo 1974a,b). These USS sources occur almost exclusively in rich clusters of galaxies. Some of them were classified as head-tail galaxies and some as cluster radio halos. Blumenthal & Miley (1979) pointed out that the fraction of sources identified on the Palomar Sky Survey was $\sim$ 75 per cent for the 38 MHz USS sample, but only $\sim$ 20 per cent for the 178 MHz USS sample. This difference strengthened the conclusion that samples of USS sources selected at 38 MHz are dominated by different populations of sources than samples selected at 178 MHz. This implies that the spectral characteristics of the sources in the two samples are different. There are two possible explanations for this difference:

1. The spectra of the 178-MHz selected USS sources tend to flatten at the lowest frequencies and are therefore not contained in USS samples selected at 38 MHz.
2. The spectra of the 38-MHz cluster sources flatten at frequencies higher than 178 MHz and are therefore not contained in USS samples selected at 178 MHz.

To investigate the first possibility, we consider flux density measurements at frequencies $\sim$ 38 MHz for the distant radio sources from the 4C sample of Chambers et al. (1987).

Two important surveys at ultra-low frequencies are those of Williams et al. (1966) at 38 MHz and of Viner & Erickson (1975) at 26.3 MHz. Except for 4C41.17 which is reportedly contained in the survey of Viner & Erickson (1975), none of the 4C high-redshift sources of Chambers et al. (1987) are listed in these two surveys**. The upper limits are, however, useful. Flux densities for the high-redshift sources at 178 MHz and 4995 MHz are given in Tielens et al. (1979). It is difficult to establish a good flux scale for flux density measurements at the lowest frequencies (e.g. Rees 1990a). An error of 20 per cent in the flux scale will, however, only result in an error of 0.1 in spectral index α_{178}^{38}, and this should not affect any of the conclusions.

We find that the mean value of the observed low frequency curvature as parameterised by $\alpha_{178}^{38} - \alpha_{4995}^{178}$ is $< 0.24 \pm 0.23$, indicating that the spectra of high-z radio galaxies are curved at the lowest frequencies. A substantial part of the flux from such objects arises from high brightness regions that might well undergo synchrotron self-absorption at low frequencies (see Leahy et al. 1989) resulting in this curvature. Indeed, low frequency curvature seems to affect the general source population in samples selected at 38 MHz: Lacy et al. (1992) find that in a complete sample of sources from the 8C 38 MHz survey (Rees 1990b), the median α_{151}^{38} is -0.81, compared to a median α_{4850}^{151} of -0.91.

The second possibility that might explain the difference in the fractional identification content for the 38-MHz and 178-MHz selected samples is flattening of the 38-MHz USS sources at frequencies $>$ 178 MHz. The data used by Tielens et al. to investigate the identification statistics was based on the 38 MHz USS sample of Slingo (1974a,b). We shall follow Tielens et al. and omit sources that may have unreliable 38 MHz flux density measurements due to confusion. White and Becker (1992) have produced a source list for both the 1400 MHz and the 4850 MHz NRAO Green Bank northern sky survey (Condon & Broderick 1985; Condon & Broderick 1986; Condon et al. 1989). The use of these surveys in our search for USS sources will be

**We note that Viner & Erickson (1975) give a flux of 36 Jy at 26.3 MHz for 4C41.17, conflicting with the upper limit of 14 ± 4 Jy by Williams et al. (1966). However, since none of the other sources were detected by Viner & Erickson (1975), their results do not affect our deduction that the low frequency spectra of distant USS sources are curved.

© European Southern Observatory • Provided by the NASA Astrophysics Data System

1994A&AS..108...79R

discussed later. Within a $1' \times 1'$ box around the source position as given by Slingo (1974a,b) we searched for sources in the 1400 and 4850 MHz source list of White & Becker (1992). For 13 out of 20 sources we found both a 1400 MHz and 4850 MHz flux density measurement.

Except for 4C07.41, the NRAO Green Bank 1400 MHz fluxes agreed to within $\sim$ 15 per cent with the measurements at 1400 MHz of Slingo (1974a,b). The sources that did not have a 4850 MHz flux were assigned an upper limit of 15 mJy. The flux densities for these sources are given in Table 1. The mean curvature taken as $\alpha_{178}^{38} - \alpha_{5000}^{178}$ for the 13 sources having a 4850 MHz flux density in the list of White & Becker (1992) is -0.53 ± 0.15, indicating that majority of the 38 MHz sources flatten at frequencies higher than 178 MHz. In many cases this is due in practice to confusion with other radio sources in the galaxy clusters which typically surround these USS sources (Slingo 1974a,b). The USS source itself generally steepens at high frequency (Roland et al. 1985).

Table 1. Radio data for the Slingo 38 MHz USS sample

name	S_{38} Jy	S_{178} Jy		S_{4850} Jy	α_{178}^{38}		α_{4850}^{178}
4C12.01	52	7.8		0.380	-1.23		-0.91
4C23.1	23	2.1		0.132	-1.55		-0.84
4C17.11	27	4.0		0.247	-1.24		-0.84
4C63.10	40	3.9	<	0.015	-1.51	<	-1.68
4C74.13	33	2.2	<	0.015	-1.75	<	-1.51
4C06.36	28	3.5		0.079	-1.35		-1.15
4C67.17.1	16	2.1	<	0.015	-1.32	<	-1.50
4C26.41	27	2.2		0.103	-1.62		-0.93
4C23.37	27	2.0		0.057	-1.69		-1.08
4C38.39	50	3.5	<	0.015	-1.72	<	-1.65
4C23.39	20	2.3	<	0.015	-1.40	<	-1.52
4C07.38	37	3.9		0.191	-1.46		-0.91
4C10.40	28	2.9		0.221	-1.47		-0.78
4C07.41	119	11	<	0.015	-1.52	<	-2.00
4C45.30	25	3.5		0.341	-1.27		-0.70
4C19.53	22	2.7		0.197	-1.36		-0.79
4C71.16	17	2.1		0.145	-1.35		-0.81
4C08.66	22	2.1		0.121	-1.52		-0.86
4C20.57	55	5.2	<	0.015	-1.53	<	-1.77
4C19.78	55	5.2		0.157	-1.53		-1.06

We therefore conclude that the difference in the fractional identification content of USS selected samples selected at 38 MHz and 178 MHz is due *both* i) low frequency flattening of spectra of the distant radio sources selected at 178 MHz and ii) apparent flattening of the spectra of the 38 MHz cluster sources at higher frequencies.

2.3. *Origin of the spectral index vs. redshift correlation*

In samples of radio sources selected at 178 MHz the spectral index correlates with redshift. We review mechanisms that have been suggested to explain this.

First, the effect may be partially due to observational selection. The spectra of radio sources have a tendency to steepen at the higher frequencies. Since more-distant objects would be observed at higher (rest-frame) frequencies, they would appear to have steeper spectra. Blumenthal & Miley (1979) calculated a rest-frame spectral index assuming a redshift of $z = 2$ for the sources from the 3C and 4C for which no redshifts were available. Although the correlation between the identification fraction and spectral index is weaker when this rest-frame spectral index is used instead of the observed spectral index, it is still clearly present. This is consistent with the results of van Breugel & McCarthy (1989) and Lacy et al. (1993) who find, for a subset of the 3CR and for a complete sample of 38 MHz radio sources respectively, that if the rest-frame spectral index is used instead of the observed spectral index the $z - \alpha_{\rm rest}$ correlation is weakened, but still present.

With the flux densities for the 4C distant galaxies from the sample of Chambers et al. (1987), we can investigate whether the $z - \alpha_{\rm obs}$ correlation still persists not only between normal-spectrum and USS sources, but within samples of distant USS radio sources. In Fig. 1 the observed spectral indices α_{4995}^{178} and α_{178}^{38} and the spectral curvature index $\alpha_{178}^{38} - \alpha_{5000}^{178}$ are plotted as a function of redshift. A formal analysis of possible trends in the three plots have been made using the Spearman rank method. The correlation coefficients for the pairs of observables plotted in Fig. 1 were -0.42, 0.39 and 0.43 respectively with significance levels p of 0.23, 0.19 and 0.19. Therefore none of the correlations are significant at even the 10 per cent level. There are two factors which will reduce the correlation seen within the 4C sample, firstly both the range in α and the number of data points are much less than for the investigation over the full range of α, and secondly both van Breugel & McCarthy (1989) and Lacy et al. (1993) find that the strength of the $\alpha - z$ correlation seems to be smaller at $z \gtrsim 1$, where most of the 4C USS sources are situated. Among the four sources with $\alpha_{4995}^{178} < -1.3$, however, two are at $z = 3.8$. This suggests that increasing the number of known USS sources at $z > 2$ may establish a significant $\alpha - z$ correlation within the relatively narrow spectral range covered by USS sources.

A second possible observational selection effect which might explain the α versus z relation was discussed by Kapahi & Kulkarni (1990). They found that the dependence of redshift and luminosity on the rest-frame spectral indices for the sources from the Leiden-Berkeley Deep Survey of Windhorst et al. (1984), is weaker than that for the sources from the 3C sample. They suggest that this may be due to a selection effect arising from the steeper slope of the luminosity function at higher luminosity, which causes ultra-steep spectrum sources at high redshifts to be preferentially included in low frequency surveys. Because of this, the steepest spectrum sources in a flux-limited sample will tend to be located at the highest redshift. As our samples are mostly selected with fluxes around the peak in the radio source counts, however, it is no longer true that the source counts of the high-z sources are rising rapidly with decreasing flux, as is necessary for the Kapahi & Kulkarni selection effect to work.

© European Southern Observatory • Provided by the NASA Astrophysics Data System

1994A&AS..108...79R

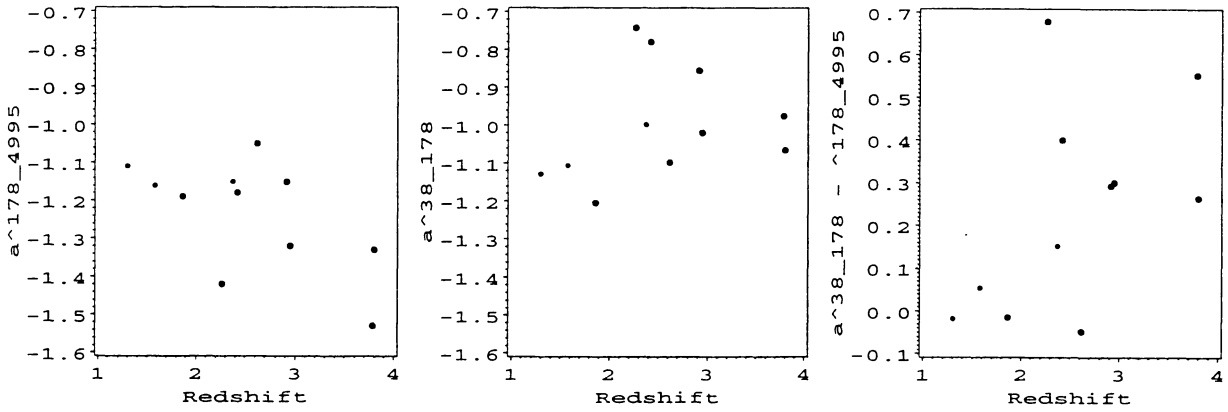

Fig. 1. Spectral indices as a function of redshift for the 4C sample of Chambers et al. (1987). Left shows α_{4995}^{178}, centre shows α_{178}^{38} and right shows the spectral curvature ($\alpha_{178}^{38} - \alpha_{5000}^{178}$)

Third, it is possible that the redshift–spectral index correlation is a secondary effect, reflecting, through the Malmquist bias, a primary correlation between the rest-frame spectral index and the luminosity. There are good physical reasons why the most powerful sources might have steeper spectra (e.g. Chambers et al. 1990; Krolik & Chen 1991), although recent statistical evidence (Lacy et al. 1993) suggests that redshift is indeed the dominant factor.

3. Description of radio catalogues

3.1. *Introduction*

During the last decades several important large–sky radio catalogues have become available. These can be used to extend the work of Tielens et al. (1979) to fainter sources and to the southern hemisphere. In this section we review the basic characteristics of some of these catalogues and briefly discuss the merits and some of the drawbacks for using them to define samples of USS sources as tracers of distant galaxies.

Some important characteristics of the catalogues are listed in Table 2.

3.2. *8C Survey (38 MHz)*

The 8C survey (Rees 1990b) is a deep radio survey of a limited region of the northern sky that has been carried out at a frequency of 38 MHz, to a limiting flux density nearly an order of magnitude deeper than previous surveys at similar frequencies. Special attention has been given to the absolute flux density scale at 38 MHz and no systematic effects at levels higher than 5 per cent are believed to be present (Rees 1990a).

3.3. *6C2 Survey (151 MHz)*

The 6C Cambridge Survey of radio sources will ultimately cover most of the sky north of $\delta = 30°$ at a frequency of 151 MHz. Maps of a circular area of radius 10° centered on the north celestial pole plus the design and operation of the telescope have been discussed by Baldwin et al. (1985). We have used a more southern region (Hales et al. 1988), because a significant fraction of sources from this region are also contained in the Texas and NRAO catalogues, allowing spectral indices to be obtained.

3.4. *Texas Survey (335 – 380 MHz)*

The Texas catalogue is a large sky radio survey carried out at an effective frequency of 365 MHz with the Texas interferometer. A sky strip covering the declination range from 13 deg 35′ to 22 deg 42′ was published in 1980 (Douglas et al. 1980). Since then the catalogue has been regularly updated. Dr. Douglas kindly provided us with updated versions.

Since the longest baseline of the Texas Interferometer was ∼ 3000 meters, the positional accuracy is excellent (0.5−1 arcsec). However, the dilute spatial frequency sampling of the system gives rise to lobe–shift problems and a complicated set of angular-size dependent selection effects. In compiling the catalogue, a model fitting technique was used to derive basic source parameters such as position and flux density. For each source, a parameter indicating the reliability of the fit is specified in the catalogue.

The Texas interferometer operates at three closely separated frequencies (335, 365 and 380 MHz). For sources that have sufficient signal to noise, a crude spectral index is determined using the available small range in observing frequency.

The Texas Catalogue is a unique compilation of low frequency radio sources and has played an important role in our sample selection. However, there are several inherent problems with it which are considered below.

1. There is a systematic uncertainty in flux density introduced by the modelling procedure. The three different source models that were fitted to the *uv* data were i) a

© European Southern Observatory • Provided by the NASA Astrophysics Data System

1994A&AS..108...79R

Table 2. Various catalogues used for sample definition

	Unit	4.85 GHz Sky Survey	1400 MHz Sky Survey	Molonglo
Frequency	MHz	4850	1400	408
Wavelength	cm	6.2	21.4	73.5
Sky coverage		$0° < \delta < 75°$	$-5° < \delta < 82°$	$-85° < \delta < 18.5°$ $\lvert b\rvert > 3$
Sky area	sr	6.0	6.8	7.85
Source density	sr^{-1}	$10^4, S > 25$ mJy	$3 \times 10^3, S > 150$ mJy	$1 \times 10^3, S > 1000$ mJy
Resolution		$3.7' \times 3.3'$	$12.7' \times 11.1'$	$2.7'$
Position uncertainty		$10'' - 30''$	$30'' - 70''$	$3'' - 10''$
Rms system noise	mJy	5	–	200
Rms confusion	mJy	1	25	–
Intensity proportional error		10%	5%	4-10%
Flux-scale		Baars *et al.* (1977)	Baars *et al.* (1977)	Wyllie (1969a; 1969b)
Reference		Condon *et al.* (1989)	Condon *et al.* (1985; 1986)	Large *et al.* (1981)

	Unit	Texas	6C2	8C
Frequency	MHz	365	151.5	37.8
Wavelength	cm	82.2	198	795
Sky coverage		$-35° < \delta < 70°$	$30° < \delta < 51°$ $08^h30^m < \alpha < 17^h30^m$	$\delta > 60°$
Sky area	sr	9.5	0.65	0.84
Source density	sr^{-1}	$7 \times 10^3, S > 250$ mJy	$1.3 \times 10^4, S > 200$ mJy	$6 \times 10^3, S > 1$ Jy
Resolution		‡	$4.2' \times 5.5'$	$4.5' \times 4.8'$
Position uncertainty		$0.5'' - 1.0''$	$5'' - 10''$	$30'' - 90''$
Rms system noise	mJy	20	40	250
Rms confusion	mJy	–	16	~ 150
Intensity proportional error		5-10%		10-30%
Flux-scale		Wills (1973)	Roger *et al.* (1973)	Roger *et al.* (1973)
Reference		Douglas *et al.* (1980)	Hales *et al.* (1988)	Rees (1990b)

‡ The dirty beam of the Texas interferometer has a complicated behaviour: Sources can be successfully modelled as double sources if their extent is more than 10 arcsec and less than 2 arcmin. Smaller sources are unresolved by the system, sources larger than 2 arcmin are poorly modelled and blended, and usually flagged as such (Douglas *et al.* 1980).

single gaussian function, ii) two gaussian functions containing equal flux density and iii) two gaussian functions containing unequal flux densities. In 27% of the cases at least two models gave acceptable fits. The results from the two simplest models are listed in the catalogue. The ratio of the flux densities from these two models that are of good quality (as indicated by the code '+++' in the Texas catalogue) and are out of the galactic plane ($|b| > 17.5$ deg), is a function of flux density (see Fig. 2). For stronger sources ($S_{365} \gtrsim 1$ Jy), the differences between the two simplest models are at the 10 per cent level, but for the weaker sources ($S_{365} \lesssim 1$ Jy), these differences can be as large $20 - 55$ per cent. On average, the flux densities obtained from the second, simpler, model seem to be systematically lower by $5 - 10$ per cent than those obtained from the first model.

2. Large sources tend to be unrepresented. Due to the poor sampling of the *uv*-plane, sources with a component separation larger than ~ 2 arcmin are poorly modelled. The result is that the Texas Catalogue tends to underestimate flux densities of sources larger than $> 15''$ (Becker et al. 1991).
3. The systematic errors in the spectral index and structure model parameters have not yet been systematically assessed (Douglas et al. 1980).

3.5. *Molonglo Reference Catalogue (408 MHz)*

Compiling the Molonglo Reference Catalogue of Radio Sources (Large et al. 1981) was one of the main programmes for the Molonglo Cross Radio Telescope originally developed by Mills et al. (1963). The catalogue lists positions, flux densities and some structural information.

3.6. *NRAO Green Bank Sky Surveys (4850 and 1400 MHz)*

The NRAO Green Bank 300-foot (91-m) transit telescope was used to map most of the northern sky at 4850 MHz and 1400 MHz (Condon & Broderick 1985; Condon & Broderick 1986; Condon et al. 1989).

Both Gregory & Condon (1991, hereafter 87GB) and Becker et al. (1991, hereafter BWE), made source catalogues from the NRAO Green Bank 4850 MHz Survey using different source finding and fitting algorithms. White and Becker (1992, hereafter WB) produced a source list from the NRAO Green Bank 1400 MHz survey. This list

© European Southern Observatory • Provided by the NASA Astrophysics Data System

1994A&AS..108...79R

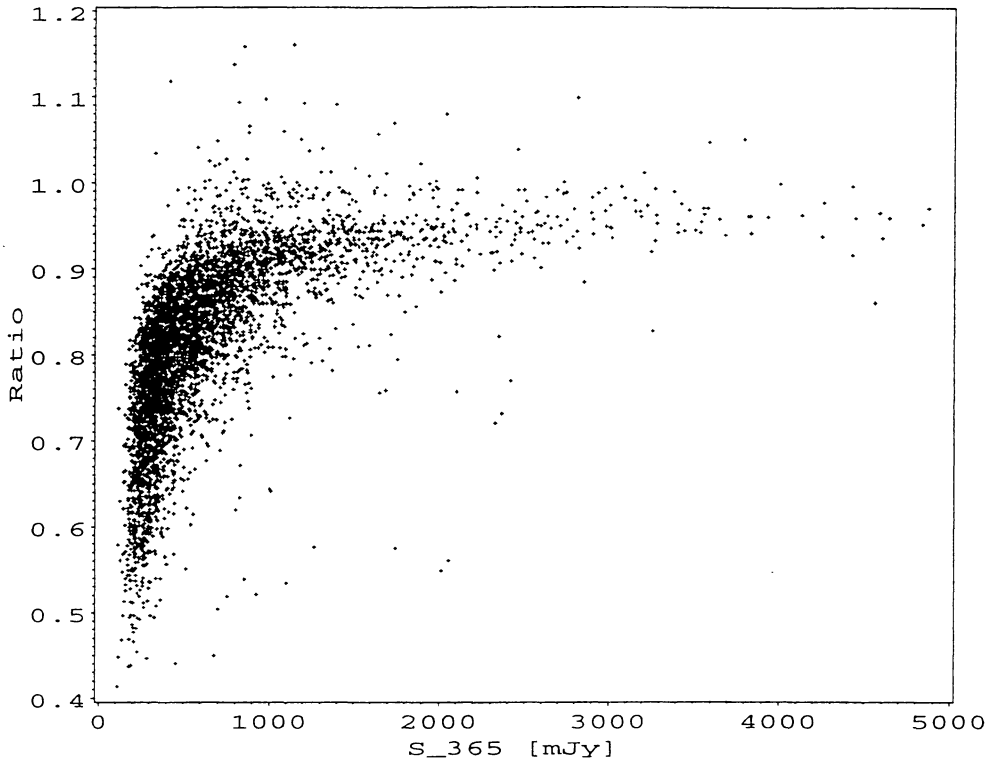

Fig. 2. The ratio of flux density derived from the most complex divided by that derived from the simplest model tabulated in the Texas catalogue for the 27 per cent of the sources where two different flux densities are listed. The ratio is plotted as a function of the flux density from the most complex model.

was kindly provided to us by the authors prior to publication.

3.7. *Parkes Catalogue (80, 178, 408, 1410, 2700 and 5000 MHz)*

The Parkes radio telescope has been used to make two important surveys of the southern sky, one at 408 MHz and one at 2700 MHz (summarised by Bolton et al. 1979). These surveys have been included in a compendium: "The Parkes Catalogue". Since 1979 improved positions, optical identifications and additional flux density measurements have been added to the catalogue. The version of the catalogue that we used is referred to as "PKSCAT85". It lists i) flux density measurements at 80, 178, 408, 1410, 2700 and 5000 MHz, ii) cross references to other catalogues such as the 4C and iii) identifications of radio sources.

4. Lack of USS sources at low finding frequencies

The relative contribution of ultra-steep spectrum sources in complete samples of radio sources can be studied as a function of finding frequency with the radio catalogues that are available to us. We now examine three two-point spectral index distributions α_{365}^{38}, α_{365}^{151} and α_{4850}^{365} taken from combinations of the 8C, 6C2, the Texas Catalogue and NRAO 4850 MHz survey (e.g. Table 2). From these combinations we have rejected sources that i) do not have a good quality Texas flux (as indicated in the Texas catalogue) ii) are inside the galactic plane ($|b| < 17.5$ deg) and iii) have position differences larger than $\sim 1\sigma$.

These spectral index distributions contain a large number of sources; The wide frequency differences result in an accurate spectral index. Since the three spectral indices have all been determined with a flux density measurement from the Texas catalogue, the inherent selection on radio sizes in the Texas catalogue ($\lesssim 1'$) will be present in the same way in the three distributions.

All sources from a radio survey with a flux density limit close to the completeness limit of the radio survey $S_{\nu_{\rm low}}^{\rm lim}$ at frequency $\nu_{\rm low}$ that have two point spectral indices $\alpha_{\nu_{\rm high}}^{\nu_{\rm low}}$, will be included in a radio survey at frequency $\nu_{\rm high}$ with a flux density limit $S_{\nu_{\rm high}}^{\rm lim}$ if

$$S_{\nu_{\rm low}}^{\rm lim} > S_{\nu_{\rm high}}^{\rm lim} \left(\frac{\nu_{\rm low}}{\nu_{\rm high}}\right)^{-\alpha_{\nu_{\rm high}}^{\nu_{\rm low}}}.$$

In Table 3 we give the flux density limits $S_{\nu_{\rm low}}^{\rm lim}$ for the three spectral indices $\alpha_{\nu_{\rm high}}^{\nu_{\rm low}}$. We have taken as the limiting spectral index $\alpha = -1.2$ to ensure a sufficient number of sources in the USS $-1.2 < \alpha < -1.1$ bin.

In Fig. 3 we plot the distribution of the two-point spectral indices α for the samples defined in Table 3. In Table

© European Southern Observatory • Provided by the NASA Astrophysics Data System

1994A&AS..108...79R

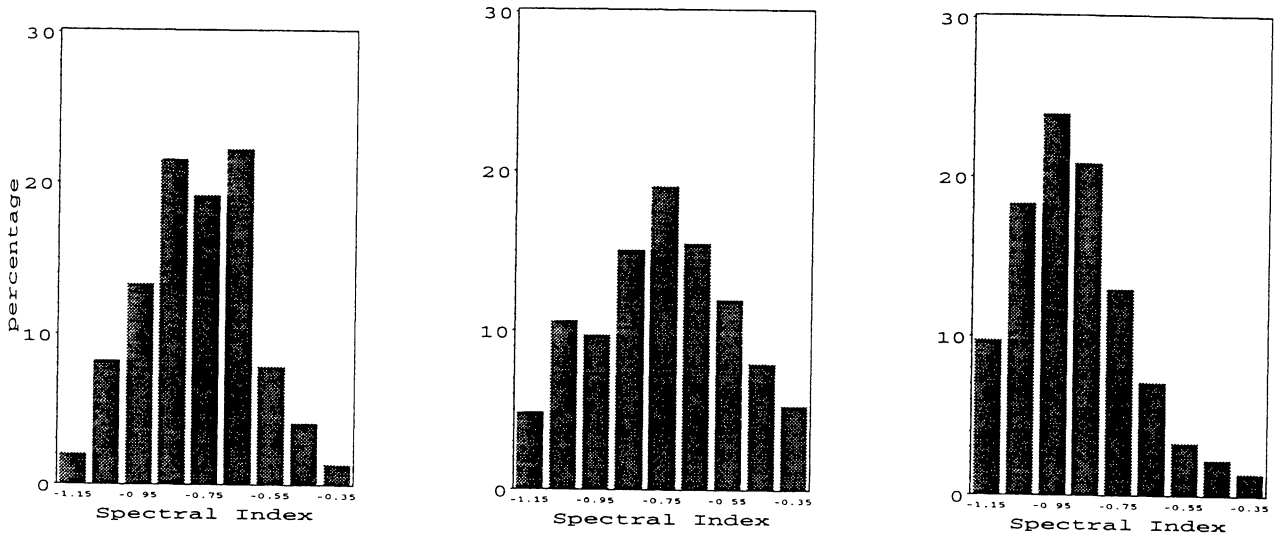

Fig. 3. From left to right the spectral index distribution for α_{365}^{38}, α_{365}^{151}, and α_{4850}^{365}

Table 3. Properties of the spectral index distributions

$\alpha_{\nu_{high}}^{\nu_{low}}$	$S_{\nu_{low}}^{lim}$ (i)	No. with $\alpha > -1.2$ (ii)	Percentage with $-1.2 < \alpha < -1.1$ (iii)	Mode (iv)
α_{365}^{38}	5.0 Jy	304	$2.0 \pm 0.8\%$	~ -0.75
α_{365}^{151}	1.0 Jy	1262	$6.1 \pm 0.7\%$	~ -0.75
α_{4850}^{365}	1.0 Jy	3129	$9.4 \pm 0.5\%$	~ -0.95

3 we give the number of sources in the distribution, the percentage of sources in the $-1.2 < \alpha < -1.1$ bin and the mode of the spectral index distribution.

From the spectral index distributions and the Table 3, it is clear that there are relatively few USS sources in the 38 MHz selected samples. To explain the differences in the three spectral index distributions properly, the radio source content of the USS samples with these angular size and flux selection needs to be studied. The following will play a role in producing the differences:

1. *Angular Size Constraints*
   Complete radio source samples selected at ultra-low frequencies (< 100 MHz) have spectral index distributions whose USS tails are well populated (Williams & Bridle 1967; Slingo 1974a,b; Baldwin & Scott 1973). As noted above, USS sources from these low frequency samples were preferentially found in clusters and had large sizes ($\gtrsim 30 - 40$ arcsec). The size selection introduced by the Texas Catalogue will result in many of these sources being missed.
2. *Curvature in the Radio Spectra*
   The curvature in the radio spectra of many distant radio sources pointed out earlier in this paper will lead to the steepest spectral index bin of the 38 MHz samples containing relatively fewer of these sources.
3. *Radio Source Density at High Redshift and the Geometry of the Universe*
   If the $\alpha - z$ relation is mainly due to a combination of spectral curvature and radio "K-correction", the highest-redshift galaxies should appear in USS samples selected at the lowest frequencies. The underpopulation of the USS bin in the 38 MHz samples is indicative of the effects of the cosmic evolution of the radio source population and the geometry of the Universe on the spectral index distribution, and points to at least a flattening off in the rapid rise in number density of radio sources observed between $z = 0 - 2$, as is predicted by recent models for the evolution of the radio source population (e.g. Dunlop & Peacock 1990).

5. Selection of samples

5.1. *Considerations*

There are several parameters which are important when defining the samples:

1. the finding frequency at which the "base" survey was made.
2. the range of flux densities.
3. angular size constraints.

Let us consider the effect of each of these parameters in turn.

© European Southern Observatory • Provided by the NASA Astrophysics Data System

1994A&AS..108...79R

5.1.1. Finding frequency

The variation of source content of USS surveys with frequency, discussed in Sect. 2.2, requires that selections over a range of frequencies is needed to optimise our chance of detecting high-z galaxies and disentangle the dependence of subsequent results on various radio properties.

5.1.2. Flux densities

The range of flux densities for the USS samples is, of course, mainly dictated by the available radio catalogues. To illustrate the relative sensitivity of the various catalogues a plot of the limiting flux density of the catalogues versus frequency is shown in Fig. 4. For reference the flux density limit of the 3C is also plotted.

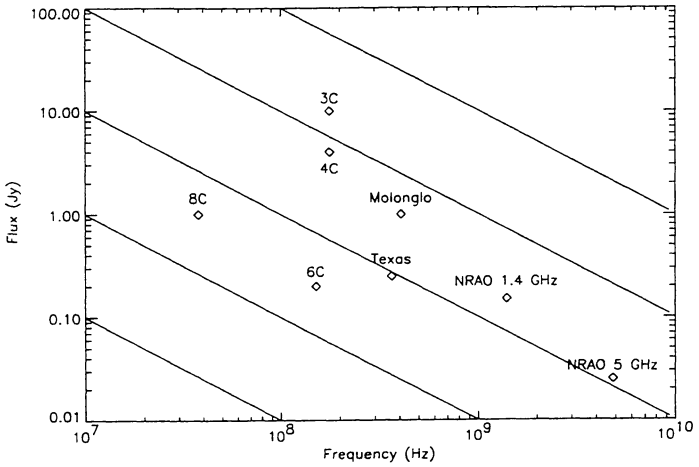

Fig. 4. The flux density limits of various radio catalogues as a function of frequency. The lines corresponds to a source with a spectral index $\alpha = -1.0$

Besides the flux density limits of the catalogues, there are two additional considerations. It is now well established that there is a good linear correlation between the emission line and radio luminosity for samples of bright radio sources (e.g. Rawlings et al. 1989; Baum & Heckman 1989; McCarthy & van Breugel 1989). The Ly α emission of the few $z > 3$ radio galaxies known are so bright that they could still be detected with a 4-metre class telescope in less than a few hours of integration time even if the Ly α emission line were a factor of $5 - 10$ fainter. If the relation between line luminosity and radio power also holds in the $z > 3$ universe, it should still be possible to detect Ly α emission for radio sources having radio flux densities fainter than the 4C USS sample by a factor $5 - 10$.

A second consideration comes from differential source counts. At $S_{408} \sim 1$ Jy the observed counts exceed the predictions of the nonevolving models by the greatest factor (e.g. Condon 1984). This suggests that the largest fraction of high redshift sources in radio samples are contained in samples selected at these flux density levels and that the greatest concentration of the very highest redshift objects will appear at flux levels at or just below this.

We conclude that the optimum strategy for seeking high-z radio galaxies will include studies of USS samples covering a range of finding frequencies reaching a limiting flux density of about $0.2 - 0.5$ Jy at 408 MHz.

5.1.3. Angular size

A decrease of the median size of the radio sources associated with quasars as a function of redshift was first found by Miley (1968). Using both bright and faint samples of radio sources, Oort (1987) and Kapahi (1989) found that the redshift dependence of the linear size $l_{\rm med}$ of radio galaxies is $l_{\rm med} \sim P^{0.3}(1+z)^{-3}$ where P is the power of the radio source. Using recently obtained data, Gopal–Krishna & Kulkarni (1992) found that this relation probably holds to at least $z \sim 2$. Selecting steep spectrum ($\alpha < -0.5$) sources smaller than 60 arcsec from the complete 3CR sample (Laing et al. 1983) selects 70 per cent of the $z > 0.1$ galaxies and 100 per cent of the $z > 1.5$ quasars, while rejecting 95% of the nearby $z < 0.1$ sources. However, we note that a $z = 2.4$ galaxy from the Chambers et al. (1987) 4C USS sample has an angular size of 55 arcsec (Chambers, priv. com.). Although restricting our samples to smaller sources optimises the chance of finding high-z galaxies and avoids some of the problems inherent in catalogues such as Texas, one should be aware of the selection effect that such a constraint imposes.

5.2. *Selections*

Our sample selection "evolved" during the course of the project because catalogues became accessible that were not initially available. For example, we originally selected the 365 MHz samples based on the very crude estimates of spectral index given in the Texas Catalogue. VLA observations were essential to confirm the spectral indices. When the NRAO Green Bank 1400 and 4850 MHz catalogues were produced, genuine USS sources could be defined with a high degree of confidence from a direct comparison between the Texas and NRAO Green Bank catalogues.

Based on the considerations listed above, we have defined 9 samples of USS or candidate USS sources. In all cases we rejected sources located close to the galactic plane ($|b| < 17.5$ deg) in order to avoid confusion with galactic sources. We labelled each sample by the lowest frequency that contributed in the spectral selection (usually the frequency at which the sample is flux limited). Details of the selection criteria are given in Table 4 together with the numbers from each sample that were observed with the VLA (Col. 8).

408A: The Parkes Catalogue lists flux densities at 6 different frequencies (80, 178, 408, 1410, 2700, 5000 MHz). Excluding the flux density point at 80 MHz, we can form 4 low frequency spectral indices

© European Southern Observatory • Provided by the NASA Astrophysics Data System

1994A&AS..108...79R

Table 4. Samples of ultra-steep spectrum sources

Sample (1)	Frequency (2)	Sky Coverage* (3)	No. at Finding Frequency (4)	Initial Spectral Selection (5)
408A	408/1400/2700/5000	$-30° < \delta < 19°$	1742	$\alpha^{\dagger} < -1.1$
408B	408	$-35° < \delta < 19°$	6657	$\alpha^{\dagger} < -1.1$
365A	365	$-35° < \delta < 45°$	40,367	$\alpha \leq -1.1, \epsilon_{\alpha} \leq 0.4$
365B	365/4850	$0° < \delta < 20°$	12,439	$\alpha^{365}_{4850} < -1.15$
178	178/408/1400/2700/5000	$-6° < \delta < 27°$	1361	$\alpha^{\dagger} < -1.1$
151	151/365/4850	$8^h30^m < \alpha < 17^h30^m$ $30° < \delta < 51°$	8278	$\alpha^{151}_{365} < -1.0, \alpha^{365}_{4850} < -1.0$
38A	38/151/4850	$60° < \delta < 75°$§ $8^h50^m < \alpha < 16^h20^m$	970	$\alpha^{38}_{151} < -1.0, \alpha^{151}_{4850} < -0.9$
38B	38/365/4850	$60° < \delta < 70°$	2642	$\alpha^{38}_{365} < -0.95, \alpha^{365}_{4850} < -1.0$
38C	38/4850	$60° < \delta < 75°$	3748	$\alpha^{38}_{S^{Upper}_{4850}=15mJy} < -1.0$

Sample (1)	Additional Selection (6)	No. Selected (7)	No. Observed (8)	No. good maps‖ (9)	Final Selection (10)	Final No.¶ (11)
408A	no identification in Parkes Catalogue	50	48	48		48
408B		28	25	25	$\alpha_l < -1.0$	16
365A	size $< 40''$, $S_{365} < 1.5$ Jy, flag='+++'	372	259‡	259	$\alpha_l < -1.0$	150
365B	$(\Delta\alpha, \Delta\delta)^{365}_{4850} < (15'', 15'')$ $S_{4580} > 15$mJy	75	70	68		68
178	no identification in Parkes Catalogue	72	65	64		64
151	$(\Delta\alpha, \Delta\delta)^{151}_{365} < (15'', 15'')$ flag='+++' $(\Delta\alpha, \Delta\delta)^{365}_{4850} < (45'', 45'')$	64	64	64		64
38A	see text	39	38	37		37
38B	-	37	36	36		36
38C	-	71	71	20†		20

* excluding galactic plane $|b| < 17.5°$.
† see text.
‡ the more southern sources had higher priority during the scheduling of the observations.
§ three sources with $\delta > 80°$ were added to the samples.
‖ For some sources the VLA maps did not show a radio source. Possible reasons are (i) the Texas source is spurious, (ii) the source has only smooth structure on scales $\gtrsim 30$ arcsec and is therefore not detected in our 20 cm A-array observations.
¶ Note that 16 sources appear in more than one sample.

(α^{178}_{1410}, α^{178}_{2700}, α^{408}_{2700}, α^{408}_{1410}) and 2 high frequency spectral indices (α^{1410}_{5000}, α^{2700}_{5000}). We included sources in the USS sample if the available low frequency spectral indices were < -1.1 and the high frequency spectral indices were either < -1.0 or not present in the catalogue. The sources that have a flux density measurement at 178 MHz form the '178' sample, and are effectively a '4C' sample. The others form the '408A' sample and are effectively a "Parkes sample".

408B: Although the Molonglo survey does not list spectral indices, we obtained spectral information by comparison with the Parkes catalogue. We included sources from the Molonglo samples in the USS sample if:

1. $\alpha^{408}_{2700} < -1.1$, provided that the Parkes catalogue lists a 2700 MHz flux density for the source.
2. If a source from the Molonglo catalogue does not have a listed flux density in the 2700 MHz survey we have assumed that its 2700 MHz flux density is fainter than the limiting flux density of the survey. We included such sources if their upper limit to the spectral index of $\alpha^{408}_{2700} < -1.1$.

365A: Since at the time of our first VLA observing session, there were no additional flux density measurements available for the majority of the fainter Texas sources, we decided to base our initial selection on the crude internal spectral indices listed in the Texas catalogue. Since only the brighter sources ($\gtrsim 1$ Jy) have such spectral indices listed, the resulting flux density cutoff of this sample was ~ 1 Jy.

Because the Texas Catalogue has a tendency of underestimating the flux density of sources larger than $15''$ (Becker et al. 1991) and because the angular size of high-z sources are statistically expected to be small, we only included sources with sizes $< 40''$ in this sample.

Furthermore, 12 sources with $\alpha^{365}_{4850} < -1.15$ were taken from the MIT-Green Bank 5 GHz Survey (Bennett et al. 1986). These sources were 0012+137, 0050+176, 0736+167, 1152+186, 1506+142, 1626+

© European Southern Observatory • Provided by the NASA Astrophysics Data System

1994A&AS..108...79R

147, 1635+159, 1649+169, 1718+192, 1725+167, 1732+160 and 2141+192. This list was kindly provided by J. Roland.

365B: This sample was selected by matching Texas sources to sources on the NRAO Green Bank 4850 MHz survey. We restricted our attention to the most reliable sources from the Texas catalogue, i.e. those that had no indication of position or structure lobe shifts and whose structures were well modelled (code ='+++', see Douglas et al. 1980). At the location of these Texas sources a gaussian brightness distribution was fitted to the 4850 MHz maps using the standard program 'JMFIT' from the NRAO image processing system AIPS. This yielded a position and a flux density at 4850 MHz for most of the Texas sources. Although the background noise in the 4850 MHz maps is not dominated by confusion, some of the 4850 MHz sources will be confused. In these cases the fitting algorithm can be unstable and give incorrect answers. Rejecting sources that have 4850 MHz positions that differ from the Texas positions by more than $\sim 1\sigma$ alleviates this problem. However, with this rejection criterion the number of USS sources will be incomplete and biased against sources whose structures and centroid positions change with frequency.

For the sources from the Texas catalogue that had no counterpart in the NRAO Green Bank 4850 MHz maps, the upper limit to the 4850 MHz flux densities was taken to be 15 mJy, i.e. 3 times the rms noise, considerably lower than the limits of the source catalogues of Becker et al. (1991) and Gregory & Condon (1991). The motivation for this is twofold.

First, since we looked for sources at the position of known Texas sources, the a posteriori chance that the source is real is larger than by searching at random positions on the maps. Second, the main aim of defining this sample was to find sources at fainter flux density levels than our previously defined Texas sample. A few spurious sources will not hamper this and would be rejected at a later stage on the basis of VLA observations.

The declination range has been chosen such that the sample is visible from the European Southern Observatory (ESO) at La Silla.

32 sources with $\delta > 20$ deg were selected from the Texas Catalogue with the same criteria as those used for selecting sample 365A. This sample of sources was observed at the Westerbork radio telescope to measure the flux at 1400 MHz. Two sources (0028+409 and 1329+485) with a USS spectrum were added to this sample.

178: for details see the selection for **408A**. This is effectively a "4C" sample.

151: This sample was selected from a combination of the 6C 151 MHz catalogue, the Texas 365 MHz catalogue and the NRAO Green Bank 4850 MHz catalogue. To minimise problems due to confusion, we constrained the accepted position differences between the positions of the radio sources from the two catalogues to about $1\ \sigma$.

38A: The initial spectral selection from the combination of the 38 MHz survey, the 6C and the NRAO Green Bank 4850 MHz was on α_{151}^{38} and $\alpha_{4850}^{151} < -1.0$ and yielded 74 sources. Subsequent removal of sources that i) are confused on the 38 MHz maps (9 sources), ii) lie within the bounds of cluster as drawn by Zwicky & Herzog (1968) (14 sources), or have been identified on the Palomar Observatory Sky Survey (POSS) Prints (13 sources) yielded 38 sources. CCD imaging and spectroscopy of this sample will be described by Lacy et al. (in prep.).

38B: This sample is formed from a combination of the 8C, Texas and the NRAO Green Bank 4850 MHz surveys. Since only 37 out of 2642 sources had an ultra-steep spectrum, we did not impose here the restriction that the position differences between the three surveys should be less than 1σ. Although this sample is likely to contain more confused sources than the other samples, VLA observations will be used to reject the confused sources.

38C: As can be seen from Fig. 4, the fainter steep spectrum sources from the 8C will be too faint to be included in the NRAO Green Bank maps. Assuming an upper limit of 15 mJy ($\sim 3\sigma$) for the 4850 MHz flux density, we included sources for which this upper limit implied a spectral index $\alpha_{4850}^{38} < -1.0$. The purpose of this was to obtain a sample of relatively faint USS sources selected at 38 MHz.

6. VLA observations

6.1. *Objectives*

The VLA snapshot observations of the USS samples had several goals. The most important was to obtain the radio positions so that the identifications of the radio sources could be established. Second, the measurement of radio structures was important both for investigating such phenomena as the radio/optical alignment effect (McCarthy et al. 1987; Chambers et al. 1987; Rigler et al. 1992) and for determining the optimum position angles for orienting the slit of the optical spectrograph. Third, for the sources for which no reliable spectral index was available (e.g. sample 365A), an additional flux density point would be obtained and the suspected ultra-steep spectrum could be confirmed or rejected. Fourth, radio sources that are confused in the finding survey could be established. Since in these cases their USS nature could be an artifact of the confusion, they could be rejected from the samples.

© European Southern Observatory • Provided by the NASA Astrophysics Data System

1994A&AS..108...79R

6.2. *Observations and reduction*

The observations were carried out with the VLA in A-array (e.g. Thompson et al. 1980). The samples 178, 365A, 408A, and 408B were observed on 26 and 27 Nov. 1988 during a 48 hour observing session, using the VLA J2000 coordinate system. The samples 38A, 38B, 38C, 151 and 365B were observed on 20 and 21 May 1990 during a 36 hour observing session using the VLA B1950 coordinate system.

The observing configurations used in the two observing sessions were identical. The observations were made in L band (1465 MHz) with a standard bandwidth of 50 MHz. Typical observing times for an individual source were 1×5 minutes. The sources from the 38A sample were observed for 2×5 minutes separated by 3 hours to improve the coverage of the uv-plane. The flux density scale was established by observing one of the primary VLA calibrators 3C286 and 3C48 a few times per day. The phases were calibrated using standard nearby VLA phase calibrators, observed about every half hour.

The Fourier transform, CLEANing and self-calibration were carried out in the normal way using the NRAO image processing system AIPS. Two sets of maps were produced at different resolution. The first set was at full resolution with a restoring circular beam of 1.5 arcsec FWHM and a field size of $4'16'' \times 4'16''$. The second set of lower resolution maps was obtained by tapering the visibilities and using a restoring circular beam of 4.5 arcsec FWHM. The maps were CLEANed using the ungridded subtraction method (Schwab 1984) as implemented in the AIPS task MX.

Self calibration (Cornwell & Wilkinson 1981) was applied only to the smoothed maps from the first observing session, with one iteration on the phases alone and two on both phases and amplitude. For the high resolution maps no self calibration was applied. In this case the quality of the maps for the stronger sources were in general sufficient to achieve our goals. For the weaker sources, the signal to noise was too low to apply self calibration

The 38A sample was analysed separately. One iteration of self-calibration was applied to observations with a sufficient signal-to-noise to warrant it, and the maps were then CLEANed and restored with a 1.5 arcsec FWHM circular beam. The noise on these 10 min observations was typically 0.3 mJy beam^{-1}. Sources in this sample which had angular sizes on the VLA maps $\gtrsim 1$ arcmin, or which were suspected of having large amounts of flux resolved out by the VLA were mapped at 151 MHz with the Cambridge Low Frequency Synthesis Telescope (CLFST). Analysis followed the procedure outlined in Lacy et al. (1992), with suitable phase calibrators being chosen separately for each source. The beam is $70 \times 70\,\mathrm{cosec}\,\delta$ arcsec^2, and the noise typically $30 - 50$ mJy beam^{-1}.

In Appendix A we present the maps for the sources that are clearly resolved (sizes $\gtrsim 3''$). The contour levels are at $(-6,-3,3,6,12,24,50,100,200,400,800,1600, 3200,6400, 12800)$ times the map noise, typically 0.5 to 1.5 mJy beam^{-1}.

6.3. *Determination of source parameters*

Positions and peak brightnesses of the main components of the radio sources were determined by fitting a quadratic function to the local brightness maxima in the high resolution maps. The fitting algorithm MAXFIT in the reduction package AIPS, as incorporated in the MIT-AIPS procedures by J. Léhar, was used. The reliability of the positions was checked visually.

The integrated flux densities were measured from the tapered VLA maps (resolution 4.5 arcsec) by summing the pixels within a box around the radio source. The ratio of the integrated VLA flux densities to the flux densities obtained from the NRAO Green Bank 1400 MHz sometimes shows large discrepancies (e.g. Fig. 5). The number of VLA sources that have flux densities that are significantly lower than those of the NRAO Green Bank by more than 3 sigma (sigma of the NRAO Green Bank 1400 MHz flux densities) is 10 per cent.

Possible explanations that might account for this discrepancy are:

1. *Insensitivity to large scale structure*
   The largest angular size over which the uv coverage of a VLA A-array snapshot at 1465 MHz satisfies the sampling theorem and thus permits mapping is approximately 30 arcsec (Bridle 1989). Components having sizes larger than ~ 30 arcsec cannot be mapped adequately with the VLA in this configuration. In these cases flux from large-scale structures such as halos and bridges might be underestimated. To illustrate this we plot the ratio between the 1400 MHz NRAO Green Bank flux density and the 1465 MHz VLA snapshot flux density for the sources that have 1400 MHz NRAO Green Bank flux densities versus the radio source extensions as measured by the VLA (Fig. 5). The error bars are determined by the uncertainties in the NRAO Green Bank measurements.
2. *Errors in CLEANing the snapshots*
   For the snapshot observing mode, the high side lobe levels of the VLA beam worsen confusion problems. Also it was not possible to completely remove the effects of noise spikes due to interference in the data taken at some baselines.
   Because of these problems the flux density as determined in an aperture around the source will be underestimated, since in the CLEANing process some of the flux from a radio source will not have been concentrated at the proper radio source position.
3. *Confusion in the NRAO Green Bank flux densities*
   Since the noise in the 1400 MHz Green Bank data is primarily due to confusing objects, a bias in the NRAO Green Bank flux might be expected (e.g Fig. 5).

© European Southern Observatory • Provided by the NASA Astrophysics Data System

1994A&AS..108...79R

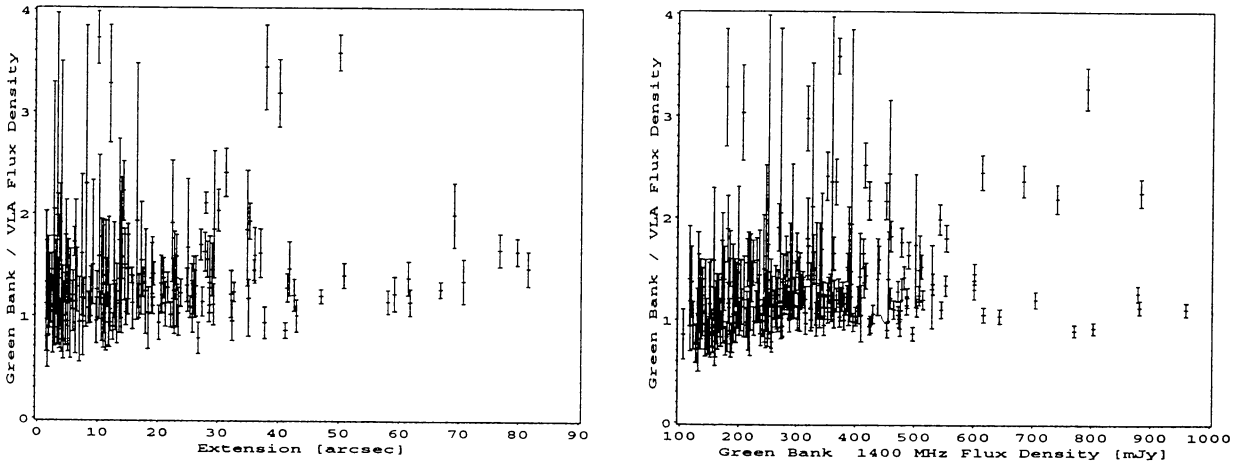

Fig. 5. The ratio between the NRAO Green Bank 1400 MHz flux density and VLA 1465 MHz flux density plotted as a function of the radio source extension as measured by the VLA snapshot measurements (left) and as a function of the NRAO Green Bank 1400 MHz flux density (right)

The discrepancy between the VLA and the Green Bank flux densities agrees with the findings of Downes et al. (1986) and Lawrence et al. (1986) that for their comparable surveys a simple VLA snapshot at A array is in general not sufficient to determine a reliable flux density and that additional measurements (single beam telescope, smaller array) are necessary to get reliable flux densities. Hence, if a 1400 MHz NRAO Green Bank measurement was available, we used this flux density instead of the integrated VLA flux density.

For the well resolved sources, the angular sizes and the position angles were measured from the location of the source extremities. For objects with simple morphologies this is straightforward. For sources that have complex diffuse emission, the measurement is signal-to-noise dependent. For small sources (< 3 arcsec), the angular sizes and the position angles were determined from an elliptical gaussian function fitted to the source brightness distribution.

We classified the source morphologies into point sources (< 3 arcsec), doubles, triples, multi-components sources and diffuse sources, although obviously the classification is a function of both resolution and dynamic range. Fortunately, the size distribution is such that most of the sources are well resolved.

For sources with sufficient data we calculated two spectral indices. A two point low frequency spectral index $\alpha_{\rm l}$ is based on either a 38 MHz flux density measurement from 8C or a 80 MHz flux density measurement listed in the Parkes Catalogue combined with the next low frequency flux density point available (either 151, 178, 365 or 408 MHz). For the high frequency spectral index ($\alpha_{\rm h}$), we fitted a power-law to the available flux density points at frequencies higher than 150 MHz.

In Appendix A we give a table with the source parameters for the sources. The contents of the various columns of this table are as follows:

1. Name of the samples to which the source belongs (see previous sections).
2. The source name in IAU B1950.0 format.
3. A component designator. A number indicates that the component belongs to the main central radio source. A letter indicates that the object is a bright (presumably) serendipitous source visible in the VLA map in a $4' \times 4'$ region surrounding the source. A 'C' after a number indicates that this component is probably the core component. The distinction between a "main component" and a "serendipitous source" is based on i) a large separation ($\gtrsim 2'$) and ii) no morphological indication that the two components are connected.
4. The VLA position determined by fitting a quadratic function to the local intensity maxima.
5. The epoch of the coordinate system B1950 or J2000
6. The measured peak brightness for the component in mJy/beam.
7. The integrated flux density (mJy) determined from the 1465 MHz VLA snapshot observations.
8. The ratio of the measured VLA flux density to the NRAO Green Bank 1400 MHz flux density taken from the 1400 MHz source list of WB.

9.–10. The low frequency spectral index and its uncertainty.

11.–12. The high frequency spectral index and its uncertainty.

13. Codes indicating which flux densities have been used in calculating the low and high frequency

© European Southern Observatory • Provided by the NASA Astrophysics Data System

1994A&AS..108...79R

Table 5. Codes indicating the radio catalogues that have been used in the spectral index calculations as presented in Appendix A

Frequency	MHz	38	80	151	178	365	365	408
Catalogue		8C	PKS	6C2	PKS	TXS	TXS:BWE	PKS
Code		a	b	c	d	e	f	g

Frequency	MHz	408	1400	1400	1410	1465	2700	4850
Catalogue		MOL	NRAO	WB	PKS	VLA	PKS	NRAO
Code		h	i	j	k	l	m	n

Frequency	MHz	4580	4580	4580	5000
Catalogue		87GB	BWE	WB	PKS
Code		o	p	q	r

spectral index. The flux densities are labeled as indicated in Table 5.

14. Various flags indicating catalogue problems and/or confusion: Flags *a* to *h* have been directly copied from three catalogues at 1400 and 4850 MHz (WB, BWE and 87GB).
Flags *r* to *x* indicate inconsistencies and how various upper limits have been treated.
   * The spectral index/indices is/are unreliable, since there are warnings in one of the three 1400/4580 MHz catalogues (flags *a* to *h*) and/or there is a bright confusing source in the VLA field (flag *z*).
   a: In WB a 1400 MHz source is reported to match more than one 1400 MHz or 365 MHz source so that confusion is likely
   b: In WB a 1400 MHz source is reported to be extended at 1400 MHz.
   c: In WB a 1400 MHz source is reported to be extended at 4850 MHz .
   d: In BWE a 4850 MHz source is reported to be extended at 4850 MHz. Note that the flags c and d are not always simultaneously present.
   e: In the BWE the separation between the NRAO 4850 MHz and the Texas 365 MHz positions is reported to be greater than 100 arcsecs.
   f: In 87GB a source is reported to be extended or a blend of two or more point sources (Flag E in the original catalogue).
   g: In 87GB a source has a warning that it is a weak source with a large zero offset, a narrow minor axis, or possibly confused; less reliable than most (Flag W in the original catalogue).
   h: In 87GB a source is reported to be confused near a stronger source or its side lobes (Flag C in the original catalogue)
   q: Difference of 4850 MHz flux densities of 87GB and our fitting routines are greater than 10 mJy
   r: Difference in the 365 MHz flux densities from the version of the Texas catalogue that we used and the version that WB used.
   u: Since no Texas flux density is present in WB catalogue, we used the flux density from our version of the Texas Catalogue.
   v: No 1400 MHz flux densities in WB.
   w: Since no 4850 MHz flux densities is present in WB, we used the 87GB 4850 MHz flux density.
   x: No WB and 87GB 4850 MHz flux densities. Our determination for the 4850 MHz NRAO flux densities is used if this flux density > 15 mJy.
   z: A bright serendipitous source in the VLA field.
15. Structure classification D–*Double;* DF–*Diffuse;* P–*Point Source* ($\lesssim 3''$); T–*Triple*; M–*Multi component sources* (> 3).
16. Angular size measured from the VLA maps
17. Position angle measured from the VLA maps.

7. Refinement of samples

7.1. *Refinement of spectral indices*

As we stated above, one of the goals of the VLA observations was to refine the spectra for samples for which only crude spectral index information was available.

The VLA flux density measurement for the sample 365A complemented the Texas flux density so that the two point spectral index α_{1465}^{365} could be determined. When the 1400 and 4850 MHz NRAO Green Bank catalogues became available, this goal became less important for the northern sources ($\delta > 0$) from this sample and for these sources the spectra could be better defined.

For the sample 408B the only flux information available was the density at 408 MHz, and an upper limit at 2700 MHz. With the new VLA measurements the spectral indices could be better defined.

In the 38A sample 4 sources were rejected after the 6C flux scale in this part of the sky was finalised, showing in fact that $\alpha_{151}^{38} > -1$.

© European Southern Observatory • Provided by the NASA Astrophysics Data System

1994A&AS..108...79R

Using the VLA and NRAO Green Bank spectral information the various samples were refined. The number of objects in sample 365A was reduced from 372 to 150 and in sample 408B from 28 to 16. The results of these refinements are given in Table 4

7.2. *Sample 38C*

Sample 38C was selected from the 8C catalogue in combination with an upper limit on the 4850 MHz NRAO Green Bank maps. Only in 30% of the cases did a source appear on the VLA snapshot maps. Most of the remaining sources had some flux at the shortest spacing indicating that the field contained a source with an angular size $\gtrsim 1$ arcmin. The characteristics of these sources are presented in the appendices. Since such sources are not expected to be located at large distances, we rejected these sources as good candidates for distant galaxies.

8. Statistical results

We shall now briefly discuss some statistical properties of the samples, namely i) the range of flux densities, ii) relative content of radio morphologies and iii) angular size distributions of the various samples.

8.1. *Flux densities*

In selecting our samples of USS sources we attempted to cover a range in flux density larger than that of the 4C USS sample. We compare the flux ranges at 365 MHz of the 4C USS sources and the samples we have defined in this paper, since the majority of the sources in the samples defined in this paper are selected at 365 MHz or at the nearby frequency of 408 MHz. For the sources that did not have a measured 365 MHz flux, we have fitted a power-law to the flux measurement at frequencies > 150 MHz and obtained a 365 MHz flux density estimate.

The distribution over this 365 MHz flux density is given in Fig. 6. For reference the distribution of the 365 MHz flux density for the 4C USS samples (Chambers et al. 1987) is also given.

The 365 MHz flux densities range from ~ 0.3 to ~ 4 Jy with most occurring near 1 Jy. The 4C samples covered a flux density range from 1 to 5 Jy. The new samples have significantly more sources than the 4C USS sample and reach a factor of ~ 3 fainter in flux density.

8.2. *Angular size distribution as a function of finding frequency*

The angular size distribution can be studied as a function of finding frequency with the samples that we have observed with the VLA. By considering the distributions for the samples 38B, 151, 365A+B (see Table 4), we cover a large range in finding frequency. Further, this combination of samples has the advantage that all contain a Texas flux point, so that the angular size selection $\lesssim 1'$ introduced by the Texas catalogue is present in all four samples. The surveys at the other frequencies have large beams ($\gtrsim 3$ arcmin), so that the angular size selection is negligible compared to the Texas angular selection. The distribution of the angular sizes has a median value of 26 ± 5, 15 ± 3 and 10 ± 1 arcseconds for the sources from the samples 38B, 151 and 365A+B respectively. (e.g. Table 6 and Fig. 7). For complete samples of sources (e.g. no spectral selection) selected at comparable flux limits the median size also decreases as a function of finding frequency (e.g. Table 6).

To test whether this correlation might be due to the different flux limits of the three samples, we examine the median size as a function of flux density at 365 MHz for the three samples. To that end, we calculated the median size in 4 bins (in mJy) {(0,718), (718,1129), (1129,1390), (1390,∞)} that have been chosen so that the total sample (38B + 151 + 365AB) contains equal numbers in each of these bins. For these 4 bins we calculated the median flux density and the median angular size (e.g. Fig. 8).

We conclude that the difference in angular size in the three samples is mainly related to their finding frequency and not to differences in flux density at 365 MHz.

Possible explanations for the origin of this decrease in median angular size with finding frequency are:

1. *Opacity of Sources*
   The spectrum of a homogeneous synchrotron source becomes optically thick below a frequency $\nu_c \sim 25\theta^{-4/5}S^{2/5}B^{1/5}$ where θ is the angular size in arcseconds, S is the maximum flux density in Janskys and B is the magnetic field in gauss (e.g. Moffet 1968). The high-redshift radio sources have large luminosities and the structures of these sources are generally dominated by bright hotspot structures. These hotspots are typically unresolved at a resolution of ~ 1 arcsec. Assuming a size of 0.1 arcsec, corresponding to ~ 1.6 kpc in size at $z = 2$ (cf. Dreher 1981) and a magnetic field B of 10 μGauss, we find that a source of 10 Jy should have a cutoff frequency at ~ 38 MHz. Hence, many high luminosity distant sources which are found to be USS at frequencies $\gtrsim 100$ MHz might have flatter spectra at frequencies < 100 MHz and be less well represented in low frequency USS samples. More diffuse sources would not be affected by synchrotron self absorption and would continue to have USS down to frequencies well below 38 MHz.
2. *Luminosity-Linear size correlation.*
   It has been suggested that for bright double-lobed radio sources total luminosity correlates with size (e.g. Gopal-Krishna & Kulkarni (1992) and references therein; but see also Lacy et al. (1993) who find no evidence for such a correlation). If this is indeed the case, some of the sources selected at the lowest frequencies

© European Southern Observatory • Provided by the NASA Astrophysics Data System

1994A&AS..108...79R

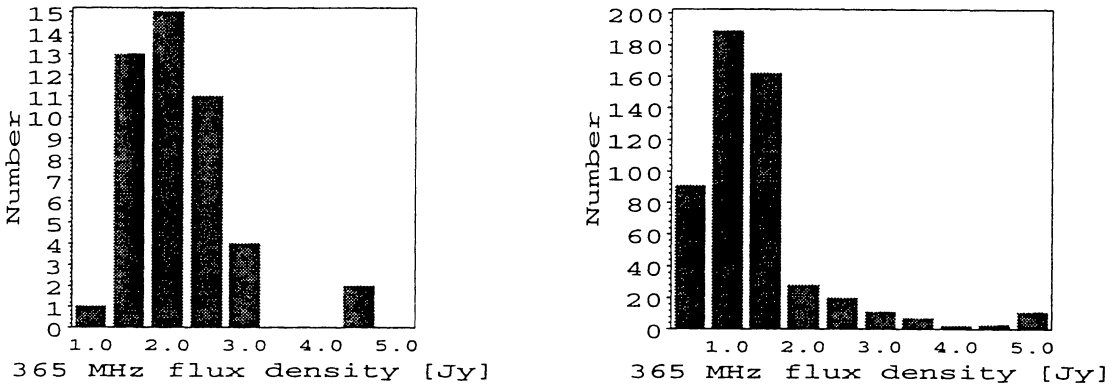

Fig. 6. Flux density distribution at 365 MHz of the 4C USS samples (left) and of the samples that have been defined in this paper

Table 6. Median sizes of sources

	38 MHz	151 MHz	365 MHz
Median Size USS samples [arcsec]	26 ± 5	15 ± 3	10 ± 1
Median size complete samples [arcsec]	18[1]	14[2]	12[3]

1. Lacy *et al.* (1992)
2. Eales (1985)
3. Allington–Smith (1982, 408 MHz)

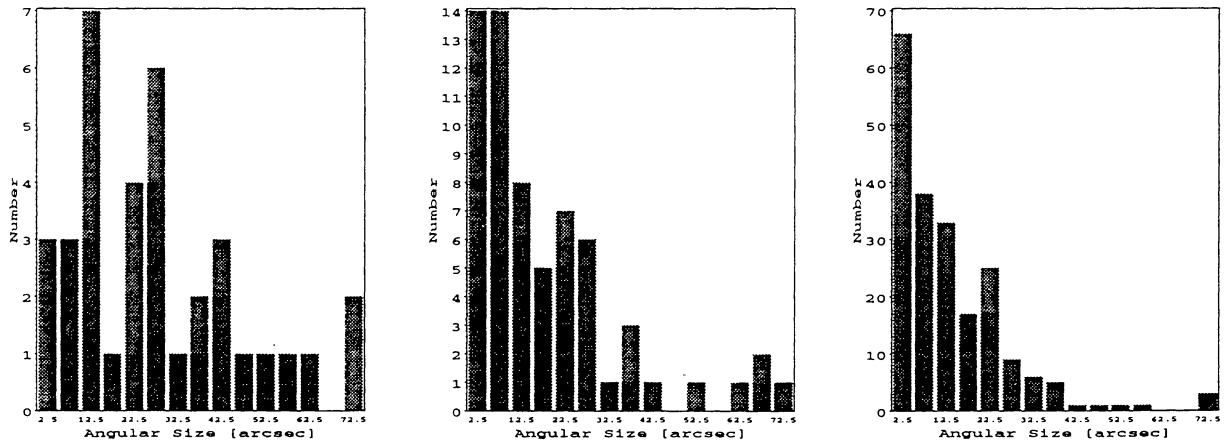

Fig. 7. Angular size distribution for the three USS samples, 38B sample (left), the 151 sample (middle) 365 A+B sample (right)

might be the most powerful and thus have the largest linear size.

3. *Redshift Selection.* We can argue that, on the one hand, if the $\alpha - z$ relation is at least partly due to spectral curvature, some of the highest redshift objects are expected in 38 MHz selected USS samples. On the other hand, sources at high redshifts are expected to have small ($\lesssim$ 10 arcsec) angular sizes, but USS samples selected at 38 MHz contain a relatively low fraction of these small sources. This suggests that USS samples selected at 38 MHz might contain a few of the highest redshift sources, but possibly fewer than the samples selected at 178 MHz. Spectroscopic redshifts of the small sources from the USS samples selected at 38 MHz are needed in order to make this statement more quantitative.

It is interesting to note that there is a suggestion that the fainter sources from the 38B sample have smaller median angular sizes than the brighter sources from the 38B sample (e.g. Fig. 8), possibly indicating that the median angular sizes for the three samples might converge at low flux densities ($S_{365} \sim 100$ mJy). This is consistent with the finding of Lacy et al. (1993) who note that the whereas at high flux levels ($S_{38} \gtrsim 20$ Jy) the USS population is dominated by sources associated with rich clusters, the USS sources at the fainter level of the 8C NEC sample

© European Southern Observatory • Provided by the NASA Astrophysics Data System

1994A&AS..108...79R

($S_{38} \gtrsim 1.3$ Jy) are not associated with rich clusters. It is therefore possible that studying samples of USS sources selected at 38 MHz is an effective way of finding distant galaxies, provided that the sample is defined at faint levels ($S_{38} \sim 1$ Jy).

8.3. *Structures*

To study the relative content of structural types in our USS samples, we use the samples that we also used for studying the distribution of angular size as a function of finding frequency (the samples 38B, 151 and 365A+B, see Table 4), and for the same reasons.

In Table 7 we present the statistics of morphological types for the samples observed with the VLA.

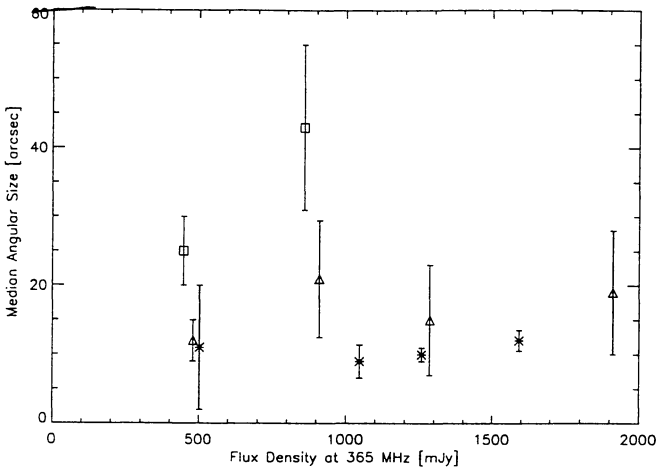

Fig. 8. Median angular sizes as a function of flux density at 365 MHz for the three samples 38B (□), 151 (△) and 365AB (⋆)

Table 7. Distribution of structural types for samples with different finding frequencies

	Samples			
Morphology	38B	151	365AB	Total
Point source (P) : $\lesssim 3''$	2	7	47	56
Double (D)	21	36	128	185
Triple (T)	5	8	18	31
Diffuse (DF)	8	11	16	35
Complex (M)		2	4	6
Total	36	64	213	313

Just as is the case for the median sizes, the structure is a clear function of finding frequency. Relatively large sources as well as sources with diffuse structures are more common in USS samples with lower finding frequencies. The lack of the Point sources at low frequency, and the very similar proportions of Double sources in the three samples, suggest that the Point sources are being lost at low frequency, presumably through becoming optically thick (cf. Lacy et al. 1992, who find marginal evidence for this effect in a complete 8C sample). The larger angular size of sources and the larger content of diffuse sources in the 38 MHz defined samples supports the conclusion that USS samples selected at the lowest finding frequencies contain a somewhat different source population than USS sources selected at $\gtrsim 150$ MHz.

9. Conclusions

We have defined new samples of radio sources with ultra-steep spectra. These samples are selected at a range of frequencies from 38 MHz to 408 MHz and flux limits fainter by a factor of three than the previously well-studied 4C samples. The samples provide candidates for distant galaxies which will be investigated using optical imaging and spectroscopy.

Snapshot observations of sources from these samples with the VLA at high resolution (1.5 arcsec) were presented and yielded accurate positions, fluxes and radio structural information for a total of 605 sources.

Statistical results from the comparisons of the catalogues and the VLA imaging are:

1. Complete samples of small radio sources ($\lesssim 1$) arcmin selected at 38 MHz contain relatively fewer ultra-steep spectrum sources than samples of small radio sources selected at higher ($\gtrsim 150$ MHz) frequencies.
2. USS radio sources selected at the lowest finding frequencies contain a higher proportion of diffuse sources, and a lower proportion of small ($\lesssim 3$ arcsec) sources than those selected at higher frequencies.

These results can be interpreted as due to a combination of i) low frequency curvature in the radio spectra, perhaps due to synchrotron self-absorption of compact components in small radio sources, and ii) the effects of radio source evolution.

Acknowledgements. It is a pleasure to thank Peggy Perley and Dave Wunkler from the NRAO with their help conducting and calibrating the VLA observation. We thank S. Hales, J. Condon, J. Douglas and R. Becker for providing us with electronic versions of their radio catalogues, Renate Reijns for reducing the Westerbork data and E. Waldram for providing the CLFST maps, Hedy Versteege, Irma Eggenkamp and Arend Sluis for their assistance in the project and Frits Bijleveld and Joseph Léhar for their software assistance. We acknowledge the EEC for support from the Science Stimulation Programme. ML thanks the SERC for a postdoctoral fellowship.

References

Allington-Smith J.R. 1982, MNRAS 199, 611
Andernach H., Sievers A., Kus A., Schnaubelt J. 1986, A&AS 65, 561

© European Southern Observatory • Provided by the NASA Astrophysics Data System

1994A&AS..108...79R

Baars J.W.M., Genzel R., Pauliny-Toth I.I.K., Witzel A. 1977, A&A 61, 99
Baldwin J., Scott P. 1973, MNRAS 165, 259
Baldwin J.E., Boysen R., Hales S. et al. 1985, MNRAS 217, 717
Baum S.A., Heckman T.M. 1989, ApJ 336, 702
Becker R., White R., Edwards A. 1991, ApJS 75, 1
Bennett C.L., Lawrence C.R., Burke B.F., Hewitt J.N., Mahoney J. 1986, ApJS 61, 1
Blumenthal G., Miley G. 1979, A&A 80, 13
Bolton J.G., Wright A.E., savage A. 1979, Aust. J. Phys. Astroph. Suppl. 46, 1
Bridle A.H. 1989, eds. R. Perley, F. Schwab, A. Bridle, Synthesis Imaging in Radio Astronomy, 443
Bridle A.H., Kesteven M.J.L., Guidon B. 1972, ApJ 11, 27
Chambers K.C., Miley G. 1989, ed. R.G. Kron, The Evolution of the Universe of Galaxies: The Edwin Hubble Centennial Symposium (San Francisco: Astro. Society of the Pacific) 373
Chambers K.C., Miley G.K., van Breugel W. 1987, Nature 329, 604
Chambers K.C., Miley G.K., van Breugel W.J.M. 1990, ApJ 363, 21
Condon J. 1984, ApJ 284, 44
Condon J., Broderick J 1985, AJ 90, 2450
Condon J., Broderick J. 1986, AJ 91, 1051
Condon J., Broderick J., Seielstad G. 1989, AJ 97, 1064
Conway R.G., Burns B.J., Vallee J.P. 1977, A&AS 27, 155
Cornwell T.J., Wilkinson P.N. 1981, MNRAS 196, 1067
Douglas J.N., Bash F., Torrence G.W., Wolfe C. 1980 The University of Texas Publications in Astronomy 17, 1
Downes A.J.B., Peacock J.A., Savage A., Carrie D.R. 1986, MNRAS 218, 31
Dreher J.W. 1981, ApJ 86, 833
Dunlop J., Peacock J. 1990, MNRAS 247, 19
Eales S. 1985, MNRAS 217, 149
Efstathiou G., Rees M.J. 1988, MNRAS 230, 5P
Gopal-Krishna, Kulkarni V.K. 1992, 257, 11
Gregory P.C., Condon J.J. 1991, ApJS 75, 1011
Hales S.E.G., Baldwin J.E., Warner P.J. 1988, MNRAS 234, 919
Hanish R. 1987, eds. C.P. O'Dea, J.M. Uson, Radio Continuum Processes in Clusters of Galaxies, NRAO workshop No. 16, NRAO, 191
Hanish R.J. 1982, A&A 111, 97
Heeschen D. 1960, PASP 72, 368
Jaffe W.J., Rudnick L. 1979, ApJ 233, 453
Kapahi V.K. 1989, AJ 97, 1
Kapahi V.K., Kulkarni V.K. 1990, AJ 99, 1397
Krolik J.H., Chen W. 1991, AJ 102, 1659
Lacy M., Hill G.J., Kaiser M.E., Rawlings S.G. 1993, MNRAS 263, 707
Lacy M., Rawlings S., Warner P.J. 1992, MNRAS 256, 404
Laing R., Peacock J.A. 1980, MNRAS 190, 903
Laing R.A., Riley J.M., Longair M.S. 1983, MNRAS 204, 151
Large M.I., Mills B.Y., Little A.G., Crawford D.F., Sutton J.M. 1981, MNRAS 194, 693
Lawrence C.R., Bennett C.L., Hewitt J.N. et al. 1986 ApJS 61, 105
Leahy J.P., Muxlow T.W.B., Stephens P.W. 1989, MNRAS 239, 401
Liu R., Riley J., Warner P., Pooley G., Alexander P. 1989, MNRAS 240, 501
Macleod J.M., Doherty L.H. 1972, Nature 238, 88
Malofeev V.M., Malov I. 1980, Sov. Astron. 24, 54
McCarthy P., Kapahi V.K., van Breugel W., Subrahmanya C. 1991a, AJ 100, 1014
McCarthy P., van Breugel W., Kapahi V., Subrahmanya C. 1991b, AJ 102, 522
McCarthy P., van Breugel W., Spinrad H., Djorgovski S. 1987, ApJL 321, L29
McCarthy P.J., van Breugel W. 1989, eds. E.J.A. Meurs and R.A.E. Fosbury, ESO Workshop on Extranuclear Activity in Galaxies, 55
Miley G., Chambers K. 1989, eds. E.J.A. Meurs and R.A.E. Fosbury, ESO Workshop on Extranuclear Activity in Galaxies, 43
Miley G.K. 1968, Nature 218, 933
Miley G.K., Perola G., van der Kruit P., van der Laan 1972, Nature 237, 269
Mills B.Y., Aitchison R.E., McAdam A.G.L.W.B. 1963, Proc. Inst. Radio Engrs. Aust. 24, 56
Moffet A.T. 1975, eds. A. Sandage, M. Sandage, J. Kristian, Stars and Stellar Systems, Vol. IX, 211
O'Dea C., Owen F.N. 1985a, AJ 90, 927
O'Dea C., Owen F.N. 1985b, AJ 90, 954
Oort M. 1987, Ph. D. thesis, University of Leiden
Rawlings S., Eales S., Warren S. 1990, MNRAS 243, 14p
Rawlings S., Saunders R., Eales S., Mackay C. 1989, MNRAS 240, 701
Rees N. 1990a, MNRAS 243, 637
Rees N. 1990b, MNRAS 244, 233
Rigler M., Lilly S., Stockton A., Hammer F., Le Fèvre O. 1992, ApJ 385, 61
Roger R.S., Bridle A.H., Costain C.H. 1973, AJ 78, 1030
Roland J., Hanish R.J., Véron P., Fomalont E. 1985, A&A 148, 323
Sarazin C. 1986, Rev. Mod. Phys. 34, 1
Schwab F.R. 1984, AJ 89, 1076
Sieber W. 1973, A&A 28, 237
Slingo A. 1974a, MNRAS 166, 101
Slingo A. 1974b, MNRAS 168, 307
Taylor J.H., Manchester R.N., Lyne A.G. 1993, ApJS 88, 529
Thompson A.R., Clark B.G., Wade C.M., Napier P.J. 1980, A&AS 44, 151
Tielens A., Miley G., Willis A. 1979, A&AS 35, 153

© European Southern Observatory • Provided by the NASA Astrophysics Data System

1994A&AS..108...79R

van Breugel W., McCarthy P.J. 1989, eds. E. Meurs and R. Fosbury, ESO Worshop on Extranuclear Activity in Galaxies, 227
Veron M.P., Veron P., Witzel A. 1972, A&A 18, 82
Viner M.R., Erickson C. 1975, AJ 80, 931
White R.L., Becker R.H. 1992, ApJS 79, 331
Williams P., Bridle A.H. 1967, Observatory 87, 280
Williams P.J.S., Kenderdine S. and Baldwin J.E. 1966, Mem. R. Astr. Soc. 70, 53
Wills B. 1973, ApJ 180, 335
Windhorst R.A., Kron R.G., Koo D.C. 1984, A&AS 58, 39
Windhorst R.A., Mathis D.F., Neuschaefer L.W. 1990, ed. R.G. Kron, ASP Conf. Ser., Vol. 10, Evolution of the Universe of Galaxies (Edwin Hubble Centennial Symposium) Provo, UT: BookCrafters, Inc., 389
Wyllie D.V. 1969a, MNRAS 142, 229
Wyllie D.V. 1969b, Proc. Astr. Soc. Aust. 1, 234
Zwicky F., Herzog E. 1968, Catalogue of Galaxies and of Clusters of Galaxies, California Institute of Technology, Vol. IV

© European Southern Observatory • Provided by the NASA Astrophysics Data System

1994A&AS..108...79R

Appendix A. Source list

Source	R.A. (h m s)	Decl (° ′ ″)		S_{peak} mJy	S_{int} mJy	$\frac{S^{VLA}_{int}}{S_{GB}}$	α_l	$\Delta\alpha_l$	α_h	$\Delta\alpha_h$			R ″	PA °
(1) (2) (3)	(4)		(5)	(6)	(7)	(8)	(9)	(10)	(11)	(12)	(13)	(14)	(15)	(16)	(17)
178 0003−019 1	0 6 11.10	−1 41 51.3	J	52	142	1.08			−1.36	0.05	djlm		D	3.3	46
0003−019 2	0 6 11.23	−1 41 49.2		52											
365B 0008+172 1	0 8 33.14	17 13 0.9	B	49	228				−1.28	0.05	elnop	*duvw	D	19.9	142
0008+172 2	0 8 32.35	17 13 15.4		56											
365A 0008−032 1	0 11 12.07	−2 59 42.8	J	42	219	0.56			−0.69	0.08	ehjl	r	D	11.0	131
0008−032 2	0 11 11.55	−2 59 35.7		68											
408B 0008−321 1	0 11 13.30	−31 50 32.2	J	205	377				−0.93	0.09	hl	v	P	4.3	35
365A 0009+058 1	0 12 13.67	6 10 7.5	J	101	229	0.95			−1.13	0.04	ehijlnopq	r	D	6.3	137
0009+058 2	0 12 13.40	6 10 11.9		58											
365A 0009+184 1	0 12 19.06	18 43 36.4	J	13	203	0.93			−1.09	0.04	ehijlnopq	r	D	8.5	81
0009+184 2	0 12 18.48	18 43 34.9		149											
365A 0010+112 1	0 13 34.81	11 28 59.3	J	52	194	0.74			−0.94	0.04	ehijlnopq	r	M	20.6	114
0010+112 2	0 13 33.43	11 29 8.3		12											
365A 0012+111 1	0 15 13.40	11 25 38.9	J	45	293	0.87			−1.12	0.03	ehijlnopq	r	D	28.7	63
0012+111 2	0 15 11.70	11 25 25.7		102											
365AB 0012+137 1	0 12 17.76	13 43 15.4	B	29	424	0.93			−1.14	0.03	ehijlnopq		P	2.6	161
365B 0013+121 1	0 13 47.06	12 10 6.5	B	34	124	1.17			−1.21	0.08	ejlnopq		D	7.6	175
0013+121 2	0 13 47.01	12 10 14.2		56											
408B 0013−316 1	0 16 14.61	−31 23 18.2	J	5	140				−1.77	0.08	hl	v	DF	16.9	106
0013−316 2	0 16 13.36	−31 23 13.6		12											
365B 0014+078 1	0 14 7.71	7 50 37.0	B	131	141	0.73			−1.17	0.07	ejlnopq		P	< 1.5	
365A 0015−114 1	0 18 22.07	−11 11 39.0	J	199	262				−1.03	0.07	ehl	uv	D	5.1	86
0015−114 2	0 18 21.73	−11 11 39.3		15											
408B 0016−028 1	0 18 47.74	−2 33 49.6	J	125	230	0.71			−1.14	0.08	hjlm	*b	P	3.5	111
365B 0017+154 1	0 17 50.16	15 24 11.8	B	564	1921	0.86			−1.17	0.03	ejlnopq		D	10.5	143
0017+154 2	0 17 49.73	15 24 19.9		262											
408A 0018−092 1	0 20 50.50	−8 57 25.4	J	161	603		−1.00	0.02	−1.23	0.03	bghklmr	v	D	19.9	19
0018−092 2	0 20 50.19	−8 57 44.5		175											
365A 0023+132 1	0 26 10.31	13 30 54.5	J	132	427	0.88			−0.71	0.04	ehijlnopq	r	D	4.0	80
0023+132 2	0 26 10.05	13 30 53.9		172											
365A 0023+330 1	0 25 43.92	33 16 48.5	J	29	289	0.84			−1.05	0.05	eijlnopq	r	P	< 1.5	
365A 0024+325 1	0 27 7.76	32 46 35.7	J	234	294	1.18			−1.13	0.03	eijlnopq	r	D	7.0	96
0024+325 2	0 27 7.23	32 46 36.4		35											
365A 0024−277 1	0 27 29.69	−27 31 18.4	J	154	395				−0.96	0.06	ehl	uv	D	14.3	136
0024−277 2	0 27 28.98	−27 31 8.2		137											
365B 0028+051 1	0 28 57.42	5 8 28.1	B	36	132	0.75			−1.30	0.06	ejln	x	D	22.6	158
0028+051 2	0 28 57.41	5 8 31.8		7											
0028+051 3	0 28 56.85	5 8 48.8		37											
365B 0028+409 1	0 28 7.72	40 54 20.3	B	127	233	0.83			−1.24	0.06	jlopq		D	5.8	84
0028+409 2	0 28 7.23	40 54 19.6		67											
178 0031+024 1	0 33 39.42	2 42 49.2	J	4	300	0.88			−1.31	0.07	dghijlmn	x	D	58.1	177
0031+024 2	0 33 39.30	2 43 46.9		6											
365A 0031−118 1	0 33 33.10	−11 32 20.0	J	164	236				−0.96	0.08	ehl	uv	D	3.7	75
0031−118 2	0 33 32.87	−11 32 20.9		20											
365A 0033+206 1	0 36 28.22	20 52 32.9	J	49	213	1.02			−1.16	0.04	eijlnopq	r	D	14.0	110
0033+206 2	0 36 27.30	20 52 37.9		36											
365A 0036+205 1	0 39 36.39	20 49 13.5	J	56	204	0.89			−0.81	0.06	eijlnopq	r	D	10.3	29
0036+205 2	0 39 36.10	20 49 6.4		22											
365B 0040+064 1	0 40 58.76	6 25 24.4	B	27	399	0.78			−1.15	0.05	ejlnopq		P	3.0	160
178 0041−000 1	0 44 30.56	0 14 20.5	J	6	112	0.28			−1.06	0.13	djlm	*b	D	8.1	119
0041−000 2	0 44 30.11	0 14 24.2		29											
408A 0043−003 1	0 46 30.75	−0 5 32.2	J	110	180	0.91			−1.08	0.06	ghjlm		P	2.3	129
365A 0044+107 1	0 46 41.44	11 2 52.4	J	223	256	1.01			−0.94	0.04	ehijlnopq	r	P	< 1.5	
365A 0050+176 1	0 53 17.70	17 54 27.4	J	69	364	0.97			−1.28	0.03	ehijlnopq	r	T	8.8	45
0050+176 2c	0 53 17.79	17 54 29.4		28											
0050+176 3	0 53 18.11	17 54 33.6		112											
365A 0050+204 1	0 53 39.01	20 46 3.4	J	52	201	0.52			−1.02	0.04	eijlnopq	r	D	35.3	90
0050+204 2	0 53 36.55	20 46 3.6		46											
365B 0054+090 1	0 54 53.12	9 1 37.2	B	186	497	0.91			−1.20	0.04	ejlnopq		D	19.2	36
0054+090 2	0 54 53.88	9 1 52.9		71											
408B 0102−335 1	1 4 39.37	−33 14 57.5	J	15	383				−1.02	0.08	hl	v	M	8.1	9
0102−335 2	1 4 39.68	−33 14 56.5		12											
0102−335 3	1 4 39.32	−33 14 55.3		70											
0102−335 4	1 4 39.57	−33 14 52.2		79											
38C 0105+747 1	1 5 4.99	74 40 56.5	B	28	82		−0.87	0.03	−0.87	0.03	alp	v	D	4.6	52
0105+747 2	1 5 5.93	74 40 59.8		11											
365B 0106+144 1	1 6 56.36	14 26 14.3	B	57	316	0.84			−1.19	0.05	ejlnopq		D	16.8	146
0106+144 2	1 6 55.72	14 26 28.1		85											
365A 0106+183 1	1 9 3.87	18 39 19.2	J	31	228	0.91			−0.91	0.04	ehijlnopq	r	M	3.7	48
0106+183 2	1 9 3.69	18 39 15.5		5											
0106+183 3	1 9 4.03	18 39 21.5		76											
365A 0111+074 1	1 13 53.86	7 43 53.5	J	112	242	0.98			−1.05	0.04	ehijlnopq	r	D	18.0	105
0111+074 2	1 13 52.69	7 43 58.4		28											
408B 0111−325 1	1 14 13.69	−32 18 2.7	J	53	334				−1.06	0.09	hl	v	D	56.0	144
0111−325 2	1 14 11.07	−32 17 17.2		118											
365A 0116+052 1	1 19 11.31	5 30 58.4	J	199	314	0.94			−0.90	0.04	ehijlnopq	r	P	2.6	119
365A 0116+052 1	1 19 11.31	5 30 58.4	J	199	314	0.94			−0.90	0.04	ehijlnopq	r	P	2.6	119
408B 0116−329 1	1 18 19.66	−32 40 20.5	J	74	498				−0.85	0.08	hl	v	DF	14.7	164
0116−329 2	1 18 19.39	−32 40 6.5		44											
178 0117+024 1	1 20 28.78	2 43 0.5	J	148	166	1.30			−0.98	0.07	dijlmnopq		D	5.5	124
0117+024 2	1 20 29.08	2 42 57.8		6											
365A 0117+126 1	1 20 24.92	12 54 5.7	J	214	347	0.88			−0.66	0.04	ehijlnopq	r	P	3.5	107
365B 0123+168 1	1 23 39.99	16 50 32.7	B	10	77	0.66			−1.16	0.09	ejln	x	D	12.7	159
0123+168 2	1 23 39.69	16 50 44.6		49											
365A 0124−167 1	1 26 56.64	−16 30 1.3	J	166	238				−1.12	0.07	ehl	uv	P	2.7	36
365A 0125+210 1	1 28 29.01	21 17 24.0	J	4	209	0.46			−0.73	0.03	eijlnopq	r	T	25.0	107
0125+210 2c	1 28 27.89	21 17 27.9		26											
0125+210 3	1 28 27.31	21 17 30.1		22											
0125+210 4	1 28 27.41	21 17 33.4		21											
408A 0128−264 1	1 30 28.41	−26 10 5.3	J	613	300		−1.49	0.02	−1.16	0.19	bghklmr	v	D	33.8	131
0128−264 2	1 30 26.56	−26 9 43.1		205											
365A 0136−231 1	1 38 57.38	−22 54 55.3	J	60	366				−0.95	0.06	ehl	uv	M	8.1	8
0136−231 2	1 38 57.46	−22 54 47.5		178											
408A 0139−167 1	1 42 24.99	−16 28 27.7	J	282	951		−1.05	0.02	−1.29	0.03	bghklmr	v	D	10.3	10
0139−167 2	1 42 25.08	−16 28 17.8		368											
365A 0141+095 1	1 43 50.89	9 46 55.7	J	22	234	0.51			−1.00	0.08	ehijlnopq	*acdfr	D	17.3	139
0141+095 2	1 43 50.13	9 47 8.9		22											
365A 0141+356 1	1 44 27.91	35 55 23.6	J	109	248	0.86			−0.92	0.05	eijlnopq	*rz	D	4.0	28
0141+356 2	1 44 28.05	35 55 27.1		67											
0141+356 A	1 44 32.82	35 56 31.5		10											

© European Southern Observatory • Provided by the NASA Astrophysics Data System

1994A&AS..108...79R

Appendix A. continued

Source	R.A.	Decl	S_{peak}	S_{int}	$\frac{S^{VLA}_{tot}}{S_{GB}}$	α_l $\Delta\alpha_l$	α_h $\Delta\alpha_h$			R	PA
	h m s	° ′ ″	mJy	mJy						″	°
(1) (2) (3)	(4)	(5)	(6)	(7)	(8)	(9) (10)	(11) (12) (13)	(14)	(15)	(16)	(17)
0141+356 B	1 44 32.44	35 56 37.4	6								
365A 0145+102 1	1 48 28.88	10 28 21.3 J	45	447	1.05		−0.73 0.04 ehijlnopq	r	P	< 1.5	
365B 0153+041 1	1 53 16.60	4 7 46.6 B	20	146	0.41		−1.16 0.03 ejlnopq		D	31.3	71
0153+041 2	1 53 14.63	4 7 35.9	52								
365A 0200+015 1	2 2 43.03	1 49 9.0 J	109	183	0.92		−1.17 0.04 ehijlnopq	r	D	5.1	155
0200+015 2	2 2 42.90	1 49 13.6	56								
365A 0201−141 1	2 3 27.46	−13 56 4.4 J	53	280			−1.00 0.07 ehl	uv	D	4.4	108
0201−141 2	2 3 27.20	−13 56 3.0	65								
365A 0203+333 1	2 6 17.22	33 36 51.7 J	3	68	0.33		−1.56 0.08 eijlnpq	r	DF	4.0	15
0203+333 2	2 6 17.45	33 37 8.8	2								
365A 0207+325 1	2 10 16.80	32 49 33.8 J	175	255	1.01		−0.81 0.03 eijlnopq	r	P	2.9	66
38C 0208+684 1	2 8 16.10	68 26 39.0 B	8	59		−1.06 0.03	−1.06 0.03 al	v	DF	101	61
0208+684 2	2 8 0.06	68 25 48.9	6								
365B 0209+071 1	2 9 48.32	7 7 55.0 B	153	588	0.95		−1.23 0.03 ejlnopq		D	13.9	16
0209+071 2	2 9 48.57	7 8 8.2	142								
178 0211+120 1	2 13 43.61	12 19 34.8 J	91	286	0.80		−1.15 0.03 dghijlmnopq		D	7.0	15
0211+120 2	2 13 43.74	12 19 41.5	46								
365A 0211−122 1c	2 14 17.38	−11 58 46.7 J	5	189			−1.27 0.07 ehl	uv	T	16.2	102
0211−122 2	2 14 17.76	−11 58 47.3	79								
0211−122 3	2 14 16.70	−11 58 43.7	31								
365A 0212+360 1c	2 15 18.05	36 18 7.3 J	6	284	0.85		−1.09 0.04 eijlnopq	r	T	30.9	155
0212+360 2	2 15 18.34	36 17 51.5	157								
0212+360 3	2 15 17.32	36 18 19.2	12								
365A 0214+183 1	2 17 25.79	18 36 59.2 J	26	268	0.88		−1.05 0.05 ehijlnopq	r	D	5.9	177
0214+183 2	2 17 25.76	18 37 5.2	215								
365A 0214+350 1	2 17 35.15	35 17 21.9 J	99	248	0.81		−1.06 0.05 eijlnopq	r	D	2.2	84
0214+350 2	2 17 34.98	35 17 21.6	146								
365A 0215+356 1	2 18 28.61	35 49 57.5 J	112	333	0.81		−0.86 0.03 eijlnopq	r	T	6.6	50
0215+356 2c	2 18 28.81	35 49 59.5	48								
0215+356 3	2 18 28.99	35 50 1.9	58								
365A 0216+335 1	2 19 48.73	33 48 12.2 J	110	331	0.87		−0.72 0.03 eijlnopq	r	D	12.1	180
0216+335 2	2 19 48.75	33 48 24.2	151								
365A 0218+007 1	2 21 3.69	−0 59 39.8 J	27	287	0.79		−1.00 0.05 ehijlnopq	r	P	< 1.5	
365A 0224+096 1	2 26 44.78	9 51 36.2 J	127	219	0.66		−1.03 0.04 ehijlnopq	r	D	5.1	109
0224+096 2	2 26 44.46	9 51 37.7	34								
365B 0226+129 1	2 26 11.69	12 57 8.4 B	42	285	0.81		−1.20 0.06 ejlnopq	*b	D	13.7	144
0226+129 2	2 26 11.14	12 57 19.6	21								
365A 0226−293 1	2 28 14.53	−29 4 38.2 J	175	328			−0.96 0.07 ehl	uv	P	4.3	30
365A 0229−141 1	2 31 30.81	−13 54 13.7 J	191	335			−1.04 0.06 ehl	uv	P	3.9	29
408A 0230−102 1	2 33 21.72	−10 0 28.4 J	122	395		−1.14 0.02	−1.34 0.06 bghkl	v	D	5.5	149
0230−102 2	2 33 21.54	−10 0 23.9	65								
365A 0233+159 1	2 36 26.91	16 8 54.8 J	43	256	0.66		−0.85 0.03 ehijlnopq	r	D	29.4	49
0233+159 2	2 36 28.42	16 9 14.2	14								
178 0238−018 1	2 40 54.52	−1 38 25.5 J	10	103	0.31		−1.06 0.09 djlmpq	*b	D	40.1	161
0238−018 2	2 40 53.69	−1 37 48.4	7								
365A 0241+348 1	2 44 33.94	35 1 31.4 J	143	191	1.26		−1.20 0.05 eijlnopq	r	D	6.3	13
0241+348 2	2 44 34.04	35 1 37.2	27								
365B 0245+013 1	2 45 12.25	1 18 48.4 B	122	251	1.04		−1.22 0.06 ejlnopq		D	13.6	47
0245+013 2	2 45 12.91	1 18 57.6	82								
365A 0247+044 1	2 49 39.92	4 40 28.7 J	286	368	0.77		−0.77 0.04 ehijlnopq	r	D	3.3	167
0247+044 2	2 49 39.98	4 40 25.6	28								
365B 0251+008 1	2 51 7.01	0 48 27.4 B	57	450	0.89		−1.16 0.03 ejlnopq		D	20.8	25
0251+008 2	2 51 7.59	0 48 46.4	179								
365A 0253+365 1	2 56 11.85	36 42 19.5 J	164	202	1.55		−0.96 0.09 eijlnopq	r	P	1.7	159
365B 0254+151 1	2 54 36.55	15 6 31.2 B	71	92	0.79		−1.19 0.11 ejln	x	P	2.0	117
408A 0254−236 1	2 56 14.37	−23 25 7.7 J	33	984		−1.17 0.02	−1.17 0.05 bghklmr	v	D	34.9	34
0254−236 2	2 56 15.63	−23 24 39.1	80								
365A 0255+114 1	2 58 20.64	11 36 50.9 J	22	195	0.46		−0.78 0.03 ehijlnopq	r	D	14.0	73
0255+114 2	2 58 19.72	11 36 47.2	42								
365A 0256+324 1	2 59 55.75	32 37 39.5 J	62	233	0.80		−1.06 0.03 eijlnopq	r	D	6.3	70
0256+324 2	2 59 55.30	32 37 37.4	103								
365A 0300+187 1	3 3 1.76	18 54 28.0 J	162	208	0.96		−1.04 0.04 eijlnopq	r	P	< 1.5	
365A 0301+080 1	3 4 4.14	8 17 18.9 J	83	189	0.81		−1.18 0.05 ehijlnopq	r	D	3.7	56
0301+080 2	3 4 4.32	8 17 20.8	105								
365B 0309+049 1	3 9 9.89	4 56 47.3 B	34	451	0.95		−1.17 0.03 ejlnopq	*g	P	1.6	150
178 0309−047 1	3 11 36.84	−4 34 42.3 J	14	300	0.59		−1.06 0.09 dhjlmr	*z	D	22.8	127
0309−047 2	3 11 34.50	−4 34 14.7	8								
0309−047 A	3 11 53.20	−4 38 27.1	8								
365A 0309−260 1	3 11 46.94	−25 53 26.0 J	5	300			−0.93 0.08 ehl	uv	DF	18.0	53
0309−260 2	3 11 47.86	−25 53 14.4	3								
365B 0310+051 1	3 10 48.23	5 5 59.5 B	28	89			−1.18 0.07 eln	uvx	T	14.5	135
0310+051 2c	3 10 47.94	5 6 2.7	3								
0310+051 3	3 10 47.56	5 6 9.7	15								
408A 0315−146 1	3 17 28.82	−14 30 51.7 J	102	534		−1.10 0.02	−1.24 0.04 bghklmr	v	D	27.2	134
0315−146 2	3 17 27.52	−14 30 32.7	119								
365A 0318−083 1	3 21 5.15	−8 12 53.9 J	38	286			−1.11 0.07 ehl	uv	T	21.3	70
0318−083 2c	3 21 4.23	−8 12 57.3	19								
0318−083 3	3 21 3.85	−8 13 1.0	115								
365A 0321+045 1	3 24 7.22	4 41 58.2 J	22	260	0.80		−1.08 0.03 ehijlnopq	r	M	8.8	24
0321+045 2	3 24 7.34	4 42 0.3	110								
0321+045 3	3 24 7.32	4 42 3.3	20								
408A 0324−228 1	3 27 4.68	−22 39 47.2 J	86	432			−1.28 0.05 ghlmr	v	D	9.6	160
0324−228 2	3 27 4.43	−22 39 38.6	277								
365A 0325−096 1	3 27 50.91	−9 29 17.3 J	150	199			−1.31 0.07 ehl	uv	P	2.2	77
365A 0327+241 1	3 29 59.23	24 16 41.5 J	41	133	0.21		−0.64 0.06 eijlnopq	r	DF	1.8	122
178 0328+248 1	3 31 6.65	24 58 45.7 J	142	290	1.05	−0.76 0.10	−1.20 0.03 bdijklmnopq		D	6.3	87
0328+248 2	3 31 6.22	24 58 45.7	81								
365A 0336+123 1	3 39 3.91	12 29 32.6 J	185	361	0.92		−0.79 0.03 ehijlnopq	r	D	3.7	71
0336+123 2	3 39 4.12	12 29 33.7	113								
408A 0338−093 1	3 41 7.56	−9 11 28.4 J	155	305			−1.13 0.06 ghlm	v	P	2.5	4
365A 0338−259 1	3 40 40.47	−25 47 35.6 J	16	243			−1.15 0.07 ehl	uv	T	20.2	100
0338−259 2c	3 40 39.70	−25 47 34.1	9								
0338−259 3	3 40 39.05	−25 47 31.8	45								
365A 0346−063 1	3 49 7.30	−6 10 54.6 J	57	287			−1.28 0.07 ehl	uv	T	9.9	152
0346−063 2c	3 49 7.16	−6 10 50.5	24								
0346−063 3	3 49 7.00	−6 10 45.9	34								
408A 0346−130 1	3 48 44.52	−12 55 6.4 J	286	506			−1.23 0.05 ghlmr	v	D	18.4	72
0346−130 2	3 48 43.36	−12 55 11.8	14								
365A 0348+013 1	3 50 57.33	1 31 2.3 J	21	147	1.09		−1.23 0.07 ehijlnopq	*gr	D	4.8	15
0348+013 2	3 50 57.43	1 31 6.6	17								

© European Southern Observatory • Provided by the NASA Astrophysics Data System

1994A&AS..108...79R

Appendix A. continued

Source	R.A. (h m s)	Decl (° ′ ″)		S_{peak} mJy	S_{int} mJy	$\frac{S^{VLA}_{int}}{S_{GB}}$	α_l	$\Delta\alpha_l$	α_h	$\Delta\alpha_h$			R ″	PA °
(1) (2) (3)	(4)		(5)	(6)	(7)	(8)	(9)	(10)	(11)	(12)	(13)	(14)	(15)	(16)	(17)
178 0348+175 1	3 51 15.27	17 43 16.4	J	7	157	0.34			−1.17	0.03	dghjlmopq		DF	16.5	75
0348+175 2	3 51 14.05	17 43 11.6		7											
178 0350+038 1	3 52 45.87	3 58 14.9	J	17	273	0.50			−0.89	0.08	djlmopq		D	4.8	85
0350+038 2	3 52 45.58	3 58 14.6		125											
365B 0353+106 1	3 53 45.67	10 39 22.3	B	17	202	0.74			−1.20	0.07	ejlnopq		D	25.7	76
0353+106 2	3 53 47.36	10 39 27.8		32											
365A 0355−037 1	3 57 48.31	−3 34 11.4	J	49	188	1.14			−1.43	0.08	ehjl	r	D	11.8	120
0355−037 2	3 57 47.64	−3 34 5.6		91											
365A 0357−112 1	4 0 4.49	−11 8 32.1	J	68	269				−0.97	0.07	ehl	uv	D	2.6	22
0357−112 2	4 0 4.54	−11 8 30.0		175											
365B 0400+020 1	4 0 33.45	2 3 16.4	B	104	158				−1.23	0.04	eln	uvx	P	3.4	71
365B 0400+020 1	4 0 33.45	2 3 16.4	B	104	158				−1.23	0.04	eln	uvx	P	3.4	71
365A 0403+036 1	4 5 54.82	3 49 32.2	J	69	192	0.57			−1.19	0.08	ehijlnopq	r	D	3.7	168
0403+036 2	4 5 54.77	3 49 35.8		102											
365AB 0405+125 1	4 5 49.68	12 32 25.5	B	26	299	0.99			−1.21	0.04	ehijlnopq		P	< 1.5	
365A 0407+090 1	4 10 16.13	9 13 20.0	J	22	141	0.53			−1.22	0.07	ehijlnopq	r	D	6.3	50
0407+090 2	4 10 16.43	9 13 23.7		48											
408A 0410−198 1	4 12 29.04	−19 42 13.6	J	56	303				−1.12	0.09	ghlmr	v	DF	9.2	31
0410−198 2	4 12 29.37	−19 42 6.0		28											
365A 0414+160 1	4 17 6.70	16 7 35.6	J	29	240	0.59			−0.81	0.03	ehijlnopq	r	DF	27.2	11
0414+160 2	4 17 6.73	16 7 40.5		7											
0414+160 3	4 17 7.04	16 8 2.2		21											
365A 0415−115 1	4 17 48.07	−11 25 59.9	J	57	285				−1.08	0.06	ehl	uv	D	5.9	143
0415−115 2	4 17 47.84	−11 25 55.2		162											
365A 0417−181 1	4 19 43.69	−18 1 55.1	J	145	273				−1.26	0.06	ehl	uv	D	3.7	168
0417−181 2	4 19 43.64	−18 1 51.7		97											
38B 0421+600 1	4 21 51.85	60 4 17.7	B	58	112		−1.17	0.05	−1.00	0.05	aelnop	uvw	D	23.9	5
0421+600 2	4 21 52.14	60 4 41.5		12											
38C 0423+614 1	4 23 12.79	61 26 50.3	B	73	100	0.28	−0.72	0.05	−1.27	0.15	ajlopq	*a	P	3.3	40
365A 0424+027 1	4 26 42.15	2 54 21.7	J	13	177	1.20			−1.14	0.07	ehijlnopq	r	T	11.4	155
0424+027 2c	4 26 42.20	2 54 26.4		40											
0424+027 3	4 26 41.84	2 54 33.9		21											
178 0428−037 1	4 30 29.78	−3 40 34.1	J	29	165	0.40			−1.12	0.12	dghjlm	*b	D	13.6	48
0428−037 2	4 30 30.46	−3 40 25.0		51											
365B 0429+194 1	4 29 6.85	19 25 6.4	B	37	111	0.45			−1.23	0.20	ejln	*bx	D	14.3	84
0429+194 2	4 29 5.85	19 25 4.8		32											
365A 0429−267 1	4 31 59.41	−26 38 12.3	J	203	326				−1.10	0.06	ehl	uv	D	7.0	27
0429−267 2	4 31 59.63	−26 38 6.3		58											
38B 0440+604 1	4 40 47.88	60 24 37.9	B	6	64		−1.04	0.05	−1.09	0.05	aelnp	uvx	D	20.0	121
0440+604 2	4 40 47.91	60 24 43.2		3											
0440+604 3	4 40 45.67	60 24 48.1		28											
365A 0447−164 1	4 50 8.00	−16 24 52.9	J	80	223				−1.27	0.06	ehl	uv	D	19.1	116
0447−164 2	4 50 6.83	−16 24 44.5		80											
365A 0447−230 1	4 49 10.30	−22 58 57.7	J	30	314				−0.97	0.10	ehl	uv	P	< 1.5	
365B 0448+091 1	4 48 31.15	9 9 25.0	B	35	129	0.44			−1.30	0.19	ejln	*bx	D	22.4	112
0448+091 2	4 48 29.76	9 9 33.2		29											
365A 0449−082 1	4 52 19.76	−8 11 44.2	J	207	350				−1.07	0.06	ehl	uv	D	2.2	23
0449−082 2	4 52 19.80	−8 11 42.4		148											
178 0451+005 1	4 53 49.65	0 40 36.4	J	12	166	0.57			−1.08	0.05	dghijlmnopq		D	16.5	174
0451+005 2	4 53 49.52	0 40 52.6		14											

Source	R.A. (h m s)	Decl (° ′ ″)		S_{peak} mJy	S_{int} mJy	$\frac{S^{VLA}_{int}}{S_{GB}}$	α_l	$\Delta\alpha_l$	α_h	$\Delta\alpha_h$			R ″	PA °
(1) (2) (3)	(4)		(5)	(6)	(7)	(8)	(9)	(10)	(11)	(12)	(13)	(14)	(15)	(16)	(17)
408A 0515−096 1	5 18 4.90	−9 37 1.9	J	33	316				−1.53	0.17	gkl	v	P	< 1.5	
365A 0523−163 1	5 26 5.99	−16 19 54.5	J	107	368				−1.05	0.06	ehl	uv	D	17.3	150
0523−163 2	5 26 5.40	−16 19 39.6		145											
365A 0524−234 1	5 26 35.00	−23 26 7.2	J	123	402				−0.93	0.07	ehl	uv	D	5.5	42
0524−234 2	5 26 34.72	−23 26 11.2		109											
365A 0527+008 1	5 30 18.79	0 52 14.4	J	33	173	0.61			−1.14	0.05	ehijlno	*frw	D	27.9	65
0527+008 2	5 30 17.14	0 52 2.9		5											
365A 0545−089 1	5 47 30.39	−8 57 55.8	J	85	213				−1.24	0.07	ehl	uv	T	13.2	100
0545−089 2c	5 47 29.91	−8 57 55.3		9											
0545−089 3	5 47 29.52	−8 57 53.3		63											
365A 0548−150 1	5 51 13.10	−15 0 5.3	J	62	276				−1.03	0.09	ehl	uv	D	25.4	109
0548−150 2	5 51 11.46	−14 59 56.8		22											
408B 0548−322 1	5 50 40.59	−32 16 16.5	J	74	144				−1.69	0.09	hl	v	DF	9.9	144
365A 0608−225 1	6 10 55.85	−22 36 43.3	J	278	487				−0.84	0.06	ehl	uv	D	3.3	3
0608−225 2	6 10 55.86	−22 36 40.3		74											
365A 0645+433 1	6 49 15.22	43 15 51.8	J	62	143	1.06			−1.09	0.05	eijlnopq	r	D	3.7	8
0645+433 2	6 49 15.26	43 15 55.2		37											
38A 0707+810 1	7 8 2.62	81 3 23.4	B	7	23		−1.62	0.10	−1.11	0.05	acl	v	D	28.0	26
0707+810 2	7 8 12.96	81 3 46.9		2											
0707+810 A	7 7 38.08	81 1 2.0		7											
365A 0710+346 1	7 13 39.74	34 31 29.2	J	89	199	0.62			−0.77	0.04	eijlnopq	r	DF	1.8	136
365A 0711+397 1	7 15 18.00	39 39 55.2	J	135	192	0.78			−1.26	0.08	eijlnopq	*fr	P	3.0	77
38A 0713+823 1	7 13 49.01	82 19 57.8	B	8	28		−1.45	0.11	−0.99	0.05	acl	v	D	30.0	125
0713+823 2	7 13 37.03	82 20 15.2		3											
365B 0725+191 1	7 25 14.42	19 8 19.8	B	165	202	0.75			−1.29	0.03	ejlnopq		D	4.2	56
0725+191 2	7 25 14.66	19 8 22.1		8											
365A 0726+282 1	7 29 44.92	28 9 27.7	J	39	234	0.75			−0.92	0.04	eijlnopq	r	T	17.6	150
0726+282 2c	7 29 44.54	28 9 35.0		12											
0726+282 3	7 29 44.28	28 9 42.8		15											
365A 0731+317 1	7 34 12.39	31 38 41.3	J	31	250	0.87			−1.22	0.03	eijlnopq	r	T	10.3	101
0731+317 2c	7 34 11.93	31 38 42.6		9											
0731+317 3	7 34 11.55	31 38 43.2		144											
38B 0732+625 1	7 32 39.24	62 35 36.3	B	9	54	0.31	−1.12	0.05	−0.99	0.13	aejlnopq	*b	DF	12.0	100
38B 0734+620 1	7 34 23.58	62 2 29.9	B	40	95		−1.04	0.05	−1.12	0.06	aelnp	uvx	D	8.0	37
0734+620 2	7 34 24.27	62 2 36.2		16											
365A 0736+167 1	7 39 24.90	16 35 6.4	J	70	356	1.06			−1.18	0.03	ehjlopq	r	D	4.4	18
0736+167 2	7 39 25.00	16 35 10.3		235											
38B 0739+641 1	7 39 47.55	64 8 50.2	B	46	137	1.05	−1.09	0.05	−1.00	0.05	aejlnopq		D	9.8	15
0739+641 2	7 39 47.93	64 8 59.6		32											
365B 0748+134 1	7 48 13.68	13 26 57.1	B	16	134	0.78			−1.46	0.09	ejln	rx	D	13.2	153
0748+134 2	7 48 13.27	13 27 8.8		51											
365A 0749+379 1	7 52 29.22	37 50 44.6	J	31	245	0.72			−0.89	0.03	eijlnopq	r	T	28.7	144
0749+379 2c	7 52 28.56	37 50 53.6		7											
0749+379 3	7 52 28.06	37 50 59.6		18											
0749+379 4	7 52 27.95	37 51 11.1		9											
365A 0752+342 1	7 55 49.26	34 8 0.3	J	6	185	1.18			−1.17	0.07	eijlnopq	r	D	18.4	15
0752+342 2	7 55 49.62	34 8 18.1		176											
365A 0759+347 1	8 2 13.87	34 35 25.3	J	160	229	1.01			−1.00	0.03	eijlnopq	r	D	5.9	51
0759+347 2	8 2 14.23	34 35 29.0		19											
365B 0801+197 1	8 1 59.07	19 47 12.9	B	87	167	1.31			−1.19	0.07	ejlnopq		P	4.3	130

© European Southern Observatory • Provided by the NASA Astrophysics Data System

© European Southern Observatory • Provided by the NASA Astrophysics Data System

1994A&AS..108...79R

Appendix A. continued

Source	R.A.	Decl	S_{peak}	S_{int}	$\frac{S^{VLA}_{int}}{S_{GB}}$	α_l $\Delta\alpha_l$	α_h $\Delta\alpha_h$		R	PA
	h m s	° ′ ″	mJy	mJy					″	°
(1) (2) (3)	(4)	(5)	(6)	(7)	(8)	(9) (10)	(11) (12) (13)	(14)	(15)	(16) (17)
365A 0801+364 1	8 5 4.54	36 19 9.2 J	47	219	0.79		−0.87 0.03 eijlnopq	*cdr	D	9.9 130
0801+364 2	8 5 3.92	36 19 15.5	131							
365A 0816+367 1	8 20 8.84	36 36 11.5 J	179	205	0.64		−1.16 0.04 eijlnopq	*afqr	P	< 1.5
178 0819+024 1	8 22 6.56	2 17 46.3 J	48	161	0.74		−1.12 0.05 dijlmnopq		D	18.0 122
0819+024 2	8 22 5.58	2 17 55.6	34							
38B 0819+672 1	8 19 12.64	67 12 54.8 B	28	104	0.77	−1.08 0.05	−1.09 0.05 aejlnopq		T	26.4 86
0819+672 2c	8 19 9.43	67 12 51.5	5							
0819+672 3	8 19 8.25	67 12 53.1	5							
365A 0820+367 1	8 23 48.63	36 32 30.0 J	41	219	1.03		−1.18 0.04 eijlnopq	r	D	22.8 155
0820+367 2	8 23 47.83	36 32 51.0	99							
38A 38C 0821+695 1	8 21 1.85	69 30 25.8 B	6	8		−1.04 0.08	−2.28 0.04 acl	v	P	2.0 168
38C 0825+648 1	8 24 56.71	64 50 22.7 B	12	26		−1.25 0.03	−1.25 0.03 al	v	D	4.6 82
0825+648 2	8 24 56.04	64 50 22.0	10							
365A 0827+321 1	8 30 30.26	32 0 43.7 J	176	273	1.12		−0.96 0.04 eijlnopq	r	D	10.7 160
0827+321 2	8 30 29.98	32 0 53.9	55							
365B 0828+193 1	8 28 0.78	19 23 18.6 B	37	72			−1.23 0.08 eln	uvx	T	11.8 46
0828+193 2c	8 28 1.10	19 23 23.8	10							
0828+193 3	8 28 1.37	19 23 26.7	24							
408A 0832−076 1	8 35 5.80	−7 47 29.2 J	15	308		−1.36 0.02	−1.35 0.08 bghklm	v	DF	9.6 131
0832−076 2	8 35 5.22	−7 47 22.9	14							
38B 0833+654 1	8 33 20.98	65 24 3.1 B	187	1072	0.78	−1.11 0.05	−1.00 0.03 aejlnopq		T	35.1 93
0833+654 2c	8 33 18.12	65 24 4.2	29							
0833+654 3	8 33 16.08	65 24 6.2	183							
0833+654 4	8 33 15.41	65 24 5.0	89							
365A 0838+325 1	8 41 13.05	32 24 54.6 J	84	339	0.46		−0.46 0.07 eijlnopq	r	D	9.2 171
0838+325 2	8 41 12.93	32 25 3.5	43							
365A 0840+114 1	8 43 42.46	11 14 11.5 J	67	354	0.97		−0.97 0.03 ehijlnopq	r	D	12.9 172
0840+114 2	8 43 42.58	11 13 58.9	136							
365B 0841+159 1	8 41 8.29	15 58 33.9 B	375	621	0.96		−1.20 0.03 ejlnopq	r	D	7.6 159
0841+159 2	8 41 8.11	15 58 41.0	115							
365A 0843+136 1	8 45 47.09	13 28 57.8 J	27	370	0.78		−0.74 0.03 ehijlnopq	r	P	2.6 75
178 0846−039 1	8 49 0.87	−4 5 37.8 J	88	245	1.12		−1.25 0.04 dghjlm		D	12.5 169
0846−039 2	8 49 0.72	−4 5 25.5	106							
365A 0847+379 1	8 50 25.15	37 46 46.5 J	12	250	0.41		−0.52 0.03 eijlnopq	r	T	29.4 170
0847+379 2c	8 50 24.72	37 47 9.4	133							
0847+379 3	8 50 24.74	37 47 13.2	12							
0847+379 4	8 50 24.75	37 47 16.0	8							
0847+379 5	8 50 24.63	37 47 23.9	8							
365A 0848+345 1	8 51 8.27	34 19 25.6 J	122	313	0.87		−1.08 0.06 eijlnopq	r	D	3.7 87
0848+345 2	8 51 7.99	34 19 25.4	111							
151I 0848+424 1	8 48 5.61	42 24 6.5 B	66	162	1.12		−1.03 0.03 cejlnopq		D	4.7 10
0848+424 2	8 48 5.69	42 24 11.0	13							
151I 0849+469 1	8 49 43.43	46 58 21.8 B	181	325	1.00		−1.05 0.02 cejlnopq		P	3.9 46
365B 0850+140 1	8 50 23.09	14 4 18.6 B	1215	2169	0.86		−1.19 0.04 ejlnopq		D	11.6 78
0850+140 2	8 50 22.34	14 4 16.4	213							
365A 0850+331 1	8 53 21.08	32 55 0.7 J	236	423	0.91		−0.69 0.03 eijlnopq	r	P	3.2 170
38A 0851+717 1	8 51 20.50	71 44 34.6 B	2	17		−1.25 0.10	−1.35 0.04 acln	v	T	22.0 2
0851+717 2c	8 51 20.10	71 44 47.1	2							
0851+717 3	8 51 20.71	71 44 55.6	2							
178 0854+038 1	8 56 59.75	3 37 41.9 J	81	258	0.88		−1.09 0.03 dghijlmnopq		D	61.8 83

Source	R.A.	Decl	S_{peak}	S_{int}	$\frac{S^{VLA}_{int}}{S_{GB}}$	α_l $\Delta\alpha_l$	α_h $\Delta\alpha_h$		R	PA
	h m s	° ′ ″	mJy	mJy					″	°
(1) (2) (3)	(4)	(5)	(6)	(7)	(8)	(9) (10)	(11) (12) (13)	(14)	(15)	(16) (17)
151I 0855+411 1	8 55 7.58	41 8 45.2 B	84	208	0.95		−1.04 0.03 cejlnopq		D	1.8 19
0855+411 2	8 55 7.64	41 8 46.9	95							
178 0857+036 1	9 0 14.32	3 24 7.6 J	143	175	1.23		−1.25 0.05 dghjlm		D	4.0 40
0857+036 2	9 0 14.47	3 24 10.8	20							
38C 0900+627 1	9 0 27.39	62 44 58.2 B	7	72		−1.07 0.03	−1.07 0.03 al	v	D	71.5 36
0900+627 2	9 0 21.12	62 43 59.7	9							
365A 0902−123 1	9 4 25.83	−12 32 46.3 J	24	290			−1.18 0.06 ehl	uv	D	19.1 7
0902−123 2	9 4 25.75	−12 32 43.2	21							
0902−123 3	9 4 26.08	−12 32 31.1	9							
0902−123 4	9 4 25.98	−12 32 27.1	61							
365A 0903+153 1	9 5 57.63	15 7 47.1 J	33	325	0.84		−1.01 0.04 ehijlnopq	r	P	< 1.5
151I 0903+428 1	9 3 9.42	42 51 5.6 B	40	265	0.58		−1.01 0.05 cejlnop	*buw	D	6.1 50
0903+428 2	9 3 9.83	42 51 9.5	77							
151I 0905+399 1	9 5 1.26	39 55 37.4 B	35	207	0.89		−1.22 0.04 cejlnopq		D	108 104
0905+399 2	9 5 10.40	39 55 12.0	12							
38A 0906+691 1	9 5 57.04	69 11 40.0 B	2	26		−1.18 0.09	−1.34 0.04 acln	v	DF	120 130
151I 0908+380 1	9 8 54.84	38 3 48.0 B	90	968	0.82		−1.10 0.02 cejlnopq		D	18.4 127
0908+380 2	9 8 53.32	38 4 0.1	80							
38A 0908+712 1	9 8 33.06	71 14 11.0 B	22	74		−1.03 0.09	−1.01 0.03 acl	v	D	10.0 8
0908+712 2	9 8 33.29	71 14 20.7	10							
151I 0910+486 1	9 10 37.58	48 39 54.4 B	5	116	0.63		−1.28 0.03 cejlnopq		DF	36.1 104
0910+486 2	9 10 35.08	48 40 4.1	3							
408A 0912−132 1	9 14 44.44	−13 29 31.6 J	178	544			−1.10 0.03 ghklmr	v	T	8.1 85
0912−132 2c	9 14 44.25	−13 29 32.0	29							
0912−132 3	9 14 43.90	−13 29 32.2	241							
408A 0912−163 1	9 15 14.66	−16 30 47.0 J	66	783			−1.19 0.12 ghklm	v	P	2.0 23
178 0915+025 1	9 17 42.05	2 19 12.7 J	36	115	0.76		−1.06 0.10 djlmopq		D	4.8 160
0915+025 2	9 17 41.94	2 19 17.1	37							
365A 0924−134 1	9 26 41.65	−13 40 15.5 J	168	302			−1.17 0.06 ehl	uv	D	21.7 145
0924−134 2	9 26 40.82	−13 39 57.9	6							
151I 0925+419 1	9 25 11.37	41 55 29.5 B	52	90			−1.11 0.05 celn	uvx	P	1.8 28
178 0927+064 1	9 30 16.83	6 15 24.9 J	15	198	0.68		−1.18 0.03 dghijlmnopq		D	81.6 161
0927+064 2	9 30 14.48	6 16 35.8	3							
151I 0928+420 1	9 28 28.30	42 2 59.8 B	73	120	0.88		−1.26 0.04 cejlnopq		P	3.7 176
178 0933+045 1	9 36 32.02	4 22 10.1 J	76	861	1.12	−0.78 0.10	−1.41 0.03 bdghijklmnopqr		P	< 1.5
365A 0933+276 1	9 36 36.44	27 25 35.1 J	92	309	0.84		−0.89 0.03 eijlnopq	r	T	7.7 160
0933+276 2c	9 36 36.25	27 25 42.1	12							
0933+276 3	9 36 35.67	27 25 58.7	3							
151I 0933+430 1	9 33 42.97	43 2 34.9 B	10	136	0.82		−1.04 0.03 cejlnopq		D	32.2 149
0933+430 2	9 33 41.46	43 3 2.0	53							
38B 0935+607 1	9 35 49.62	60 47 37.9 B	39	106		−1.07 0.05	−1.08 0.05 aelnop	uvw	D	46.9 49
0935+607 2	9 35 54.44	60 48 9.0	19							
365A 0940−287 1	9 42 28.81	−28 59 42.4 J	209	309			−0.98 0.07 ehl	uv	D	4.0 180
0940−287 2	9 42 28.82	−28 59 38.7	61							
151I 0942+425 1	9 42 52.94	42 32 17.3 B	10	154	0.90		−1.05 0.03 cejlnopq		D	29.3 106
0942+425 2	9 42 50.42	42 32 25.0	33							
38A 38B 0942+676 1	9 42 39.97	67 40 33.6 B	6	70		−1.31 0.08	−1.48 0.06 aceln	uv	DF	34.0 116
365A 0943−109 1	9 45 35.15	−11 11 11.2 J	165	338			−1.08 0.06 ehl	uv	D	16.5 133
0943−109 2	9 45 34.36	−11 10 59.9	83							
365A 0943−242 1	9 45 32.61	−24 28 50.1 J	45	245			−1.20 0.08 ehl	uv	D	3.7 74

1994A&AS..108...79R

Appendix A. continued

Source	R.A. h m s	Decl ° ′ ″		S_{peak} mJy	S_{int} mJy	$\frac{S^{VLA}_{int}}{S_{GB}}$	α_l	$\Delta\alpha_l$	α_h	$\Delta\alpha_h$			R ″	PA °
(1) (2) (3)	(4)		(5)	(6)	(7)	(8)	(9)	(10)	(11)	(12)	(13)	(14)	(15)	(16)	(17)
0943−242 2	9 45 32.86	−24 28 49.2		176											
408A 0945+003 1	9 47 44.53	0 4 36.5	J	504	783	0.89	−0.66	0.05	−1.11	0.02	bghijklmnopqr		D	3.7	2
0945+003 2	9 47 44.53	0 4 39.9		212											
38C 0945+633 1	9 44 54.69	63 19 38.2	B	33	77		−1.28	0.03	−1.28	0.03	al	v	D	5.4	132
0945+633 2	9 44 54.35	63 19 40.4		23											
365A 0945−111 1	9 48 5.86	−11 21 24.8	J	266	329				−1.02	0.06	ehl	uv	D	3.3	67
0945−111 2	9 48 5.66	−11 21 25.9		13											
408A 0946−182 1	9 48 44.18	−18 28 30.0	J	138	435		−1.19	0.02	−1.13	0.08	bghklmr	v	D	23.5	143
0946−182 2	9 48 43.23	−18 28 11.4		117											
151I 0949+448 1	9 49 29.55	44 53 54.8	B	39	94				−1.03	0.03	celnp	uvx	D	3.3	146
0949+448 2	9 49 29.38	44 53 57.3		17											
151I 0949+499 1	9 49 31.57	49 59 49.2	B	89	139				−1.07	0.03	celnop	uvw	D	10.7	11
0949+499 2	9 49 31.80	49 59 59.6		25											
38A 0950+708 1	9 50 6.33	70 48 52.2	B	5	130		−1.01	0.08	−1.08	0.03	aclnop	vw	T	54.0	149
0950+708 2c	9 50 4.06	70 49 6.5		3											
0950+708 3	9 50 0.21	70 49 37.0		5											
365A 0950−111 1	9 52 56.64	−11 21 53.9	J	61	313				−0.98	0.07	ehl	uv	D	8.5	94
0950−111 2	9 52 56.16	−11 21 52.3		47											
178 0951+009 1	9 54 23.79	0 43 52.0	J	25	236	0.77			−1.11	0.04	dghjlmopq		D	5.9	67
0951+009 2	9 54 23.51	0 43 49.2		75											
151I 0952+456 1	9 52 21.63	45 40 30.4	B	39	120	0.69			−1.04	0.03	cejlnopq		D	29.1	142
0952+456 2	9 52 19.95	45 40 53.0		11											
151I 0956+475 1	9 56 7.98	47 35 34.9	B	132	431				−1.25	0.03	celnop	uvw	D	5.6	2
0956+475 2	9 56 8.01	47 35 40.4		107											
151I 1001+425 1	10 1 20.86	42 33 52.1	B	15	77				−1.14	0.04	celn	uvx	D	2.5	131
1001+425 2	10 1 20.70	42 33 53.5		48											
365A 1007+376 1	10 10 10.10	37 23 53.6	J	21	228	0.93			−0.98	0.04	eijlnopq	r	D	22.8	133
1007+376 2	10 10 8.74	37 24 9.3		81											
151I 1009+434 1	10 9 6.96	43 27 53.7	B	79	165	0.98			−1.22	0.03	cejlnopq		T	11.2	28
1009+434 2c	10 9 7.07	43 27 56.7		18											
1009+434 3	10 9 7.46	43 28 3.6		6											
365A 1010+337 1	10 13 0.57	33 27 54.3	J	166	204	0.79			−0.86	0.03	eijlnopq	r	P	1.8	124
365A 1010−116 1	10 12 41.69	−11 56 0.7	J	23	284				−1.20	0.07	ehl	uv	D	35.7	55
1010−116 2	10 12 43.67	−11 55 40.0		34											
151I 1012+425 1	10 12 30.75	42 34 38.6	B	54	239	0.99			−1.08	0.03	cejlnopq		D	22.6	49
1012+425 2	10 12 32.31	42 34 53.5		33											
151I 1014+420 1	10 14 12.57	42 0 27.0	B	30	88	0.73			−1.05	0.04	cejln	x	DF	19.0	48
365A 1015+187 1	10 17 46.39	18 32 31.0	J	228	289	1.00			−1.04	0.04	ehijlnopq		P	2.0	5
365A 1015−047 1	10 17 59.49	−4 58 40.7	J	56	275	0.77			−0.86	0.07	ehjl	r	D	15.1	178
1015−047 2	10 17 59.45	−4 58 25.8		91											
365A 1017+372 1	10 20 39.70	36 56 58.7	J	79	324	0.90			−1.06	0.03	eijlnopq	r	D	7.4	47
1017+372 2	10 20 40.14	36 57 3.7		190											
365A 1021−217 1	10 23 45.60	−21 58 31.6	J	110	292				−1.06	0.06	ehl	uv	D	4.0	177
1021−217 2	10 23 45.59	−21 58 27.8		124											
38A 1022+625 1	10 22 45.77	62 35 15.8	B	3	31		−1.23	0.09	−1.23	0.04	acln	v	DF	39.0	124
1022+625 2	10 22 41.49	62 35 35.3		3											
408A 1022−186 1	10 25 16.88	−18 51 13.9	J	88	384				−1.18	0.05	ghlm	v	D	6.6	160
1022−186 2	10 25 16.73	−18 51 7.7		163											
38C 1024+721 1	10 24 38.74	72 10 45.1	B	8	41		−1.13	0.03	−1.13	0.03	al	v	D	50.8	176
1024+721 2	10 24 38.28	72 10 52.4		3											
1024+721 3	10 24 37.89	72 11 36.4		5											
365A 1025−293 1	10 28 2.72	−29 37 8.4	J	73	360				−1.08	0.06	ehl	uv	DF	7.0	126
365A 1028−111 1	10 30 34.74	−11 25 35.7	J	46	321				−1.06	0.07	ehl	uv	D	14.3	59
1028−111 2	10 30 35.56	−11 25 28.5		179											
408B 1028−334 1	10 31 11.98	−33 39 30.6	J	48	496				−0.73	0.09	hl	v	P	< 1.5	
151I 1032+498 1	10 32 55.00	49 48 39.2	B	62	233	0.86			−1.03	0.02	cejlnopq		D	11.8	36
1032+498 2	10 32 55.70	49 48 48.8		95											
38A 1032+706 1	10 32 56.22	70 40 21.8	B	9	53		−1.15	0.08	−1.21	0.03	acln	v	D	12.0	90
1032+706 2	10 32 54.44	70 40 21.9		8											
365A 1033−041 1	10 36 11.70	−4 23 59.8	J	140	242	0.97			−0.94	0.09	ehjl	r	P	3.9	100
365A 1035+208 1	10 38 42.46	20 35 40.9	J	161	229	0.81			−1.15	0.03	eijlnopq	r	P	3.2	4
151I 1035+486 1	10 35 18.38	48 41 22.5	B	24	198	0.84			−1.03	0.03	cejlnopq		DF	20.6	85
1035+486 2	10 35 16.33	48 41 20.5		37											
365A 1038+334 1	10 41 48.20	33 8 49.6	J	138	249	0.81			−1.16	0.03	eijlnopq	r	D	23.9	8
1038+334 2	10 41 48.46	33 9 12.9		21											
151I 1039+504 1	10 39 8.85	50 28 38.2	B	40	696	0.79			−1.12	0.03	cejlnopq		D	66.9	136
1039+504 2	10 39 4.48	50 29 26.3		57											
1039+504 3	10 39 4.04	50 29 26.0		221											
38A 1039+681 1	10 39 9.08	68 6 8.5	B	31	232	0.87	−1.03	0.08	−1.07	0.03	acjlnopq		D	15.0	74
1039+681 2	10 39 8.43	68 6 8.0		7											
1039+681 3	10 39 6.71	68 6 4.6		102											
365A 1040+317 1	10 43 19.04	31 30 50.6	J	9	242	0.31			−0.47	0.04	eijlnopq	r	DF	16.5	162
1040+317 2	10 43 18.65	31 31 6.0		29											
365A 1041+366 1	10 43 53.88	36 21 1.8	J	102	187	1.10			−1.07	0.04	eijlnopq	r	P	4.0	105
178 1042+109 1	10 44 43.48	10 38 18.0	J	34	119	0.89			−0.98	0.08	dijlmnopq		M	15.8	156
1042+109 2	10 44 43.07	10 38 32.3		15											
151I 1042+481 1	10 42 41.84	48 7 30.6	B	14	139	0.64			−1.00	0.04	cejlnopq		DF	28.7	72
1042+481 2	10 42 39.15	48 7 21.6		5											
365A 1043+372 1	10 46 11.91	36 58 43.1	J	66	228	0.87			−1.19	0.04	eijlnopq	r	D	3.7	178
1043+372 2	10 46 11.90	36 58 46.6		57											
408A 1043−216 1	10 45 30.87	−21 53 42.1	J	241	415				−1.15	0.04	ghlm	v	D	3.3	110
1043−216 2	10 45 30.66	−21 53 41.1		81											
178 1044−019 1	10 46 36.42	−2 13 25.5	J	37	99	0.75			−0.97	0.08	djlmpq		D	16.5	9
1044−019 2	10 46 36.74	−2 12 53.5		5											
365A 1045+340 1	10 48 12.64	33 47 43.7	J	168	256	0.96			−1.09	0.03	eijlnopq	r	D	14.7	111
1045+340 2	10 48 11.55	33 47 49.0		42											
38B 1046+679 1	10 46 40.56	67 55 22.5	B	11	51		−1.10	0.05	−1.18	0.05	aeln	uv	DF	10.0	163
365A 1052+380 1	10 55 44.55	37 46 0.8	J	150	184	0.96			−1.32	0.04	eijlnopq	r	P	< 1.5	
365A 1052−163 1	10 55 25.41	−16 35 2.4	J	20	251				−1.16	0.07	ehl	uv	D	7.0	49
1052−163 2	10 55 25.78	−16 34 57.7		203											
365A 1103−080 1	11 6 2.55	−8 18 51.4	J	127	232				−1.18	0.07	ehl	uv	D	11.8	77
1103−080 2	11 6 3.33	−8 18 48.9		27											
365A 1103−132 1	11 5 48.17	−13 31 22.3	J	30	318				−1.00	0.08	ehl	uv	P	< 1.5	
365A 1104+089 1	11 7 9.24	8 41 30.7	J	48	158	1.05			−1.21	0.05	ehijlnopq	u	M	10.7	43
1104+089 2	11 7 9.40	8 41 31.5		16											
1104+089 3	11 7 9.62	8 41 35.4		6											
1104+089 4	11 7 9.71	8 41 38.5		10											
38A 38B 1104+619 1	11 4 32.25	61 58 20.2	B	21	93		−1.10	0.08	−1.35	0.05	aceln	uv	D	23.0	151
1104+619 2	11 4 30.66	61 58 40.7		12											
408A 1107−227 1	11 9 50.72	−23 2 52.2	J	47	526		−1.17	0.02	−1.57	0.08	bghlm	v	DF	66.2	128

© European Southern Observatory • Provided by the NASA Astrophysics Data System

1994A&AS..108...79R

Appendix A. continued

Source	R.A. h m s	Decl ° ′ ″		S_{peak} mJy	S_{int} mJy	$\frac{S^{VLA}_{int}}{S_{GB}}$	α_l $\Delta\alpha_l$	α_h $\Delta\alpha_h$			R ″	PA °
(1) (2) (3)	(4)		(5)	(6)	(7)	(8)	(9) (10)	(11) (12) (13)	(14)	(15)	(16)	(17)
1107−227 2	11 9 46.82	−23 2 11.1		160								
408B 1111−317 1	11 14 0.42	−32 0 16.6	J	14	261			−1.21 0.09 hl	v	M	8.1	54
1111−317 2	11 14 0.91	−32 0 12.2		161								
365A 1113−178 1	11 16 14.72	−18 6 29.9	J	55	256			−1.19 0.06 ehl	uv	D	10.3	168
1113−178 2	11 16 14.59	−18 6 20.0		127								
408B 1116−320 1	11 19 17.68	−32 18 18.0	J	62	281			−1.16 0.09 hl	v	D	26.8	116
1116−320 2	11 19 15.81	−32 18 5.8		22								
365A 1119+173 1	11 21 40.46	17 6 14.9	J	72	171	0.99		−1.44 0.05 ehijln	rx	T	23.5	87
1119+173 2	11 21 40.08	17 6 15.4		4								
1119+173 3c	11 21 39.76	17 6 15.3		33								
1119+173 4	11 21 38.85	17 6 14.0		27								
151I 1123+441 1	11 23 7.12	44 8 0.3	B	73	78			−1.01 0.03 celn	uvx	P	< 1.5	
365A 1125+127 1	11 28 5.64	12 30 2.3	J	164	277	1.16		−1.13 0.04 ehijlnopq	r	D	4.4	105
1125+127 2	11 28 5.38	12 30 3.3		20								
365A 1126−175 1	11 28 34.51	−17 49 28.8	J	41	254			−1.15 0.07 ehl	uv	DF	9.9	140
1126−175 2	11 28 34.99	−17 49 35.6		21								
365A 1127+326 1	11 30 33.58	32 21 27.3	J	37	264	0.60		−1.03 0.05 eijlnopq	r	D	23.2	12
1127+326 2	11 30 33.95	32 21 49.9		38								
365A 1127+380 1	11 29 55.51	37 48 4.8	J	128	204	0.82		−0.98 0.03 eijlnopq	r	D	4.8	134
1127+380 2	11 29 55.24	37 48 7.9		15								
38A 1127+831 1	11 27 26.66	83 6 23.1	B	8	40		−1.31 0.10	−0.96 0.04 acln	v	T	29.0	162
1127+831 2c	11 27 23.38	83 6 41.0		1								
1127+831 3	11 27 21.78	83 6 50.1		2								
365A 1128−268 1	11 31 4.03	−27 5 18.7	J	119	285			−1.02 0.07 ehl	uv	D	7.0	104
1128−268 2	11 31 3.53	−27 5 17.1		71								
38A 1131+704 1	11 31 29.95	70 24 30.9	B	8	46		−1.21 0.09	−1.08 0.04 acl	v	DF	11.0	15
1131+704 2	11 31 30.10	70 24 33.7		6								
1131+704 3	11 31 30.36	70 24 40.9		9								
408A 1131−077 1	11 34 25.28	−8 0 24.9	J	42	351			−1.13 0.05 ghlm	v	D	14.3	71
1131−077 2	11 34 26.04	−8 0 21.4		89								
1131−077 3	11 34 26.21	−8 0 19.9		48								
408A 1131−269 1	11 33 31.56	−27 15 22.9	J	34	394			−1.35 0.05 ghlm	v	P	< 1.5	
365A 1132+112 1	11 35 21.30	10 56 17.0	J	69	202	0.83		−1.18 0.05 ehijlnopq	r	D	7.7	142
1132+112 2	11 35 20.98	10 56 22.8		19								
38C 1137+601 1	11 37 42.10	60 10 23.0	B	31	41		−1.09 0.03	−1.09 0.03 al	v	P	2.6	92
365A 1137−103 1	11 40 24.47	−10 37 36.0	J	113	306			−1.00 0.07 ehl	uv	M	7.0	36
1137−103 2	11 40 24.73	−10 37 30.3		22								
178 1138+234 1	11 41 35.75	23 9 5.5	J	43	411	0.81	−0.77 0.10	−1.12 0.02 bdijklmnopq		D	32.7	151
1138+234 2	11 41 34.62	23 9 34.2		104								
408A 1138−262 1	11 40 48.91	−26 29 8.8	J	199	728		−1.27 0.02	−1.30 0.03 bghklmr	v	D	11.4	87
1138−262 2	11 40 48.30	−26 29 8.2		27								
178 1139−025 1	11 42 9.40	−2 50 0.3	J	36	272	0.76		−1.09 0.04 dghjlm		D	20.6	18
1139−025 2	11 42 9.82	−2 49 40.9		65								
408A 1140−114 1	11 42 34.94	−11 41 48.5	J	879	300		−1.34 0.02	−1.17 0.19 bghklmr	v	D	4.0	74
1140−114 2	11 42 35.19	−11 41 47.5		109								
178 1142+010 1	11 45 8.31	0 43 28.8	J	82	291	0.74		−1.10 0.03 dghijlmno	*fw	D	11.8	135
1142+010 2	11 45 7.78	0 43 36.9		63								
408B 1142−341 1	11 45 20.36	−34 26 6.5	J	9	145			−1.65 0.09 hl	v	DF	19.5	135
1142−341 2c	11 45 20.17	−34 26 1.0		15								
1142−341 3	11 45 19.54	−34 25 57.8		5								

Source	R.A. h m s	Decl ° ′ ″		S_{peak} mJy	S_{int} mJy	$\frac{S^{VLA}_{int}}{S_{GB}}$	α_l $\Delta\alpha_l$	α_h $\Delta\alpha_h$			R ″	PA °
(1) (2) (3)	(4)		(5)	(6)	(7)	(8)	(9) (10)	(11) (12) (13)	(14)	(15)	(16)	(17)
151I 1146+507 1	11 46 33.53	50 47 56.6	B	42	87	0.66		−1.11 0.04 cejlnopq		T	14.5	87
1146+507 2c	11 46 33.19	50 47 55.4		18								
1146+507 3	11 46 32.03	50 47 56.0		6								
151I 1149+421 1	11 49 37.37	42 10 24.3	B	47	99			−1.07 0.03 celnop	uvw	D	3.8	21
1149+421 2	11 49 37.49	42 10 27.9		29								
365A 1150+041 1	11 53 30.29	3 54 34.0	J	118	277	0.80		−0.93 0.04 ehijlnopq	r	D	13.2	23
1150+041 2	11 53 30.62	3 54 46.2		92								
365A 1152+186 1	11 55 21.82	18 21 9.9	J	168	237	0.84		−1.42 0.08 ehijlnopq	r	D	4.4	51
1152+186 2	11 55 22.02	18 21 12.8		51								
365A 1152−245 1	11 54 54.51	−24 47 33.6	J	80	173			−1.27 0.08 ehl	uv	D	12.9	84
1152−245 2	11 54 53.55	−24 47 34.9		73								
408A 1154−011 1	11 57 10.90	−1 24 12.2	J	49	245	1.31		−1.11 0.06 ghjlm		D	2.6	47
1154−011 2	11 57 11.02	−1 24 10.4		111								
365A 1154−041 1	11 56 56.90	−4 26 35.6	J	55	210	0.95		−1.19 0.07 ejl	u	D	21.3	114
1154−041 2	11 56 55.61	−4 26 26.9		37								
365A 1155−067 1	11 58 11.93	−6 59 11.6	J	193	461			−0.86 0.07 ehl	uv	D	3.3	45
1155−067 2	11 58 12.08	−6 59 9.4		105								
365A 1158−275 1	12 1 9.68	−27 50 3.2	J	81	288			−1.03 0.09 ehl	uv	D	9.6	74
1158−275 2	12 1 10.37	−27 50 0.6		76								
365A 1201+060 1	12 4 3.47	5 47 25.7	J	44	431	0.84		−0.73 0.04 ehijlnopq	r	P	< 1.5	
365B 1201+167 1	12 1 46.97	16 47 29.0	B	41	107	0.34		−1.41 0.17 ejln	*bx	D	2.7	166
1201+167 2	12 1 46.93	16 47 31.7		39								
38A 1201+739 1	12 1 19.47	73 59 32.7	B	3	39		−1.03 0.09	−1.20 0.04 aclp	v	DF	46.0	30
1201+739 2c	12 1 15.51	73 59 10.0		3								
1201+739 3	12 1 14.09	73 58 52.0		1								
38A 1203+691 1	12 3 52.07	69 10 29.9	B	13	32		−1.24 0.10	−1.07 0.04 acl	v	DF	43.0	117
1203+691 2	12 3 44.90	69 10 49.3		1								
38A 1207+733 1	12 7 49.93	73 19 37.4	B	6	69		−0.89 0.09	−1.04 0.03 acl	v	DF	9.0	112
1207+733 2	12 7 48.02	73 19 41.2		16								
38A 1210+706 1	12 11 0.35	70 36 24.8	B	180	469	0.99	−0.85 0.08	−1.13 0.03 acjlopq		D	12.0	108
1210+706 2	12 10 58.02	70 36 28.4		135								
365A 1212+074 1	12 14 50.57	7 11 12.4	J	254	331	0.97		−0.91 0.04 ehijlnopq	r	P	2.6	49
408A 1213−147 1	12 16 30.81	−15 0 44.2	J	58	326			−1.18 0.05 ghlm	v	D	60.7	164
1213−147 2	12 16 29.64	−14 59 45.0		59								
365B 1216+108 1	12 16 40.18	10 49 44.5	B	18	193	0.90		−1.32 0.06 ejln	x	D	28.6	161
1216+108 2	12 16 39.53	10 50 11.2		26								
365A 1217−163 1	12 20 20.18	−16 38 7.3	J	8	258			−1.04 0.07 ehl	uv	D	20.6	32
1217−163 2	12 20 20.92	−16 37 50.5		44								
365A 1218−024 1	12 21 23.93	−2 41 49.5	J	187	393	0.44		−0.41 0.06 ehjl	r	DF	7.4	37
1218−024 2	12 21 23.66	−2 41 55.5		16								
365A 1218−123 1	12 21 23.24	−12 37 25.2	J	136	281			−1.18 0.06 ehl	uv	D	13.2	82
1218−123 2	12 21 24.11	−12 37 23.3		48								
151I 1219+438 1	12 19 47.56	43 52 23.3	B	28	126	1.07		−1.12 0.03 cejlno	w	T	11.9	138
1219+438 2c	12 19 47.16	43 52 28.5		2								
1219+438 3	12 19 46.81	43 52 32.3		75								
151I 1220+507 1	12 20 25.87	50 43 31.9	B	225	389	0.97		−1.27 0.04 cejlnopq		D	2.9	145
1220+507 2	12 20 25.70	50 43 34.3		50								
38A 1220+731 1	12 21 5.91	73 6 34.6	B	1	60		−1.08 0.09	−0.97 0.04 acl	v	DF	101	128
1220+731 2c	12 20 56.51	73 7 4.0		1								
1220+731 3	12 20 47.13	73 7 34.6		1								

© European Southern Observatory • Provided by the NASA Astrophysics Data System

1994A&AS..108...79R

Appendix A. continued

Source	R.A. (h m s)	Decl (° ′ ″)		S_{peak} mJy	S_{int} mJy	$\frac{S^{VLA}_{int}}{S_{GB}}$	α_l	$\Delta\alpha_l$	α_h	$\Delta\alpha_h$			R ″	PA °
(1) (2) (3)	(4)		(5)	(6)	(7)	(8)	(9)	(10)	(11)	(12)	(13)	(14)	(15)	(16)	(17)
365A 1221+113 1	12 24 19.82	11 7 23.3	J	263	329	0.93			−0.73	0.04	ehijlnopq	r	P	< 1.5	
38A 1223+639 1	12 23 34.25	63 56 38.3	B	4	60		−1.25	0.08	−1.09	0.03	acln	v	DF	15.0	96
1223+639 2	12 23 33.07	63 56 40.2		4											
408A 1226−105 1	12 28 41.66	−10 52 59.3	J	122	398				−1.15	0.05	ghlm	v	D	4.8	180
1226−105 2	12 28 41.67	−10 52 54.4		141											
38C 1227+609 1	12 27 13.53	60 58 14.0	B	8	54		−1.03	0.03	−1.03	0.03	al	v	D	84.6	134
1227+609 2	12 27 4.69	60 59 9.7		13											
1227+609 3	12 27 5.10	60 59 12.5		9											
365A 1228−166 1	12 30 53.39	−16 56 56.9	J	51	226				−1.21	0.10	ehl	uv	D	24.6	144
1228−166 2	12 30 52.40	−16 56 37.0		81											
365A 1231−293 1	12 33 38.75	−29 35 2.2	J	15	172				−1.26	0.08	ehl	uv	DF	30.5	103
1231−293 2	12 33 40.89	−29 35 11.9		7											
1231−293 3	12 33 41.01	−29 35 9.1		9											
365A 1234+132 1	12 36 38.65	12 58 45.4	J	6	99	0.27			−0.87	0.04	ehijlnopq	r	DF	50.0	114
1234+132 2c	12 36 38.02	12 58 51.5		6											
1234+132 3	12 36 36.92	12 58 56.3		7											
365A 1235+057 1	12 38 7.13	5 30 28.6	J	157	249	0.94			−1.06	0.05	ehijln	rx	D	3.3	119
1235+057 2	12 38 6.95	5 30 30.0		41											
178 1236+004 1	12 39 11.29	0 10 1.5	J	6	300	0.61			−0.91	0.15	djlm	*b	D	79.8	169
1236+004 2	12 39 10.33	0 11 20.6		13											
178 1237−030 1	12 39 38.96	−3 19 2.2	J	143	257	1.00			−1.27	0.04	dghjlm		P	3.3	35
365A 1238−273 1	12 41 27.16	−27 36 0.8	J	64	196				−1.22	0.10	ehl	uv	D	27.2	139
1238−273 2	12 41 28.46	−27 36 21.3		9											
365A 1239+168 1	12 41 52.59	16 33 21.3	J	69	300				−0.97	0.04	ehilnop	uvw	D	3.7	128
1239+168 2	12 41 52.39	16 33 23.5		72											
408A 1241−275 1	12 43 50.93	−27 52 14.0	J	5	121				−1.40	0.23	ghlm	v	DF	39.7	60
178 1243+036 1	12 45 38.43	3 23 18.3	J	89	310	1.21			−1.31	0.05	dghjlm		D	7.0	159
1243+036 2	12 45 38.29	3 23 23.1		88											
365A 1243−289 1	12 46 34.28	−29 14 6.1	J	58	192				−1.26	0.09	ehl	uv	D	32.4	4
1243−289 2	12 46 34.37	−29 13 34.1		39											
365A 1248−157 1	12 51 20.02	−16 3 59.5	J	96	295				−1.07	0.07	ehl	uv	D	3.7	144
1248−157 2	12 51 19.87	−16 3 56.6		116											
365B 1250+174 1	12 50 6.25	17 29 59.2	B	137	151	0.94			−1.16	0.04	ejlno	w	P	< 1.5	
408B 1250−347 1	12 53 11.26	−34 59 9.7	J	120	477				−0.81	0.08	hl	v	D	4.4	169
1250−347 2	12 53 11.18	−34 59 5.5		190											
151I 1253+432 1	12 53 24.83	43 14 36.2	B	12	407	1.02			−1.06	0.03	cejlnopq		D	5.1	139
1253+432 2	12 53 24.52	43 14 40.1		263											
408B 1255−316 1	12 57 59.03	−31 55 16.9	J	77	989				−0.27	0.08	hl	v	P	< 1.5	
38C 1257+616 1	12 57 56.83	61 35 53.0	B	46	80		−0.87	0.03	−0.87	0.03	al	v	P	4.2	7
365A 1259−149 1	13 2 22.89	−15 15 37.1	J	56	211				−1.26	0.09	ehl	uv	D	15.8	179
1259−149 2	13 2 22.87	−15 15 21.2		48											
408A 1259−200 1	13 1 52.98	−20 20 44.2	J	86	768				−1.12	0.03	ghlmr	v	D	9.6	113
1259−200 2	13 1 52.35	−20 20 40.3		515											
178 365A 1300−019 1	13 3 13.16	−2 12 54.7	J	113	182	0.95			−1.16	0.04	deghjlm	r	P	2.9	42
365A 1308+063 1	13 11 20.86	6 2 20.4	J	71	329	1.04			−1.30	0.05	ehijln	rx	D	12.9	3
1308+063 2	13 11 20.92	6 2 33.1		103											
178 1309−038 1	13 12 9.87	−4 4 38.4	J	21	192	0.67			−1.12	0.05	dghjlm		DF	6.6	37
38A 1311+670 1	13 11 3.19	67 2 22.9	B	1	40		−1.00	0.09	−1.19	0.07	acln	vx	T	22.0	111
1311+670 2c	13 11 0.68	67 2 27.5		2											
1311+670 3	13 10 59.68	67 2 30.5		17											

Source	R.A. (h m s)	Decl (° ′ ″)		S_{peak} mJy	S_{int} mJy	$\frac{S^{VLA}_{int}}{S_{GB}}$	α_l	$\Delta\alpha_l$	α_h	$\Delta\alpha_h$			R ″	PA °
(1) (2) (3)	(4)		(5)	(6)	(7)	(8)	(9)	(10)	(11)	(12)	(13)	(14)	(15)	(16)	(17)
408A 1312−187 1	13 15 5.53	−18 58 18.3	J	202	300		−1.39	0.02	−1.16	0.18	bghklmr	v	D	7.4	170
1312−187 2	13 15 5.45	−18 58 11.4		311											
365A 1313+216 1	13 15 58.96	21 20 40.3	J	97	312	0.90			−0.91	0.04	eijlnopq	r	T	12.9	126
1313+216 2c	13 15 58.49	21 20 45.1		15											
1313+216 3	13 15 58.21	21 20 48.2		54											
151L 1317+469 1	13 17 53.58	46 55 10.9	B	22	117	0.68			−1.03	0.05	cejlnopq		D	41.8	55
1317+469 2	13 17 56.83	46 55 34.1		10											
151I 1317+509 1	13 17 2.88	50 59 4.3	B	34	100	0.50			−1.08	0.05	cejlnopq	*f	D	69.2	14
1317+509 2	13 17 1.04	50 57 56.8		11											
38A 1319+683 1	13 19 37.66	68 19 29.0	B	14	42		−1.47	0.10	−0.91	0.04	acl	v	D	21.0	52
1319+683 2	13 19 40.59	68 19 42.0		13											
365A 1320−077 1	13 23 31.42	−8 3 18.6	J	116	261				−1.14	0.07	ehl	uv	P	5.9	63
365A 1320−223 1	13 23 33.70	−22 39 37.4	J	36	214				−1.10	0.08	ehl	uv	D	10.3	113
1320−223 2	13 23 33.02	−22 39 33.3		72											
38A 1321+738 1	13 21 47.97	73 50 34.9	B	1	27		−1.12	0.10	−1.27	0.04	acl	v	DF	18.0	112
1321+738 2	13 21 43.06	73 50 42.1		2											
1321+738 3	13 21 38.83	73 50 46.8		2											
365A 1323+080 1	13 25 44.81	7 48 29.9	J	206	333	0.87			−0.64	0.04	ehijlnopq	r	D	4.8	34
1323+080 2	13 25 44.98	7 48 33.9		13											
365B 1324+148 1	13 24 56.61	14 52 32.2	B	39	136	0.74			−1.34	0.07	ejln	rx	D	91.5	150
1324+148 2	13 24 53.40	14 53 51.9		12											
38A 1324+676 1	13 24 23.61	67 39 15.7	B	4	23		−1.49	0.09	−1.31	0.04	acl	v	DF	106	86
1324+676 2	13 24 5.33	67 39 7.2		3											
178 1326+070 1	13 29 13.81	6 44 30.2	J	132	332	0.82	−0.54	0.10	−1.15	0.04	bdghjlm		D	28.7	88
1326+070 2	13 29 11.92	6 44 29.3		60											
365B 1329+584 1	13 29 48.96	58 24 33.0	B	105	168	1.09			−1.30	0.05	jlopq		D	13.2	123
1329+584 2	13 29 47.55	58 24 40.0		23											
365A 1333+168 1	13 36 7.33	16 33 32.8	J	134	413	0.75			−0.86	0.05	ehijlnopq	r	D	9.9	158
1333+168 2	13 36 7.07	16 33 41.8		94											
365A 1333−041 1	13 35 54.90	−4 26 40.1	J	12	185	1.07			−1.33	0.12	ehjl	r	M	20.2	13
1333−041 2	13 35 55.24	−4 26 26.3		9											
1333−041 3	13 35 55.25	−4 26 23.4		28											
1333−041 4	13 35 55.18	−4 26 20.6		38											
365A 1333−227 1	13 35 58.21	−23 1 5.6	J	5	110				−1.59	0.08	ehl	uv	DF	22.1	101
1333−227 2	13 35 57.59	−23 1 3.8		7											
365A 1335+194 1	13 37 41.87	19 9 35.6	J	135	211	1.08			−1.22	0.04	eijlnopq	r	D	5.1	134
1335+194 2	13 37 41.63	19 9 39.2		41											
408A 1336+003 1	13 38 41.80	0 2 47.2	J	31	163	0.73			−1.10	0.06	ghijlmr		D	21.0	88
1336+003 2	13 38 40.46	0 2 46.6		17											
151I 1339+438 1	13 39 47.73	43 50 23.1	B	79	270	0.99			−1.02	0.02	cejlnopq		T	22.2	110
1339+438 2c	13 39 46.80	43 50 26.7		4											
1339+438 3	13 39 45.79	43 50 30.8		57											
38A 1339+665 1c	13 39 33.85	66 35 16.5	B	1	60		−1.03	0.09	−1.10	0.05	acln	vx	T	32.0	105
1339+665 2	13 39 35.90	66 35 14.0		19											
1339+665 3	13 39 30.83	66 35 21.9		15											
38B 1341+601 1	13 41 55.07	60 8 20.3	B	16	202	0.73	−1.13	0.05	−1.21	0.07	aejlnopq		DF	61.5	171
1341+601 2	13 41 56.09	60 7 24.8		9											
365A 1345−110 1	13 47 44.62	−11 20 50.4	J	192	426				−0.88	0.06	ehl	uv	D	11.4	1
1345−110 2	13 47 44.63	−11 20 39.2		44											
408B 1345−309 1	13 47 55.94	−31 11 42.3	J	35	132				−1.75	0.09	hl	v	DF	6.6	171

© European Southern Observatory • Provided by the NASA Astrophysics Data System

1994A&AS..108...79R

Appendix A. continued

(1)	Source (2)	(3)	R.A. h m s (4)	Decl ° ′ ″	(5)	S_{peak} mJy (6)	S_{int} mJy (7)	$\frac{S^{VLA}_{int}}{S_{GB}}$ (8)	α_l $\Delta\alpha_l$ (9) (10)	α_h $\Delta\alpha_h$ (11) (12)	(13)	(14)	(15)	R ″ (16)	PA ° (17)
151I	1347+500 1		13 47 58.60	50 0 54.4	B	29	170	0.86		−1.12 0.04	cejlnopq	r	D	12.7	150
	1347+500 2		13 47 57.94	50 1 5.3		33									
365A	1348+352 1		13 51 1.11	34 59 43.7	J	83	223	0.44		−0.81 0.03	eijlnopq	r	DF	34.9	108
38A	1349+624 1		13 49 48.57	62 28 6.5	B	9	69		−1.09 0.09	−1.05 0.03	acl	v	M	15.0	140
	1349+624 2		13 49 48.82	62 28 10.2		30									
	1349+624 3		13 49 47.41	62 28 18.6		3									
151I	1350+432 1		13 50 24.04	43 14 9.4	B	112	141	0.85		−1.37 0.04	cejln	x	P	1.9	22
38A	1350+636 1c		13 50 19.18	63 41 32.8	B	1	30		−1.16 0.08	−1.52 0.03	acln	v	T	82.0	55
	1350+636 2		13 50 24.97	63 41 50.0		1									
	1350+636 3		13 50 15.19	63 41 2.0		1									
365A	1352+082 1		13 54 41.03	8 0 46.9	J	231	316	0.82		−0.96 0.05	ehijlnopq	r	P	2.7	168
365A	1352−104 1		13 54 47.88	−10 40 59.8	J	107	675			−0.61 0.06	ehl	uv	D	20.2	85
	1352−104 2		13 54 46.53	−10 41 1.4		311									
	1352−104 3		13 54 46.01	−10 41 6.8		23									
151I	1355+471 1		13 55 52.36	47 6 4.8	B	77	140	0.87		−1.02 0.05	cejlnopq		D	5.1	147
	1355+471 2		13 55 52.09	47 6 9.0		25									
408A	1357+007 1		14 0 21.28	−0 30 21.4	J	126	233	0.79		−1.21 0.06	ghjlm		P	4.6	139
38B	1357+657 1		13 57 9.27	65 42 59.1	B	59	131	1.06	−1.05 0.05	−0.89 0.07	aejlnopq	*cdf	D	7.6	97
	1357+657 2		13 57 8.05	65 43 0.0		28									
365A	1359+103 1		14 2 15.41	10 5 24.2	J	4	277	0.63		−0.92 0.03	ehijlnopq	r	D	29.4	150
	1359+103 2		14 2 13.67	10 6 20.7		11									
38A	1400+649 1		14 0 51.82	64 59 44.5	B	4	36		−1.00 0.08	−1.44 0.03	acln	v	DF	35.0	74
	1400+649 2		14 0 51.19	64 59 42.0		3									
	1400+649 3		14 0 48.57	64 59 37.3		1									
365A	1401+092 1		14 3 33.35	8 59 43.9	J	47	534	1.01		−0.45 0.04	ehijlnopq	r	P	< 1.5	
365A 408A	1401−005 1		14 4 7.90	−0 50 7.0	J	21	238	0.69		−1.03 0.06	eghjlm	r	D	34.9	96
	1401−005 2		14 4 5.79	−0 50 2.2		25									
151I	1403+441 1		14 3 29.20	44 11 36.6	B	18	151	0.91		−0.95 0.03	cejlnopq	*cd	DF	12.1	23
	1403+441 2		14 3 29.64	44 11 47.9		21									
151I	1403+497 1		14 3 25.79	49 42 3.8	B	100	156	0.43		−1.03 0.08	cejlnopq	*b	M	10.3	161
	1403+497 2		14 3 25.33	49 42 9.2		4									
	1403+497 3		14 3 25.43	49 42 13.5		8									
151I	1404+465 1		14 4 58.81	46 31 20.8	B	19	148	0.73		−1.06 0.03	cejlnopq		D	23.1	45
	1404+465 2		14 5 0.38	46 31 37.3		14									
365B	1406+113 1		14 6 51.35	11 19 20.3	B	109	112	0.81		−1.15 0.06	ejln	x	P	< 1.5	
365A	1408+148 1		14 10 28.19	14 38 38.0	J	50	291	0.74		−0.60 0.05	ehijlnopq	r	DF	3.3	142
	1408+148 2		14 10 28.06	14 38 40.2		77									
178	1410−001 1		14 13 15.66	−0 23 7.6	J	31	179	0.97		−1.19 0.05	dghjlm		D	23.5	132
	1410−001 2		14 13 14.53	−0 22 51.8		53									
38A	1411+601 1		14 11 41.60	60 10 49.8	B	3	40		−1.21 0.09	−1.10 0.04	acl	v	DF	8.0	150
	1411+601 2		14 11 41.37	60 10 56.1		5									
	1411+601 3		14 11 40.78	60 11 1.1		3									
408A	1411−265 1		14 14 22.42	−26 48 16.0	J	111	359			−1.19 0.05	ghlm	v	DF	4.8	164
	1411−265 2		14 14 22.37	−26 48 13.9		100									
365B	1412+083 1		14 12 11.46	8 18 28.7	B	121	244	0.78		−1.30 0.05	ejlnopq		D	41.5	147
	1412+083 2		14 12 9.94	8 19 3.5		22									
365A	1412+352 1		14 14 24.80	34 58 40.4	J	102	251	0.61		−0.98 0.04	eijlnopq	r	D	15.1	60
	1412+352 2		14 14 25.85	34 58 47.9		32									
408A	1412−107 1		14 15 10.24	−10 57 47.3	J	41	484		−0.96 0.02	−1.18 0.04	bghklmr	v	P	2.4	151
408A	1414−042 1		14 17 9.76	−4 28 40.3	J	54	475	1.16		−1.19 0.06	ghjklmr		D	41.2	22
	1414−042 2		14 17 10.70	−4 28 1.4		77									
151I	1415+361 1		14 15 6.30	36 6 23.4	B	20	163	0.85		−1.10 0.03	cejlnopq		T	9.9	157
	1415+361 2c		14 15 6.15	36 6 28.6		14									
	1415+361 3		14 15 5.97	36 6 32.5		77									
151I	1416+509 1		14 16 6.41	50 59 19.3	B	58	89			−1.00 0.04	celn	uvx	P	2.4	113
408A	1417+144 1		14 19 42.33	14 13 9.4	J	30	329	1.28		−1.14 0.04	ghjlmopq		P	< 1.5	
151I	1418+443 1		14 18 6.94	44 23 19.3	B	25	127	0.67		−1.10 0.05	cejlnopq		D	3.1	56
	1418+443 2		14 18 7.18	44 23 21.1		81									
38A	1419+678 1		14 19 2.90	67 48 54.9	B	3	40		−1.18 0.08	−1.40 0.03	acln	v	DF	7.8	39
408A	1425−148 1		14 28 41.99	−15 2 31.3	J	110	400			−1.18 0.04	ghlm	v	D	10.7	132
	1425−148 2		14 28 41.47	−15 2 24.3		180									
365B	1436+157 1		14 36 43.08	15 44 10.5	B	65	138	0.64		−1.18 0.04	ejlnopq	*z	D	4.7	141
	1436+157 2		14 36 42.88	15 44 14.1		31									
	1436+157 A		14 36 35.74	15 43 27.5		18									
	1436+157 B		14 36 35.85	15 43 36.0		16									
408A	1437−247 1		14 40 36.29	−24 58 29.4	J	135	410			−1.18 0.04	ghlm	v	DF	4.0	112
365A	1439+111 1		14 41 28.29	10 55 24.2	J	26	384	0.88		−0.87 0.04	ehijlnopq	r	P	2.7	14
151I	1440+447 1		14 40 10.80	44 42 12.4	B	42	80			−1.10 0.04	celn	uvx	D	22.8	110
	1440+447 2		14 40 8.80	44 42 20.0		10									
151I	1442+441 1		14 42 57.34	44 9 54.3	B	47	297	0.72		−1.01 0.04	cejlnopq		D	50.8	16
	1442+441 2		14 42 58.65	44 10 43.3		56									
365A	1449+089 1		14 51 38.71	8 47 39.3	J	166	342	0.84		−0.81 0.04	ehijlnopq	r	D	8.8	38
	1449+089 2		14 51 39.08	8 47 46.1		17									
178	1449−004 1		14 52 24.94	−0 37 15.4	J	34	205	0.67		−1.08 0.06	djlm		D	5.5	97
	1449−004 2		14 52 24.60	−0 37 14.8		89									
365A	1451+118 1		14 54 8.56	11 37 24.4	J	94	330	0.92		−0.82 0.04	ehijlnopq	r	D	25.4	160
	1451+118 2		14 54 8.00	11 37 48.4		34									
365A	1452+066 1		14 55 9.28	6 26 52.8	J	10	253	0.55		−0.90 0.05	ehijlnopq	*br	D	11.8	24
	1452+066 2		14 55 9.61	6 27 3.9		75									
38B	1454+629 1		14 54 10.77	62 55 54.6	B	14	134	0.82	−1.08 0.05	−1.04 0.06	aejlnopq		DF	26.2	127
	1454+629 2		14 54 7.74	62 56 10.3		9									
151I	1455+463 1		14 55 12.17	46 17 51.3	B	4	63			−1.06 0.04	celn	uvx	DF	35.8	117
	1455+463 2		14 55 9.10	46 18 7.0		7									
365A	1455−212 1		14 57 54.64	−21 25 1.3	J	21	250			−1.18 0.07	ehl	uv	DF	16.5	101
	1455−212 2		14 57 53.54	−21 24 57.2		21									
38B	1456+618 1		14 56 12.77	61 52 46.3	B	52	229	0.88	−1.03 0.05	−1.17 0.04	aejlnopq		D	27.5	43
	1456+618 2		14 56 14.92	61 53 5.2		35									
	1456+618 3		14 56 15.34	61 53 6.3		49									
365A	1457+321 1		14 59 14.78	31 57 37.9	J	67	181	0.71		−1.35 0.06	eijlnopq	r	D	20.6	70
	1457+321 2		14 59 13.26	31 57 30.9		15									
38A 38B	1457+664 1		14 57 47.56	66 28 9.7	B	12	200	1.00	−1.18 0.08	−1.12 0.04	acejlnopq		D	43.0	0
	1457+664 2		14 57 47.71	66 27 19.0		4									
38A	1458+643 1		14 58 39.04	64 18 5.4	B	5	6		−1.11 0.08	−2.29 0.05	acln	v	P	< 1.5	
365A	1500+333 1		15 2 15.71	33 9 33.5	J	7	145	0.91		−1.45 0.06	eijln	rx	DF	7.0	118
	1500+333 2		15 2 15.75	33 9 36.6		10									
	1500+333 3		15 2 15.36	33 9 37.8		9									
178	1502+039 1		15 5 6.53	3 47 11.7	J	38	464	0.77	−0.78 0.10	−1.22 0.03	bdghijklmnopqr		P	2.6	80
365A	1506+142 1		15 9 15.59	14 6 14.4	J	275	384	1.01		−1.10 0.03	ehijlnopq	r	P	< 1.5	
365A	1506+191 1		15 8 39.32	18 58 59.2	J	196	266	1.00		−1.12 0.04	eijlnopq	r	P	2.8	92
365A	1509+348 1		15 11 20.10	34 39 32.8	J	49	520	1.09		−0.50 0.03	eijlnopq	r	P	< 1.5	

© European Southern Observatory • Provided by the NASA Astrophysics Data System

1994A&AS..108...79R

Appendix A. continued

(1)	Source (2)	(3)	R.A. h m s (4)	Decl ° ′ ″ (5)	S_{peak} mJy (6)	S_{int} mJy (7)	$\frac{S^{VLA}_{int}}{S_{GB}}$ (8)	α_l (9)	$\Delta\alpha_l$ (10)	α_h (11)	$\Delta\alpha_h$ (12)	(13)	(14)	(15)	R ″ (16)	PA ° (17)
178	408B 1510−006 1		15 13 30.10	−0 50 0.4 J	39	221	0.80			−1.09	0.05	dhjlm		D	1.8	76
	1510−006 2		15 13 30.34	−0 50 0.7	28											
151I	1512+452 1		15 12 40.57	45 12 17.6 B	14	85				−1.11	0.03	celn	uvx	D	5.1	72
	1512+452 2		15 12 40.12	45 12 16.1	37											
365A	1513+339 1		15 15 59.34	33 48 3.5 J	55	231	1.23			−1.00	0.08	eijlnopq	r	D	3.7	6
	1513+339 2		15 15 59.36	33 48 6.9	157											
365B	1514+072 1		15 14 16.98	7 12 16.8 B	284	2584	0.47			−1.21	0.04	ejlnopq		DF	28.0	29
365A	1514+333 1		15 16 36.87	33 7 37.1 J	111	246	0.85			−1.08	0.03	eijlnopq	r	D	25.0	99
	1514+333 2		15 16 35.76	33 7 39.2	29											
365A	1515−025 1		15 17 41.59	−2 42 12.9 J	96	166	0.70			−1.05	0.08	ehjl	r	P	2.8	131
178	1516+246 1		15 18 40.01	24 27 1.5 J	33	213	0.80	−1.82	0.10	−1.16	0.04	bdijlmnopq		DF	16.9	83
	1516+246 2		15 18 40.61	24 27 4.9	5											
	1516+246 3		15 18 39.36	24 27 4.2	4											
38A	1517+619 1		15 17 17.86	61 58 47.4 B	2	2		−1.71	0.13	−2.06	0.15	acln	v	P	< 1.5	
38A	38B 1520+659 1		15 20 49.57	65 57 54.8 B	10	100		−1.11	0.08	−1.02	0.03	acelnop	uvw	D	50.0	122
	1520+659 2		15 20 42.92	65 58 19.9	30											
151I	1522+460 1		15 22 18.82	46 1 12.9 B	95	181	1.21			−1.06	0.03	cejlnopq		D	6.3	166
	1522+460 2		15 22 18.67	46 1 19.0	36											
365A	1523+074 1		15 26 1.31	7 15 25.1 J	238	192	0.82			−1.18	0.04	ehijlnopq	r	P	< 1.5	
365A	1523−081 1		15 25 49.71	−8 16 46.1 J	67	332				−1.10	0.06	ehl	uv	T	21.0	124
	1523−081 2c		15 25 49.31	−8 16 43.3	13											
	1523−081 3		15 25 48.40	−8 16 39.5	14											
151I	1524+432 1		15 24 53.34	43 16 43.0 B	7	272	0.57			−1.04	0.07	cejlnopq		DF	15.0	112
	1524+432 2		15 24 52.03	43 16 48.1	13											
365B	1525+182 1		15 25 17.83	18 16 25.2 B	12	80				−1.21	0.06	eln	uvx	T	36.5	15
	1525+182 2c		15 25 18.26	18 16 48.6	5											
	1525+182 3		15 25 18.48	18 16 59.8	8											
151I	1527+496 1		15 27 52.52	49 41 1.1 B	4	52				−1.13	0.05	celn	uvx	DF	4.0	177
	1527+496 2		15 27 52.50	49 41 5.0	5											
365A	1531+073 1		15 34 19.06	7 10 26.8 J	195	296	1.20			−1.01	0.05	ehijlnopq	r	P	3.5	144
151I	1531+496 1		15 31 59.06	49 36 23.4 B	80	157	0.86			−1.01	0.03	cejlnopq		D	3.6	138
	1531+496 2		15 31 58.81	49 36 26.1	43											
151I	1533+508 1		15 33 10.53	50 51 18.1 B	17	76				−1.06	0.04	celn	uvx	D	16.1	97
	1533+508 2		15 33 8.84	50 51 20.0	30											
38B	1533+684 1		15 33 42.78	68 26 31.4 B	9	73		−1.03	0.05	−1.08	0.05	aeln	uv	D	23.9	92
	1533+684 2		15 33 38.48	68 26 32.2	28											
365A	1533−143 1		15 35 50.63	−14 32 8.3 J	30	291				−1.12	0.07	ehl	uv	DF	12.1	64
	1533−143 2		15 35 51.33	−14 32 3.0	22											
365A	1535+367 1		15 37 14.26	36 35 11.0 J	233	247	0.80			−0.90	0.05	eijlnopq	r	P	< 1.5	
38C	1536+620 1		15 36 17.48	62 5 19.6 B	69	130	0.76	−1.08	0.08	−1.13	0.06	acjln	*bx	D	11.5	35
	1536+620 2		15 36 18.34	62 5 28.3	27											
365B	1538+158 1		15 38 52.10	15 53 36.6 B	100	157	0.79			−1.60	0.06	ejln	x	P	3.2	137
151I	1539+409 1		15 39 19.10	40 58 33.8 B	10	123	0.95			−1.07	0.03	cejlnopq		DF	35.1	40
	1539+409 2		15 39 21.05	40 59 0.4	12											
178	1539−011 1		15 41 41.97	−1 14 43.8 J	4	55	0.19			−1.12	0.07	dghjlm		DF	7.7	145
	1539−011 2		15 41 41.24	−1 14 26.6	8											
151I	1540+313 1		15 40 50.11	31 20 1.9 B	22	85				−1.15	0.03	celn	uvx	D	22.8	74
	1540+313 2		15 40 48.42	31 19 55.6	21											
365A	1543+021 1		15 46 31.36	1 58 9.7 J	101	233	1.47			−1.02	0.08	ehijlnopq	r	D	7.0	79
	1543+021 2		15 46 30.91	1 58 8.4	66											
151I	1543+465 1		15 43 50.07	46 32 2.6 B	30	437	0.92			−1.06	0.02	cejlnopq		P	2.8	150
38B	1544+672 1		15 44 15.97	67 15 36.8 B	42	88		−0.63	0.08	−1.20	0.04	acelop	uvw	D	< 1.5	
	1544+672 2		15 44 16.34	67 15 41.0	15											
365A	1545−234 1		15 48 17.52	−23 37 5.1 J	98	222				−1.20	0.07	ehl	uv	D	6.3	159
	1545−234 2		15 48 17.37	−23 36 59.1	87											
38B	1546+679 1		15 46 24.05	67 55 55.5 B	9	84		−0.95	0.05	−1.06	0.05	aelnop	uvw	DF	11.6	108
	1546+679 2		15 46 22.12	67 55 59.1	9											
178	1547−021 1		15 49 56.78	−2 18 20.4 J	10	145	0.64			−1.16	0.05	dghjlm		DF	22.4	99
	1547−021 2		15 49 55.31	−2 18 16.6	15											
365A	1548−111 1		15 51 41.68	−11 17 42.4 J	19	184				−1.35	0.11	ehl	uv	D	5.9	175
	1548−111 2		15 51 41.66	−11 17 36.7	55											
365A	1551+368 1		15 53 24.78	36 43 28.1 J	238	263	0.83			−1.26	0.06	eijlnopq	r	P	< 1.5	
151I	1553+412 1		15 53 39.99	41 15 49.1 B	17	75				−1.11	0.03	celn	uvx	D	22.4	136
	1553+412 2		15 53 38.60	41 16 5.1	24											
365B	1554+080 1		15 54 27.01	8 4 1.1 B	20	146	0.63			−1.11	0.07	ejlnopq	*a	D	14.1	167
	1554+080 2		15 54 26.80	8 4 14.7	23											
178	1558−003 1		16 1 17.55	−0 28 47.1 J	62	343	0.91	−0.92	0.10	−1.17	0.02	bdghjlmpq		D	7.7	75
	1558−003 2		16 1 17.05	−0 28 48.9	135											
365B	1600+105 1		16 0 3.49	10 33 20.2 B	6	63	0.25			−1.21	0.22	ejln	*bx	DF	10.0	127
	1600+105 2		16 0 3.62	10 33 22.2	7											
38C	1600+727 1		16 0 0.38	72 46 42.5 B	21	82		−0.92	0.03	−0.92	0.03	al	v	D	3.1	35
	1600+727 2		16 0 0.73	72 46 44.3	19											
151I	1602+445 1		16 2 34.59	44 31 27.9 B	85	867	0.90			−1.13	0.03	cejlnopq		DF	26.0	78
	1602+445 2		16 2 36.95	44 31 33.5	145											
365A	1603+110 1		16 6 11.28	10 57 43.2 J	70	367	1.06			−0.85	0.04	ehijlnopq	r	T	12.1	85
	1603+110 2c		16 6 10.83	10 57 42.7	9											
	1603+110 3		16 6 10.46	10 57 42.1	207											
365AB	1604+183 1		16 4 42.83	18 19 31.0 B	79	227				−1.14	0.05	ehilnop	uvw	D	10.3	85
	1604+183 2		16 4 42.10	18 19 30.0	90											
38A	38C 1604+630 1		16 4 47.92	63 5 38.6 B	19	53		−1.14	0.08	−1.17	0.03	acln	v	D	6.0	153
	1604+630 2		16 4 47.51	63 5 44.1	14											
38A	1605+639 1		16 5 37.91	63 54 56.5 B	4	20		−1.46	0.11	−1.16	0.05	acln	v	DF	5.0	14
	1605+639 2		16 5 38.09	63 55 1.1	3											
365A	1607+218 1		16 9 36.34	21 41 5.2 J	270	290	0.78			−1.06	0.03	eijlnopq	r	P	1.5	72
151I	1607+305 1		16 7 17.22	30 32 54.7 B	33	127	0.81			−1.16	0.03	cejlnopq		D	8.9	42
	1607+305 2		16 7 17.67	30 33 1.2	29											
178	1608−036 1		16 11 5.53	−3 46 9.7 J	4	79	0.29			−0.90	0.14	djlm	*b	DF	37.9	0
	1608−036 2		16 11 5.43	−3 45 31.4	13											
151I	1611+452 1		16 11 17.49	45 13 27.1 B	9	96				−1.08	0.03	celno	*guvw	M	64.6	96
	1611+452 2		16 11 11.39	45 13 34.2	11											
	1611+452 3		16 11 11.08	45 13 31.2	9											
	1611+452 4		16 10 59.04	45 13 16.0	4											
38A	1611+643 1		16 11 9.85	64 22 36.3 B	9	137	0.62	−1.07	0.08	−0.98	0.03	acjlopq		DF	44.0	44
	1611+643 2		16 11 3.87	64 21 56.8	6											
365B	1612+148 1		16 12 42.75	14 52 8.8 B	234	301	0.89			−1.20	0.03	ejlnopq	r	P	< 1.5	
365A	1612−156 1		16 14 54.71	−15 45 51.6 J	82	359				−1.06	0.06	ehl	uv	DF	11.0	128
	1612−156 2		16 14 54.12	−15 45 46.2	40											
151I	1615+494 1		16 15 7.25	49 26 19.9 B	4	70				−1.24	0.04	celn	uvx	D	8.7	7
	1615+494 2		16 15 7.36	49 26 28.4	37											
38B	1618+642 1		16 18 9.41	64 14 53.3 B	59	100	0.58	−1.12	0.05	−1.15	0.13	aejln	x	P	2.8	54

© European Southern Observatory • Provided by the NASA Astrophysics Data System

1994A&AS..108...79R

Appendix A. continued

	Source	R.A. h m s	Decl ° ′ ″		S_{peak} mJy	S_{int} mJy	$\frac{S^{VLA}_{int}}{S_{GB}}$	α_l	$\Delta\alpha_l$	α_h	$\Delta\alpha_h$			R ″	PA °
(1)	(2)	(3) (4)		(5)	(6)	(7)	(8)	(9)	(10)	(11)	(12)	(13)	(14)	(15)	(16)	(17)
365B	1620+127 1	16 20 42.99	12 46 54.0	B	37	408	0.95			−1.15	0.03	ejlnopq		P	< 1.5	
151I	1624+465 1	16 24 36.31	46 33 30.4	B	91	203	1.27			−1.18	0.03	cejlnopq		D	26.8	10
	1624+465 2	16 24 36.79	46 33 56.5		29											
365A	1626+147 1	16 28 40.33	14 38 0.8	J	119	857	0.84			−1.24	0.04	ehijlnopq	r	D	47.1	103
	1626+147 2	16 28 37.19	14 38 12.9		66											
365A	1627+342 1	16 28 56.37	34 6 33.1	J	34	357	0.98			−0.78	0.03	eijlnopq	r	P	< 1.5	
178	1627−013 1	16 30 24.38	−1 29 39.8	J	47	294	1.07			−1.15	0.04	dghjlm		D	18.0	98
	1627−013 2	16 30 23.20	−1 29 37.3		55											
365B	1628+144 1	16 28 49.42	14 24 56.7	B	116	136	0.56			−1.39	0.11	ejln	rx	P	< 1.5	
38B	1630+631 1	16 30 7.40	63 7 58.0	B	6	86		−1.04	0.05	−1.06	0.05	aelnop	uvw	T	13.7	159
	1630+631 2c	16 30 7.01	63 8 4.6		9											
	1630+631 3	16 30 6.67	63 8 10.7		11											
151I	1632+503 1	16 32 22.94	50 20 29.5	B	4	87				−1.05	0.04	celnop	uvw	T	27.1	42
	1632+503 2c	16 32 22.05	50 20 19.6		6											
	1632+503 3	16 32 20.90	50 20 8.3		3											
151I	1633+420 1	16 33 5.70	42 1 11.4	B	99	229	0.79			−1.16	0.05	cejlnopq	*f	DF	5.0	22
365A	1635+159 1	16 37 48.98	15 48 54.9	J	72	481				−1.29	0.05	ehilnop	uvw	D	51.5	15
	1635+159 2	16 37 49.90	15 49 44.9		69											
365A	1635+396 1	16 36 59.66	39 30 11.9	J	45	164	0.87			−1.54	0.07	eijln	rx	D	4.8	123
	1635+396 2	16 36 59.31	39 30 14.5		83											
178	1638+209 1	16 40 42.00	20 53 5.3	J	10	119				−1.25	0.06	diklmnop	vw	D	58.1	84
	1638+209 2	16 40 37.96	20 52 59.1		9											
151I	1643+475 1	16 43 29.29	47 30 33.5	B	32	120				−1.22	0.04	celn	uvx	T	9.8	40
	1643+475 2c	16 43 29.65	47 30 38.3		4											
	1643+475 3	16 43 29.90	47 30 40.9		43											
178	1643−031 1	16 45 51.15	−3 13 52.7	J	25	168	0.49			−1.14	0.08	dghjlm		D	30.1	157
	1643−031 2	16 45 50.31	−3 13 25.6		5											
365A	1647+364 1	16 48 53.03	36 23 24.5	J	77	233	0.97			−1.23	0.03	eijlnopq	r	D	23.2	129
	1647+364 2	16 48 51.58	36 23 39.0		92											
365A	1647+388 1	16 48 49.03	38 48 9.8	J	28	211	0.71			−1.07	0.03	eijlnopq	r	T	11.4	37
	1647+388 2c	16 48 49.17	38 48 12.6		13											
	1647+388 3	16 48 49.63	38 48 18.8		54											
365A	1649+169 1	16 51 35.51	16 52 39.5	J	201	289	1.32			−1.35	0.04	ehjlopq	r	D	5.1	145
	1649+169 2	16 51 35.29	16 52 43.1		56											
178	1649−031 1	16 52 40.10	−3 12 6.4	J	43	127				−1.40	0.08	dlm	v	DF	3.7	20
365B	1652+027 1	16 52 5.48	2 43 46.5	B	66	149	0.71			−1.19	0.09	ejln	*xz	P	2.9	37
	1652+027 A	16 52 15.65	2 46 43.6		18											
178	1657+003 1	17 0 17.01	0 19 4.1	J	51	158	1.05			−1.07	0.07	dghjlmopq		D	32.4	162
	1657+003 2	17 0 16.27	0 19 35.6		18											
365A	1657+372 1	16 59 25.06	37 11 28.3	J	182	193	0.95			−1.25	0.04	eijlnopq	r	P	< 1.5	
151I	1659+440 1	16 59 8.53	44 0 46.5	B	69	189	0.68			−1.32	0.04	cejlnopq	*z	T	7.4	132
	1659+440 2c	16 59 8.26	44 0 49.7		6											
	1659+440 3	16 59 8.02	44 0 51.4		79											
	1659+440 A	16 59 18.21	44 2 24.6		17											
151I	1700+508 1	17 0 10.57	50 52 37.3	B	89	342	0.71			−1.05	0.04	cejlnopq	*af	D	19.3	17
	1700+508 2	17 0 11.17	50 52 56.0		61											
365A	1701+145 1	17 3 24.07	14 30 21.7	J	57	574	1.16			−0.83	0.04	ehijlnopq	r	P	< 1.5	
365AB	1707+105 1	17 7 46.04	10 34 57.8	B	17	220	0.78			−1.20	0.03	ehijlnpq		D	21.7	59
	1707+105 2	17 7 44.77	10 34 46.8		150											
38B	1707+666 1	17 7 15.04	66 37 53.3	B	21	96	0.53	−0.99	0.05	−1.01	0.09	aejlnopq	*b	D	13.9	40
	1707+666 2	17 7 14.01	66 37 45.6		6											
365A	1718+064 1	17 20 58.02	6 21 40.6	J	25	299				−0.95	0.05	ehilnop	uvw	D	23.2	124
	1718+064 2	17 20 56.66	6 21 54.8		47											
365AB	1718+192 1	17 18 53.56	19 14 47.7	B	260	329	0.62	−1.07	0.10	−1.21	0.03	bdeijklmnopq		P	1.6	78
38C	1718+630 1	17 18 24.64	63 1 31.6	B	3	40		−1.16	0.03	−1.16	0.03	al	v	D	92.3	51
	1718+630 2	17 18 24.67	63 1 39.0		9											
	1718+630 3	17 18 14.13	63 0 40.7		4											
365A	1722+105 1	17 24 42.44	10 30 48.8	J	9	329				−1.00	0.04	ehilnop	uvw	D	22.4	104
	1722+105 2	17 24 40.98	10 30 54.3		90											
38C	1724+610 1	17 24 44.77	61 4 33.6	B	7	44		−1.04	0.03	−1.04	0.03	al	v	D	47.7	101
	1724+610 2	17 24 38.46	61 4 42.6		9											
178 365A	1725+167 1	17 27 35.35	16 44 22.1	J	131	265				−1.15	0.04	deghilmnop	uvw	D	11.4	40
	1725+167 2	17 27 35.86	16 44 30.7		63											
178	1726+011 1	17 28 35.38	1 2 36.8	J	59	312	0.75			−1.17	0.06	dghjlmopq		D	19.1	91
	1726+011 2	17 28 32.89	1 2 37.6		27											
178	1727+197 1	17 29 50.37	19 45 28.4	J	97	263	1.22			−1.13	0.05	dijlmnopq		D	2.9	135
	1727+197 2	17 29 50.23	19 45 30.6		131											
365A	1732+160 1	17 32 27.94	16 2 22.0	B	355	963	0.72			−1.15	0.03	jlopq		D	15.7	168
	1732+160 2	17 32 27.73	16 2 37.2		177											
178	1746+093 1	17 48 44.63	9 18 52.5	J	67	379	0.83	−0.60	0.10	−1.25	0.03	bdghjlmopq	*a	D	9.2	88
	1746+093 2	17 48 44.02	9 18 52.5		256											
365A	1748+344 1	17 49 52.05	34 26 10.1	J	27	373	0.96			−1.04	0.03	eijlnopq	r	P	< 1.5	
365A	1754+366 1	17 56 9.01	36 36 18.3	J	66	268	1.07			−1.04	0.03	eijlnopq	r	D	5.1	167
	1754+366 2	17 56 8.93	36 36 23.0		142											
38B	1802+649 1	18 2 12.91	64 56 30.5	B	17	110	0.77	−1.17	0.05	−1.28	0.06	aejlnpq		D	26.0	111
	1802+649 2	18 2 9.11	64 56 39.6		43											
365A	1805+316 1	18 7 48.00	31 41 27.3	J	31	303	0.80			−0.92	0.03	eijlnopq	r	M	9.2	2
	1805+316 2	18 7 48.13	31 41 30.6		38											
	1805+316 3	18 7 48.00	31 41 36.6		21											
365A	1817+364 1	18 19 1.23	36 27 15.0	J	64	188	0.56			−1.04	0.07	eijlnopq	r	D	10.7	164
	1817+364 2	18 19 0.99	36 27 25.1		82											
365A	1827+334 1	18 29 39.47	33 27 35.3	J	187	317	0.97			−1.13	0.03	eijlnopq	r	D	4.8	105
	1827+334 2	18 29 39.12	33 27 36.5		59											
38B	1854+683 1	18 54 16.10	68 19 1.7	B	14	62		−1.52	0.05	−1.08	0.09	aelnop	uvw	DF	10.0	0
38B	1919+601 1	19 19 50.92	60 7 44.7	B	18	77		−1.15	0.05	−1.02	0.06	aeln	uvx	D	17.4	140
	1919+601 2	19 19 49.42	60 7 58.0		13											
38B	1926+644 1	19 26 58.04	64 29 55.9	B	7	28		−1.12	0.05	−1.34	0.18	aeln	uvx	DF	28.5	20
365A	1926−228 1	19 29 27.81	−22 43 13.9	J	25	431				−0.83	0.07	ehl	uv	P	2.7	129
38C	1942+631 1	19 42 48.27	63 11 28.9	B	6	49		−1.03	0.03	−1.03	0.03	al	*vz	DF	67.7	145
	1942+631 2	19 42 53.96	63 10 33.1		5											
	1942+631 A	19 43 6.89	63 8 35.1		3											
365A	1946−131 1	19 48 56.33	−13 1 11.4	J	107	308				−1.03	0.06	ehl	uv	D	4.0	155
	1946−131 2	19 48 56.21	−13 1 8.0		57											
365A	1950−144 1	19 52 56.38	−14 17 9.0	J	208	311				−1.02	0.07	ehl	uv	D	3.7	52
	1950−144 2	19 52 56.59	−14 17 6.6		32											
365A	2000−091 1	20 3 38.66	−9 2 51.7	J	7	192				−1.53	0.06	ehl	uv	T	25.4	30
	2000−091 2c	20 3 39.00	−9 2 38.8		5											
	2000−091 3	20 3 39.46	−9 2 30.4		51											
365A	2004−042 1	20 6 56.40	−4 7 45.1	J	100	307	0.55			−0.62	0.07	ehjl	r	DF	11.4	152
	2004−042 2	20 6 56.06	−4 7 35.0		9											

© European Southern Observatory • Provided by the NASA Astrophysics Data System

1994A&AS..108...79R

Appendix A. continued

(1)	Source (2)	R.A. h m s (3)	Decl ° ′ ″ (4)	(5)	S_{peak} mJy (6)	S_{int} mJy (7)	$\frac{S^{VLA}_{int}}{S_{GB}}$ (8)	α_l (9)	$\Delta\alpha_l$ (10)	α_h (11)	$\Delta\alpha_h$ (12)	(13)	(14)	(15)	R ″ (16)	PA ° (17)
365A	2007−098 1	20 10 27.93	−9 44 41.6	J	39	517				−0.79	0.06	ehl	uv	P	1.9	30
365A	2012−212 1c	20 15 32.96	−21 3 23.9	J	8	267				−1.23	0.07	ehl	uv	T	16.2	170
	2012−212 2	20 15 33.05	−21 3 31.4		50											
	2012−212 3	20 15 32.84	−21 3 15.7		54											
365A	2019−202 1	20 22 18.07	−20 7 0.8	J	50	556				−0.77	0.07	ehl	uv	P	1.6	155
408B	2021−330 1	20 24 35.59	−32 53 36.8	J	518	856				−0.42	0.08	hl	v	D	8.1	28
	2021−330 2	20 24 35.37	−32 53 38.6		101											
365B	2026+013 1	20 26 24.72	1 23 32.0	B	19	34	0.12			−1.08	0.03	ejlnopq	*aq	D	17.7	137
	2026+013 2	20 26 23.90	1 23 44.1		15											
408B	2034−309 1	20 37 55.37	−30 43 34.3	J	32	432				−0.85	0.09	hl	v	P	1.6	136
408A	2037−085 1	20 40 2.05	−8 24 38.3	J	34	648				−1.52	0.18	ghklm	v	P	4.2	139.
365B	2045+142 1	20 45 23.87	14 16 36.6	B	106	116	0.77			−1.23	0.05	ejlnopq		P	< 1.5	
178 365B	2048+136 1	20 48 52.59	13 37 34.4	B	18	134	0.62			−1.22	0.04	deghijlmnopq	r	DF	37.1	104
	2048+136 2	20 48 50.12	13 37 42.8		5											
38C	2049+647 1	20 49 37.28	64 46 56.9	B	6	24		−1.53	0.03	−1.53	0.03	al	v	DF	6.9	73
	2049+647 2	20 49 37.96	64 46 58.2		3											
365A	2050+054 1	20 53 17.79	5 37 25.2	J	67	181	0.60			−0.93	0.03	ehijlnopq	r	D	18.0	107
	2050+054 2	20 53 16.68	5 37 30.5		75											
38C	2051+672 1	20 51 53.22	67 14 31.7	B	14	111		−0.83	0.03	−0.83	0.03	al	v	D	6.2	178
	2051+672 2	20 51 53.16	67 14 37.2		45											
365A	2055+167 1	20 58 13.31	16 58 34.3	J	29	232	0.79			−1.03	0.03	ehijlnopq	*cdr	D	9.9	126
	2055+167 2	20 58 12.75	16 58 40.1		69											
178	2058−041 1	21 0 34.40	−3 55 17.9	J	71	115				−1.31	0.06	dlm	v	P	2.9	132
365B	2104+093 1	21 4 47.93	9 20 24.0	B	7	56				−1.21	0.08	eln	uvx	D	84.6	141
	2104+093 2	21 4 44.33	9 21 29.5		9											
365A	2107+190 1	21 9 41.09	19 12 51.5	J	184	210	0.69			−0.91	0.05	eijlnopq	r	P	2.4	114
408B	2110−342 1	21 13 33.22	−34 2 38.8	J	41	394				−0.90	0.09	hl	v	DF	22.1	32
	2110−342 2	21 13 34.14	−34 2 20.3		13											
365A	2112+158 1	21 14 34.95	16 6 6.2	J	19	217	1.20			−1.39	0.04	ehijlnopq	r	D	11.0	10
	2112+158 2	21 14 35.10	16 6 17.0		171											
365B	2117+120 1	21 17 13.62	12 2 59.9	B	36	82	0.52			−1.17	0.16	ejln	x	D	3.8	29
	2117+120 2	21 17 13.74	12 3 3.3		21											
365A	2120+061 1	21 23 27.88	6 22 34.6	J	39	341	0.86			−0.64	0.04	ehijlnopq	r	P	< 1.5	
365B	2125+152 1	21 25 21.39	15 14 52.5	B	83	144				−1.35	0.08	eln	uvx	P	< 1.5	
178 365B	2131+162 1	21 31 7.55	16 15 59.2	B	23	189	0.76			−1.43	0.05	deghijlmnopq		DF	5.2	68
178	2132−031 1	21 35 28.90	−2 54 7.9	J	98	208	0.83			−1.14	0.06	dghjlm		D	42.6	160
	2132−031 2	21 35 27.92	−2 53 32.2		27											
365A	2132−160 1	21 35 36.74	−15 51 22.1	J	93	423				−0.89	0.06	ehl	uv	D	3.7	14
	2132−160 2	21 35 36.78	−15 51 19.2		265											
408B	2133−337 1	21 36 52.39	−33 30 6.2	J	132	432				−0.87	0.08	hl	v	D	4.0	65
	2133−337 2	21 36 52.68	−33 30 4.7		180											
178	2135+037 1	21 38 1.81	3 59 2.7	J	181	228	0.89			−1.28	0.05	dghijlmno	w	P	1.9	172
365A	2138+086 1	21 41 22.05	8 51 54.5	J	45	505	1.11			−0.64	0.04	ehijlnopq	r	P	1.5	32
365A	2139−048 1	21 42 36.91	−4 37 44.1	J	48	589	0.84			−0.43	0.07	ehjl	r	P	< 1.5	
365A	2140+102 1	21 42 55.17	10 31 16.9	J	37	403	0.83			−0.86	0.03	ehijlnopq	r	D	12.9	34
	2140+102 2	21 42 55.26	10 31 21.4		55											
	2140+102 3	21 42 55.63	10 31 27.5		78											
365A	2141+192 1	21 44 7.51	19 29 10.6	J	129	305	1.00			−1.24	0.03	eijlnopq	r	D	8.1	176
	2141+192 2	21 44 7.48	19 29 18.8		163											
365A	2142+077 1	21 45 7.82	8 0 21.2	J	127	281	0.83			−1.07	0.04	ehijlnopq	r	M	21.3	175
	2142+077 2	21 45 7.70	8 0 42.6		6											
365A	2143+084 1	21 45 32.06	8 43 1.4	J	239	295	1.08			−0.90	0.04	ehijlnopq	r	P	1.9	116
365A	2144+092 1	21 47 10.16	9 29 46.5	J	72	874	1.09			−0.03	0.06	ehijlnopq	qr	P	< 1.5	
365A	2145+089 1	21 48 18.31	9 8 42.2	J	40	256	0.87			−1.09	0.05	ehijlnopq	r	D	2.9	55
	2145+089 2	21 48 18.46	9 8 43.9		70											
365A	2146−016 1	21 48 43.43	−1 22 38.7	J	62	336	0.66			−0.53	0.04	ehjlpq	r	DF	11.4	109
	2146−016 2	21 48 42.98	−1 22 36.7		10											
365A	2148−228 1	21 51 16.69	−22 36 57.3	J	24	298				−1.20	0.06	ehl	uv	DF	21.3	172
	2148−228 2	21 51 16.45	−22 36 36.3		40											
38B	2149+616 1	21 49 5.89	61 38 20.1	B	25	220	0.61	−1.07	0.05	−1.00	0.08	aejlnopq		D	76.9	24
	2149+616 2	21 49 10.29	61 39 30.3		65											
365A	2150−140 1	21 52 45.10	−13 49 26.8	J	55	324				−1.07	0.07	ehl	uv	D	17.6	55
	2150−140 2	21 52 46.05	−13 49 16.9		26											
178	2153+122 1	21 55 42.06	12 31 25.2	J	45	289	0.42	−1.25	0.10	−1.02	0.04	bdghijlmnopq	*b	D	8.1	164
	2153+122 2	21 55 41.92	12 31 32.8		32											
365B	2154+163 1	21 54 52.80	16 19 19.0	B	52	51				−1.18	0.08	eln	uvx	P	< 1.5	
38B	2154+691 1	21 54 5.83	69 8 57.9	B	98	204	1.07	−1.01	0.05	−1.00	0.04	aejlnopq		T	37.8	180
	2154+691 2c	21 54 5.62	69 9 16.1		4											
	2154+691 3	21 54 5.76	69 9 35.5		11											
	2154+691 4	21 54 5.02	69 9 38.9		12											
365A	2156+023 1	21 59 12.35	2 35 18.6	J	19	241	0.79			−0.84	0.04	ehijlnopq	r	DF	16.5	112
	2156+023 2	21 59 11.33	2 35 25.1		22											
408A	2159−201 1	22 2 41.80	−19 55 9.1	J	27	384				−1.50	0.12	ghklmr	v	P	2.1	150
408A	2159−201 1	22 2 41.80	−19 55 9.1	J	27	384				−1.50	0.12	ghklmr	v	P	2.1	150
38B	2201+654 1	22 1 24.92	65 24 10.1	B	97	19		−1.52	0.05	−2.08	0.06	aeln	uv	P	5.3	39
365B	2202+128 1	22 2 47.73	12 50 56.3	B	72	161	0.50			−1.25	0.14	ejlno	w	D	3.4	80
	2202+128 2	22 2 47.94	12 50 56.9		61											
178	2205−040 1	22 8 8.54	−3 48 2.7	J	39	186	0.64			−1.07	0.04	dghjlm	*a	D	28.3	78
	2205−040 2	22 8 6.71	−3 48 8.3		77											
178	2207+038 1	22 9 48.56	4 4 46.9	J	195	39	0.15			−1.08	0.06	djlm	*z	P	1.5	112
	2207+038 A	22 9 47.55	4 1 32.3		7											
408A	2211+071 1	22 14 20.35	7 26 49.1	J	43	454	1.07			−1.17	0.03	ghijlmnopq		D	7.0	24
	2211+071 2	22 14 20.52	7 26 55.3		273											
365A	2214+134 1	22 16 39.08	13 41 5.4	J	58	225	0.89			−1.08	0.04	ehijlnopq	r	D	16.9	175
	2214+134 2	22 16 38.96	13 41 22.5		75											
365A	2214+201 1	22 17 15.94	20 24 45.3	J	26	358	0.88			−0.63	0.03	eijlnopq	r	M	6.6	153
	2214+201 2c	22 17 15.83	20 24 48.9		247											
	2214+201 3	22 17 15.77	20 24 50.6		20											
408A	2215−185 1	22 18 21.94	−18 19 50.1	J	14	120				−1.17	0.14	ghlm	v	D	41.2	45
	2215−185 2	22 18 19.84	−18 20 17.9		5											
365A	2224−273 1	22 27 43.26	−27 5 1.7	J	219	233				−1.18	0.07	ehl	uv	P	< 1.5	
365B	2226+162 1	22 26 17.94	16 17 47.7	B	29	87				−1.19	0.06	eln	uvx	D	9.8	168
	2226+162 2	22 26 17.81	16 17 57.3		19											
178 365B	2231+015 1	22 31 12.24	1 34 55.6	B	77	311	0.83			−1.18	0.04	deghijlmnopq		D	6.3	0
	2231+015 2	22 31 12.23	1 35 1.8		165											
38B	2235+642 1	22 35 29.85	64 15 23.0	B	41	116		−1.08	0.05	−1.11	0.05	aelnop	uvw	D	43.9	77
	2235+642 2	22 35 23.29	64 15 12.8		9											
408A	2236−047 1	22 39 32.79	−4 29 32.4	J	58	384	0.95			−1.54	0.03	ghjlm		DF	16.5	16
365A	2238+033 1	22 40 52.98	3 36 35.8	J	89	216	0.63			−0.97	0.06	ehijlnopq	r	D	5.1	65
	2238+033 2	22 40 52.69	3 36 33.8		39											

© European Southern Observatory • Provided by the NASA Astrophysics Data System

1994A&AS..108...79R

Appendix A. continued

	Source	R.A. h m s	Decl ° ′ ″		S_{peak} mJy	S_{int} mJy	$\frac{S^{VLA}_{int}}{S_{GB}}$	α_l	$\Delta\alpha_l$	α_h	$\Delta\alpha_h$			R ″	PA °
(1)	(2)	(3)	(4)	(5)	(6)	(7)	(8)	(9)	(10)	(11)	(12)	(13)	(14)	(15)	(16)	(17)
365A	2242+274 1	22 45 5.19	27 42 47.0	J	18	236	0.95			−1.09	0.04	eijlnopq	r	T	23.2	121
	2242+274 2c	22 45 4.26	27 42 54.8		6											
	2242+274 3	22 45 3.72	27 42 59.1		140											
408B	2242−304 1	22 45 10.93	−30 12 54.0	J	13	169				−1.56	0.09	hl	v	T	32.4	128
	2242−304 2c	22 45 9.89	−30 12 41.7		4											
	2242−304 3	22 45 8.98	−30 12 34.2		17											
365B	2243+174 1	22 43 36.12	17 28 11.0	B	83	415	0.69			−1.20	0.03	ejlnopq		D	36.0	55
	2243+174 2	22 43 33.99	17 27 49.9		9											
178	2245+181 1	22 48 16.26	18 26 50.9	J	295	413	0.82			−1.11	0.03	dghjlmopq		D	5.5	98
	2245+181 2	22 48 15.89	18 26 51.7		39											
178	2246−022 1	22 48 54.94	−1 59 26.1	J	38	143	0.61			−1.22	0.04	dghjlm		DF	4.0	126
365B	2247+034 1	22 47 46.22	3 24 11.3	B	98	146	1.01			−1.22	0.05	ejln	x	P	3.0	24
178	2247+036 1	22 49 44.85	3 57 32.3	J	7	114	0.67			−1.11	0.04	dijlmnopq		D	19.1	132
	2247+036 2	22 49 42.94	3 57 58.2		9											
365B	2247+052 1	22 47 50.19	5 14 21.5	B	79	191	0.82			−1.19	0.04	ejlnopq		D	59.2	27
	2247+052 2	22 47 51.92	5 15 14.4		30											
408A	2251−089 1	22 53 40.37	−8 40 43.6	J	206	388				−1.13	0.04	ghlm	v	P	4.5	6
365A	2254+061 1	22 57 28.75	6 24 24.6	J	197	292	0.70			−0.88	0.04	ehijlnopq	*bcdr	P	3.2	127
365A	2258−109 1	23 0 45.85	−10 38 50.9	J	9	180				−1.37	0.08	ehl	uv	DF	30.1	90
	2258−109 2	23 0 44.51	−10 38 52.4		12											
	2258−109 3	23 0 44.06	−10 38 51.0		9											
38B	2259+643 1	22 59 40.96	64 20 48.4	B	35	110		−0.93	0.05	−1.15	0.06	aeln	uvx	D	85.4	164
	2259+643 2	22 59 37.33	64 22 10.7		24											
38B	2310+667 1	23 10 43.00	66 45 35.6	B	63	173	1.06	−0.93	0.05	−1.23	0.04	aejlnopq		D	4.2	58
	2310+667 2	23 10 43.57	66 45 37.8		69											
38C	2311+655 1	23 11 47.50	65 33 24.5	B	7	30		−1.24	0.03	−1.24	0.03	al	v	DF	5.0	28
408B	2311−308 1	23 14 17.37	−30 37 27.9	J	11	219				−1.42	0.08	hl	v	T	32.7	119
	2311−308 2c	23 14 15.96	−30 37 17.7		8											
	2311−308 3	23 14 15.31	−30 37 14.8		13											
365A	2313+318 1	23 15 33.32	32 10 10.3	J	70	198	0.60			−1.10	0.07	eijlnopq	*ar	D	3.3	16
	2313+318 2	23 15 33.38	32 10 13.2		126											
38B	2313+694 1	23 13 34.11	69 29 32.3	B	26	129	0.93	−0.97	0.05	−0.90	0.05	aejlnopq	*cdf	D	25.8	61
	2313+694 2	23 13 38.30	69 29 44.7		10											
365B	2317+120 1	23 17 36.47	12 5 38.3	B	69	238	1.00			−1.28	0.04	ejlnopq		D	3.6	32
	2317+120 2	23 17 36.59	12 5 41.4		129											
38B	2317+651 1	23 17 49.48	65 8 34.3	B	18	58		−1.26	0.05	−1.04	0.06	aeln	uvx	D	13.9	29
	2317+651 2	23 17 48.48	65 8 22.8		11											
38B	2319+642 1	23 19 38.63	64 12 42.0	B	92	190		−1.18	0.05	−1.03	0.03	aelnop	uvw	T	43.9	95
	2319+642 2c	23 19 35.35	64 12 40.0		5											
	2319+642 3	23 19 32.04	64 12 45.5		12											
365B	2324+071 1	23 24 2.64	7 7 12.1	B	3	146	0.74			−1.16	0.04	ejlnopq		DF	70.8	0
	2324+071 2	23 24 2.72	7 8 19.7		3											
408B	2330−319 1	23 32 47.76	−31 37 34.9	J	117	361				−1.06	0.08	hl	v	T	24.3	106
	2330−319 2c	23 32 46.82	−31 37 30.7		8											
	2330−319 3	23 32 45.95	−31 37 28.4		59											
365B	2331+095 1	23 31 37.15	9 30 12.8	B	161	182	0.89			−1.37	0.10	ejln	x	P	< 1.5	
408B	2332−348 1	23 35 35.51	−34 33 34.9	J	80	342				−1.05	0.08	hl	v	D	5.9	176
	2332−348 2	23 35 35.49	−34 33 29.3		171											
365B	2334+178 1	23 34 45.54	17 50 53.8	B	45	130	0.96			−1.20	0.05	ejlnopq		D	23.5	46
	2334+178 2	23 34 46.69	17 51 10.2		15											

	Source	R.A. h m s	Decl ° ′ ″		S_{peak} mJy	S_{int} mJy	$\frac{S^{VLA}_{int}}{S_{GB}}$	α_l	$\Delta\alpha_l$	α_h	$\Delta\alpha_h$			R ″	PA °
(1)	(2)	(3)	(4)	(5)	(6)	(7)	(8)	(9)	(10)	(11)	(12)	(13)	(14)	(15)	(16)	(17)
365A	2335−125 1	23 38 8.09	−12 18 50.9	J	170	400				−0.87	0.06	ehl	uv	P	4.1	133
178	2336−023 1	23 39 6.54	−2 4 43.0	J	33	199	0.58			−1.15	0.05	dghjlmpq		D	10.3	55
	2336−023 2	23 39 7.11	−2 4 37.2		82											
408B	2336−332 1	23 39 12.97	−33 1 10.5	J	33	298				−1.09	0.09	hl	v	P	< 1.5	
365B	2339+189 1	23 39 53.18	18 58 56.0	B	58	195	0.77			−1.17	0.04	ejlnopq		D	24.9	105
	2339+189 2	23 39 51.44	18 59 2.3		12											
178	2339+260 1	23 41 53.87	26 20 49.1	J	96	260	0.88			−1.17	0.06	djklmopq	*a	D	17.3	175
	2339+260 2	23 41 53.76	26 21 6.1		46											
408A	2339−096 1	23 42 7.49	−9 23 46.1	J	175	374				−1.16	0.04	ghlmr	v	D	3.7	77
	2339−096 2	23 42 7.24	−9 23 47.0		134											
365A	2342+071 1	23 44 59.49	7 24 13.6	J	202	224	1.26			−1.12	0.04	eijlnopq	r	P	< 1.5	
408B	2346−320 1	23 48 51.36	−31 44 11.8	J	20	283				−1.17	0.09	hl	v	D	22.4	55
	2346−320 2	23 48 49.89	−31 44 24.2		54											
365A	2350−018 1	23 52 50.23	−1 36 10.5	J	32	263	0.67			−0.74	0.07	ehjl	r	D	23.2	77
	2350−018 2	23 52 48.75	−1 36 15.3		10											
365A	2356+179 1	23 59 22.61	18 11 24.0	J	223	393	0.74			−0.82	0.04	ehijlnopq	r	D	9.2	180
	2356+179 2	23 59 22.62	18 11 33.0		27											
408A	2358−111 1	0 0 57.66	−10 54 32.4	J	188	348				−1.28	0.05	ghlm	v	P	4.3	28

© European Southern Observatory • Provided by the NASA Astrophysics Data System

1994A&AS..108...79R

1. 0141+356 A serendipitous double radio galaxy in the field is present about 1.5 minutes from components '1' and '2'.

2. 0309−047 Component 'A' is probably serendipitous.

3. 0707+810 This is resolved into two separate sources. The northern source has an asymmetric FRII structure; the southern a bright central component and low surface brightness lobes just detectable on the low-resolution VLA map. CLFST observations show that both sources have similar fluxes at 151-MHz ($\approx$ 100 mJy for the northern source and $\approx$ 150 mJy for the southern), but the southern source has a steeper spectral index; hence this object should dominate the flux at the selection frequency of 38-MHz.

4. 0906+691 The VLA map shows three diffuse components; a CLFST map shows two distinct sources, the southern of which is resolved into two components and may therefore either be a single large source or two smaller ones.

5. 1127+831 A Ryle Telescope map at 5GHz [calibrated and analysed as detailed in Lacy *et al.* (1993)] only detects component 1, but shows it to have a very steep radio spectrum ($\alpha_{5000}^{1490} = -1.1$), suggesting that it is some form of hotspot.

6. 1227+609 It is not clear whether the three components are related.

7. 1323+080 It is not clear if component '2' is real.

8. 1345−309 Diffuse radio source. Coordinates are derived from the moments of the source brightness.

9. 1350+635 This 80 arcsec source has a faint central component and diffuse lobes which barely show up on the VLA map. CLFST observations confirm the presence of the lobes.

10. 1436+157 The double radio galaxy with components 'A' and 'B' is probably not related to the double radio galaxy with components '1' and '2'.

11. 1611+452 It is not clear whether the three components belong to one source.

12. 1652+027 Two components separated by 233″, so may not be a single source.

13. 1659+440 Component A probably is probably a seperate serendipitous source.

14. 1718+630 Component '1' serendipitous or related to double radio source?

15. 1942+631 Component A related to central radio source ?

16. 2207+038 It is not clear whether the two components belong to one source.

17. 2324+071 Diffuse double lobed radio source. Position of lobes measure from the tapered maps.

18. 2335−125 It is not clear whether the two components belong to one source.

© European Southern Observatory • Provided by the NASA Astrophysics Data System

1994A&AS..108...79R

Appendix B. Radio maps

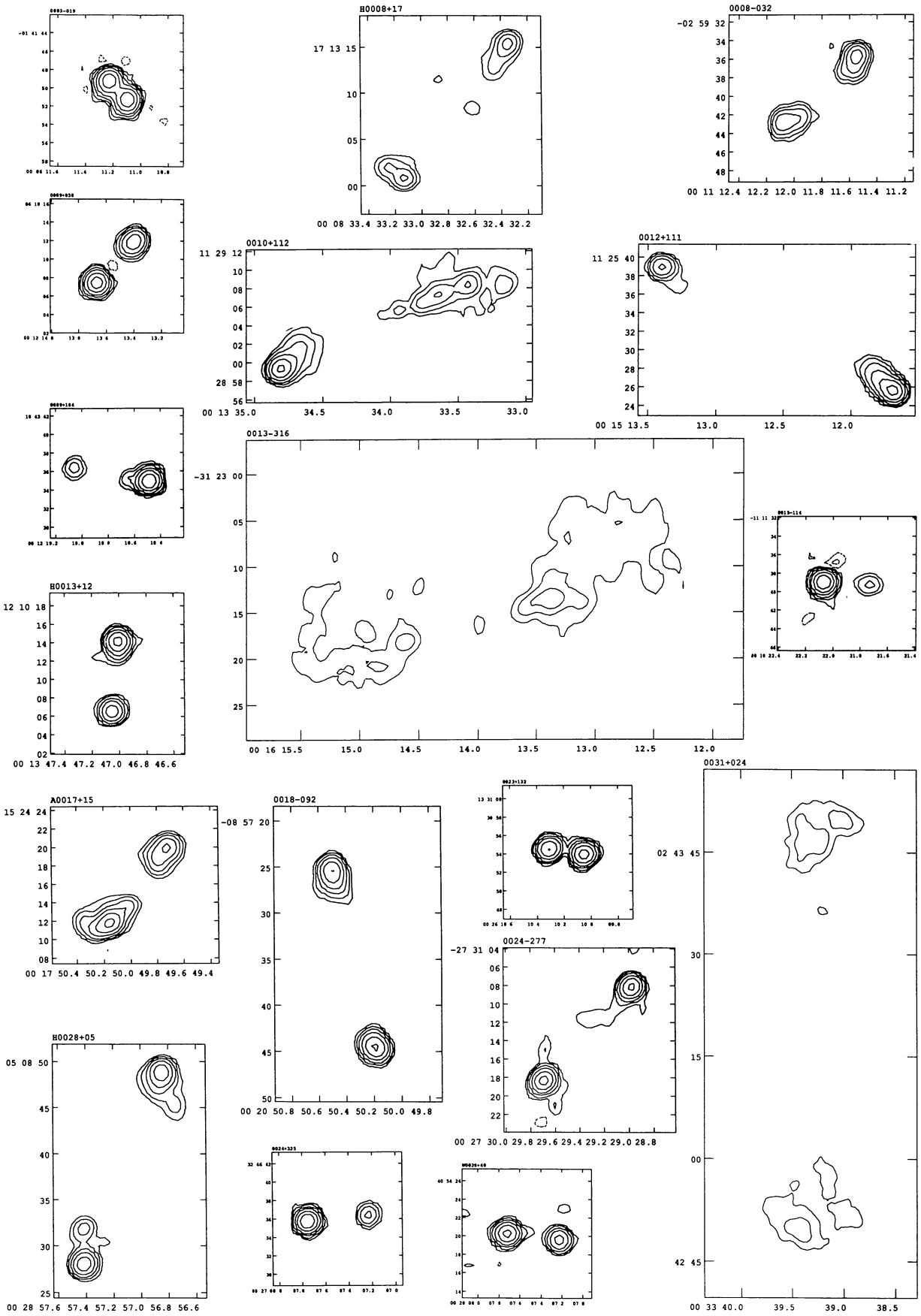

© European Southern Observatory • Provided by the NASA Astrophysics Data System

1994A&AS..108...79R

Appendix B. continued

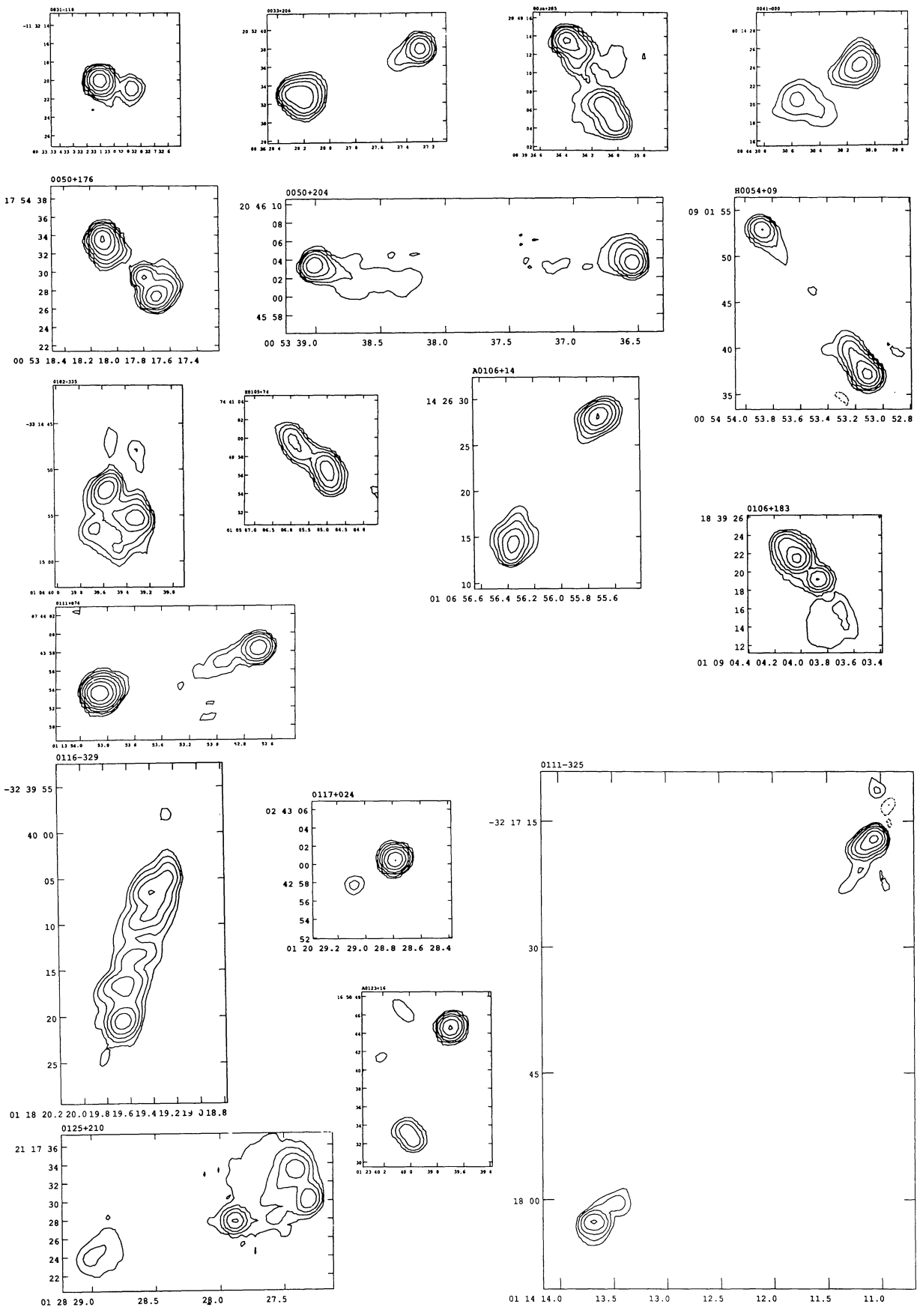

© European Southern Observatory • Provided by the NASA Astrophysics Data System

1994A&AS..108...79R

Appendix B. continued

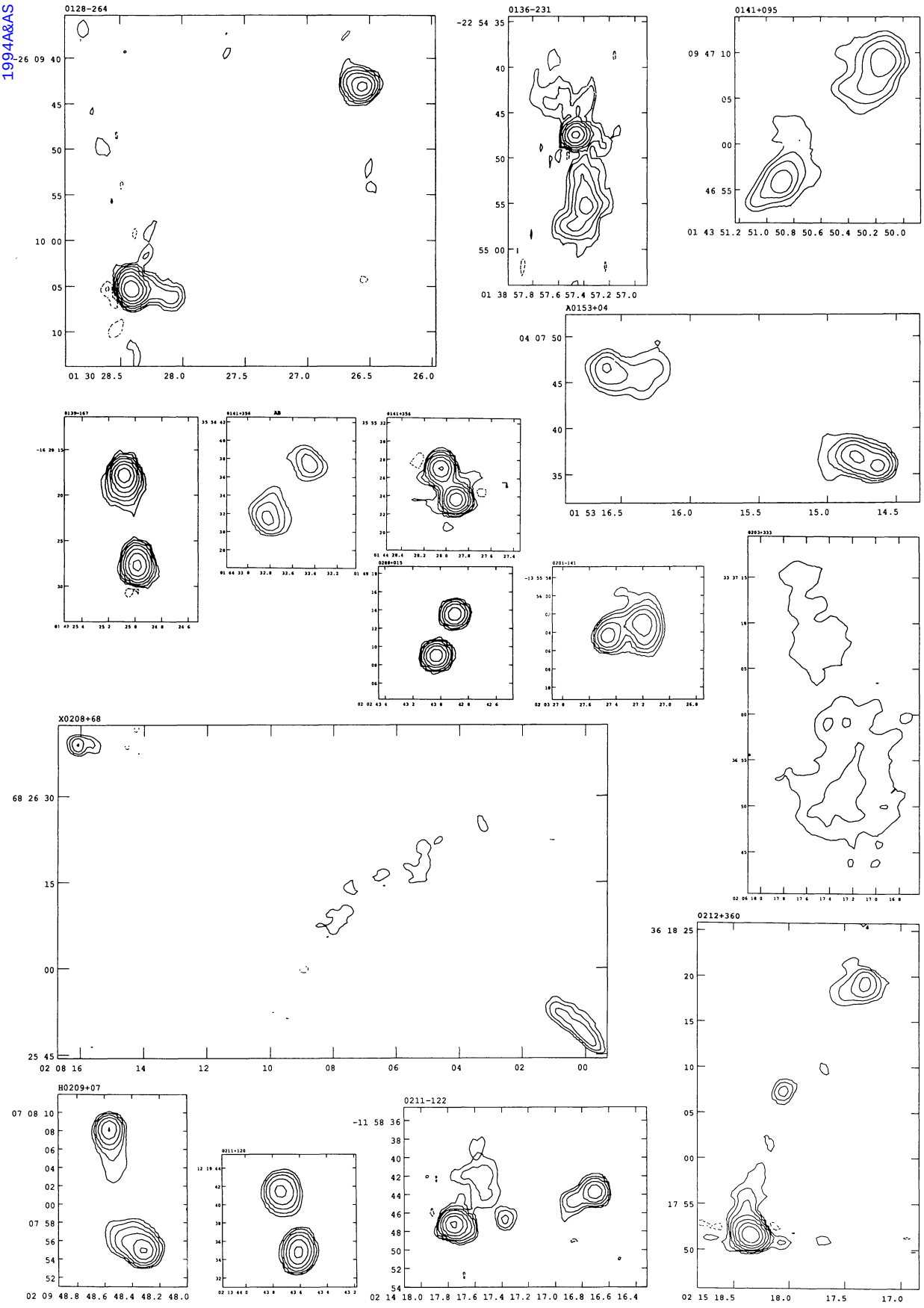

© European Southern Observatory • Provided by the NASA Astrophysics Data System

1994A&AS..108...79R

Appendix B. continued

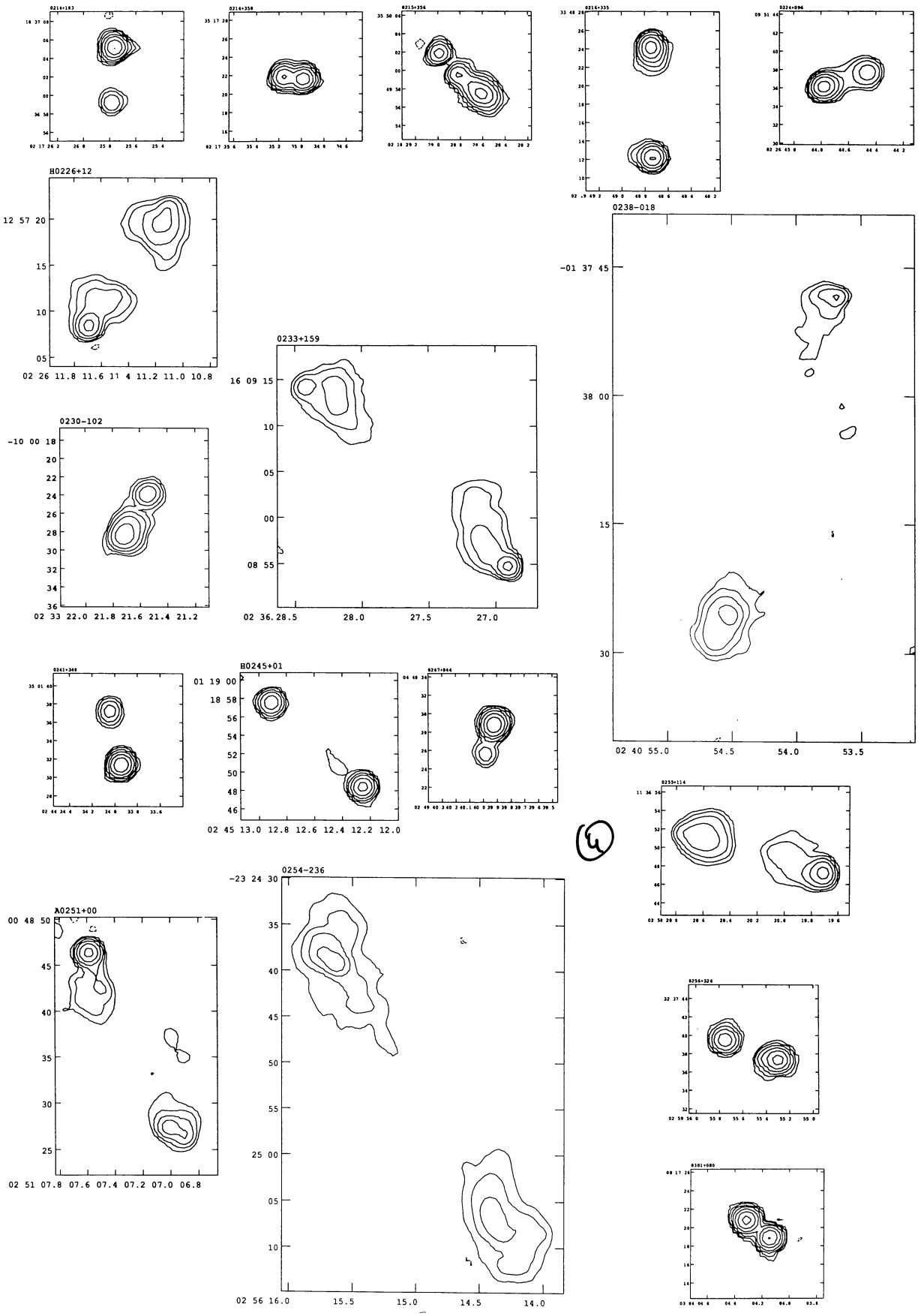

© European Southern Observatory • Provided by the NASA Astrophysics Data System

1994A&AS..108...79R

Appendix B. continued

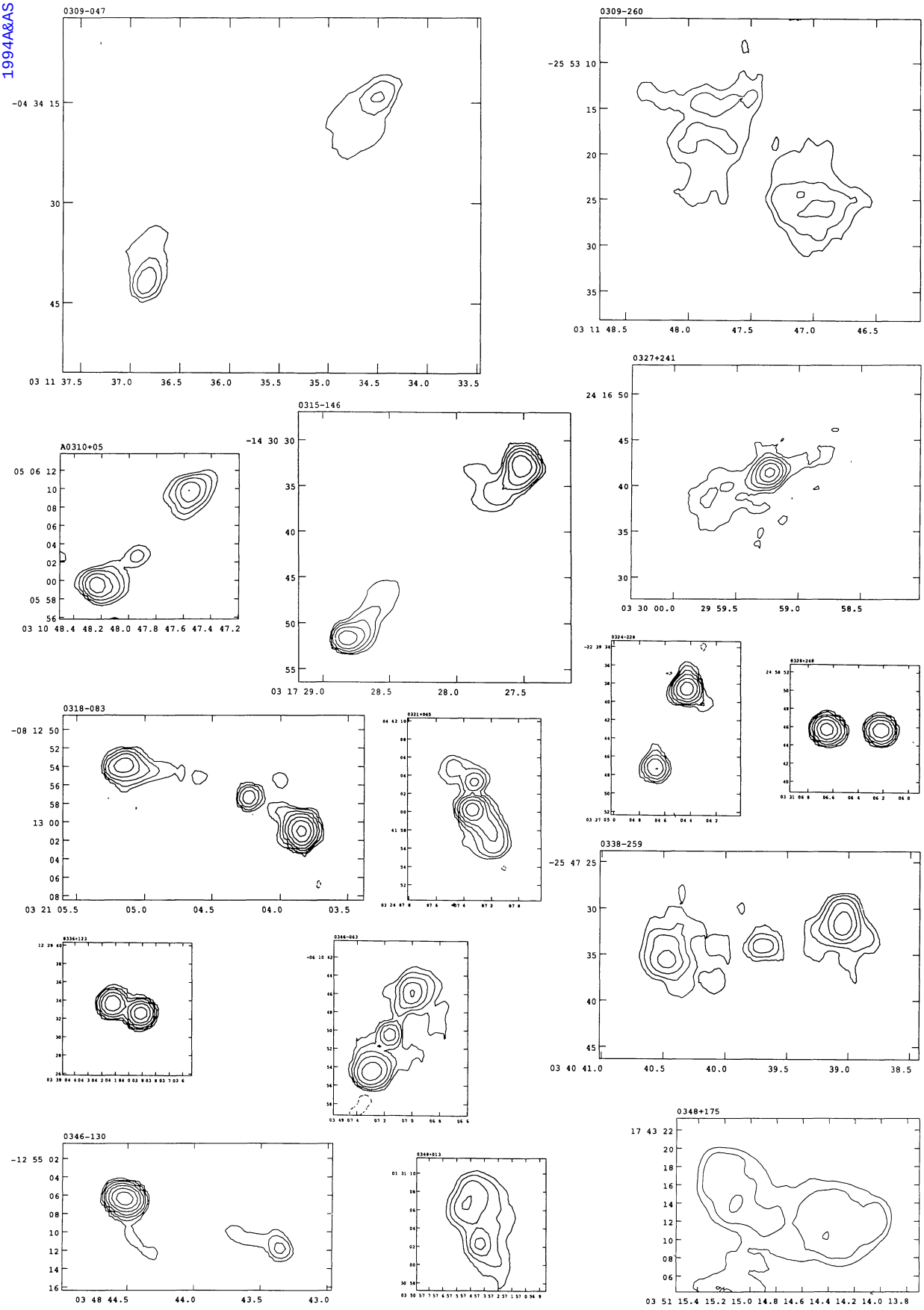

© European Southern Observatory • Provided by the NASA Astrophysics Data System

1994A&AS..108...79R

Appendix B. continued

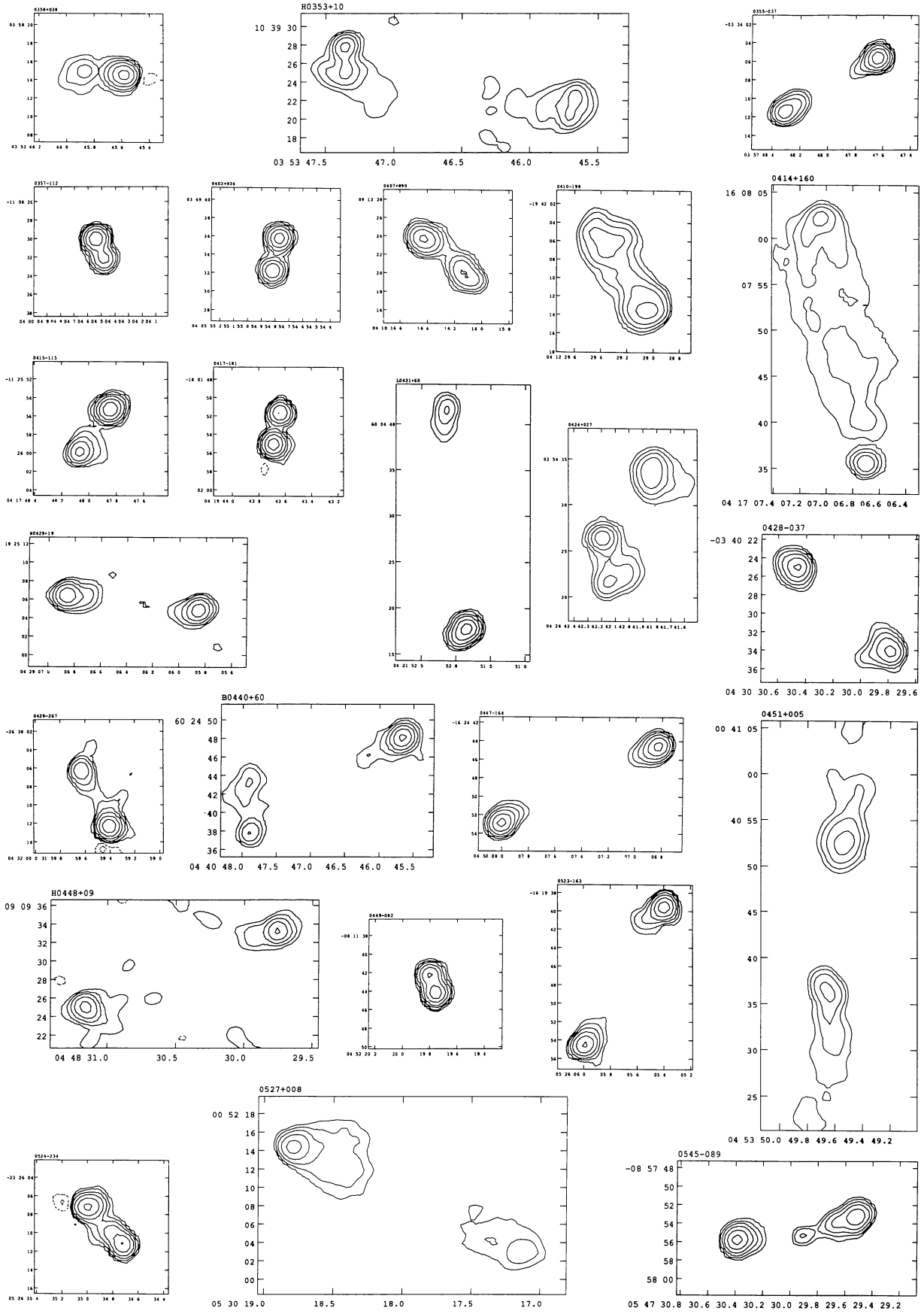

© European Southern Observatory • Provided by the NASA Astrophysics Data System

1994A&AS..108...79R

Appendix B. continued

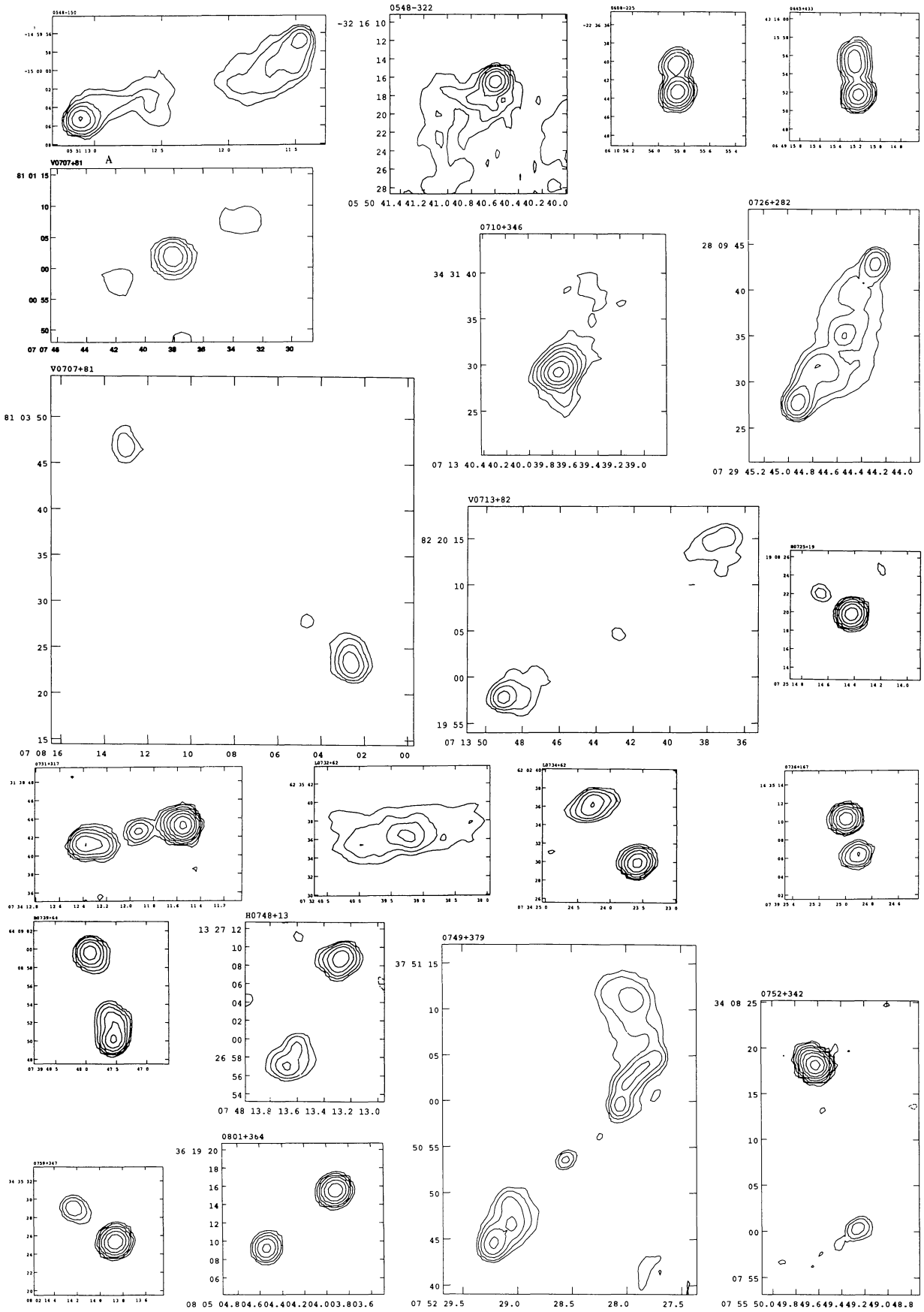

© European Southern Observatory • Provided by the NASA Astrophysics Data System

1994A&AS..108...79R

Appendix B. continued

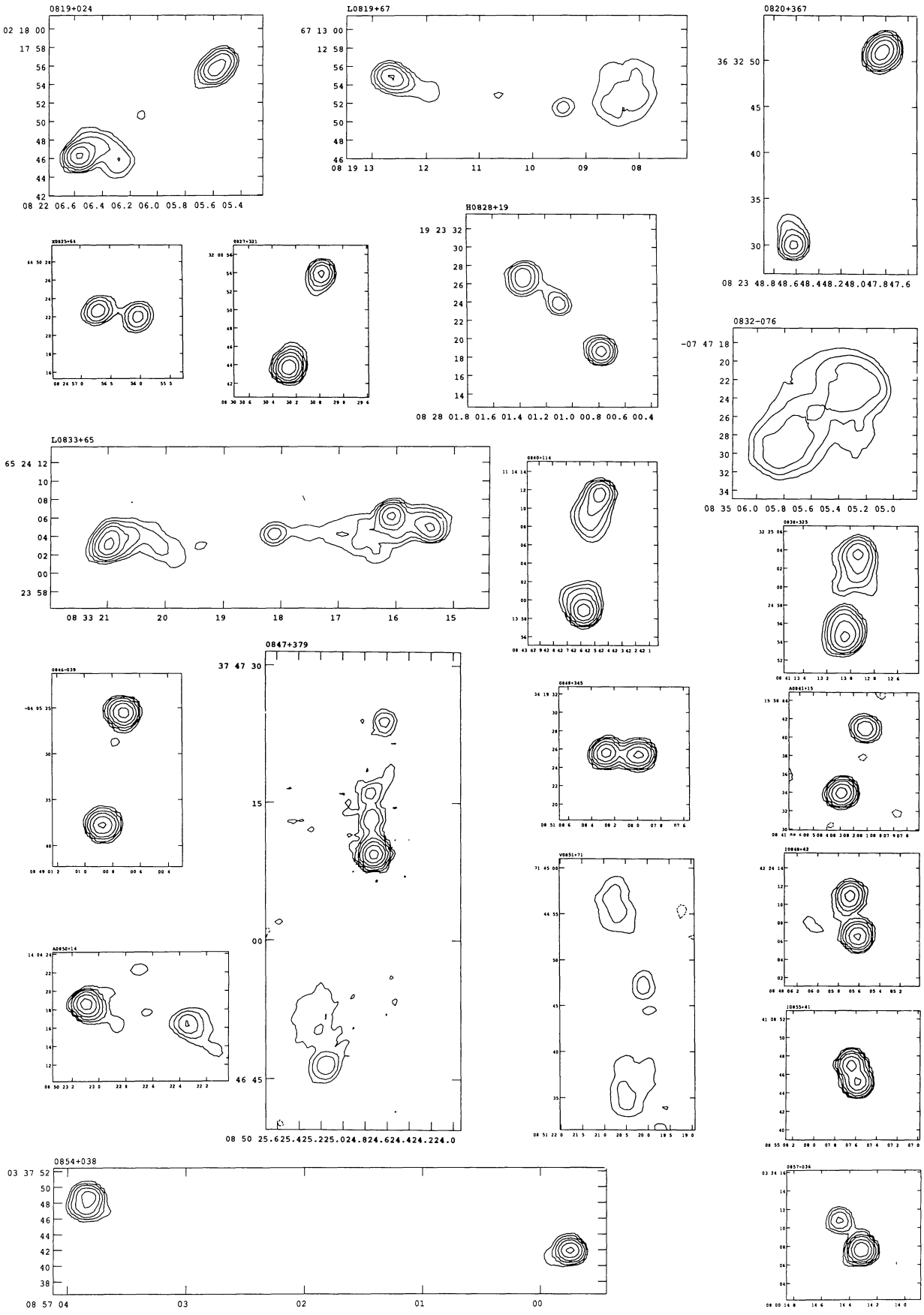

© European Southern Observatory • Provided by the NASA Astrophysics Data System

1994A&AS..108...79R

Appendix B. continued

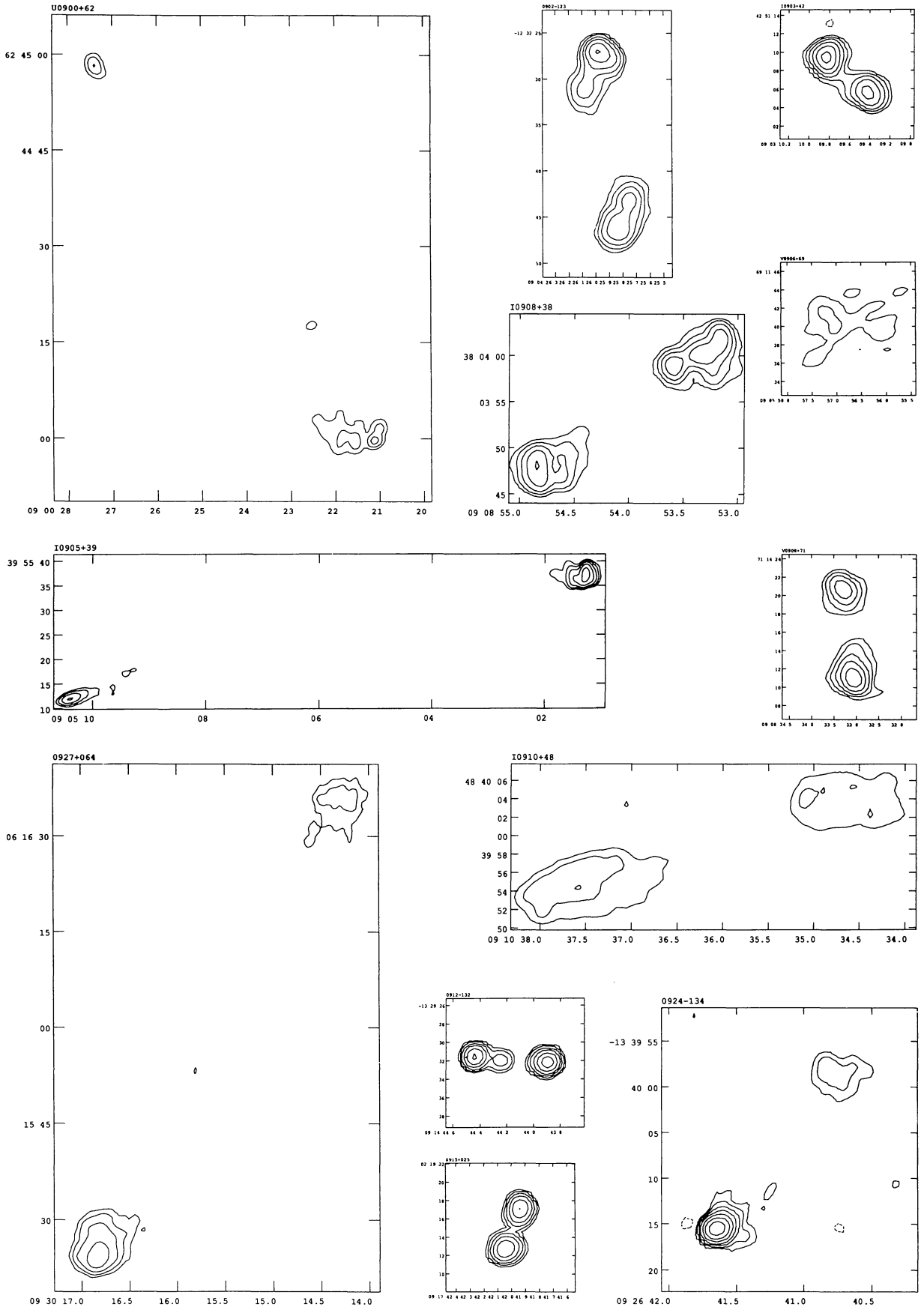

© European Southern Observatory • Provided by the NASA Astrophysics Data System

1994A&AS..108...79R

Appendix B. continued

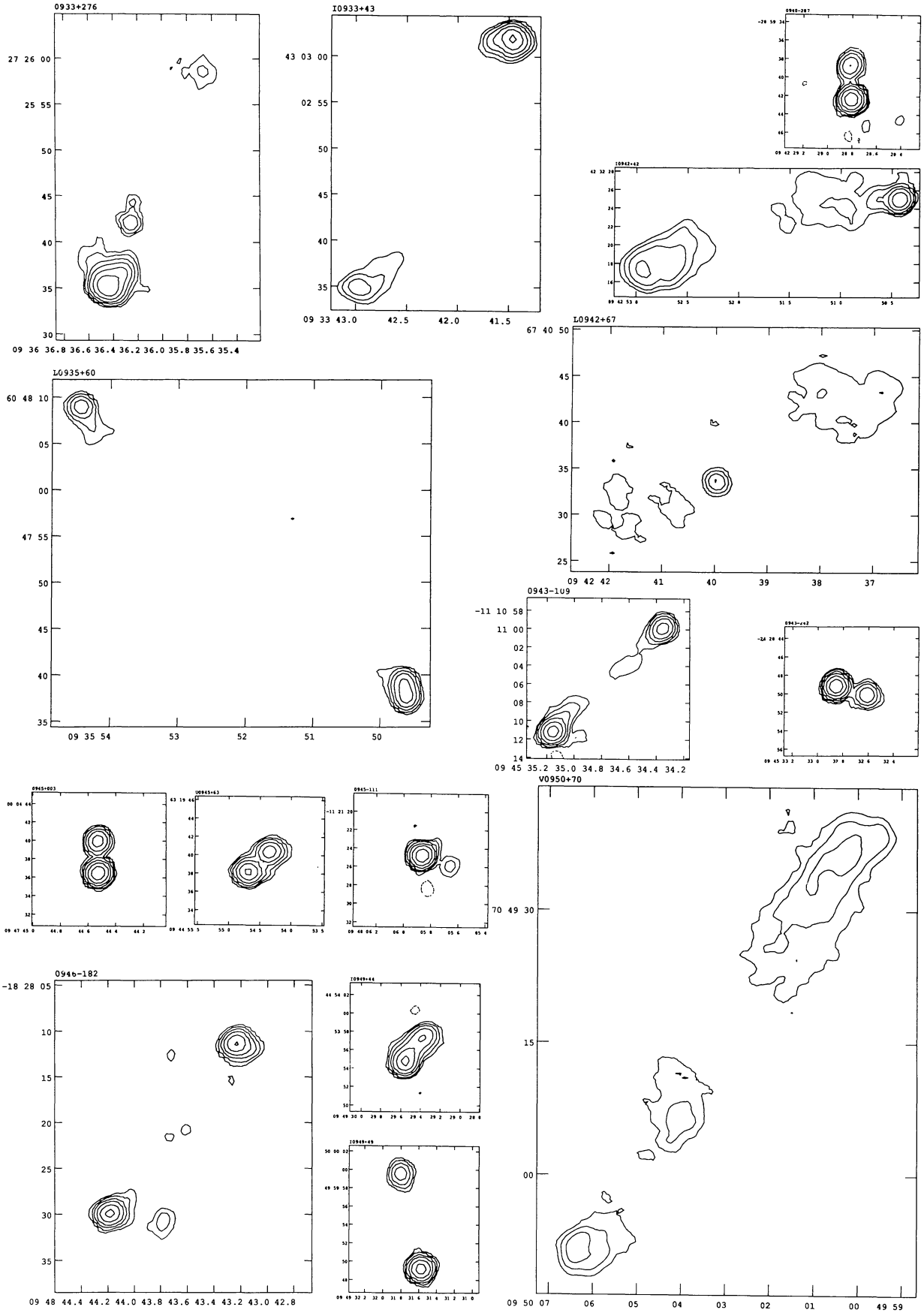

© European Southern Observatory • Provided by the NASA Astrophysics Data System

1994A&AS..108...79R

Appendix B. continued

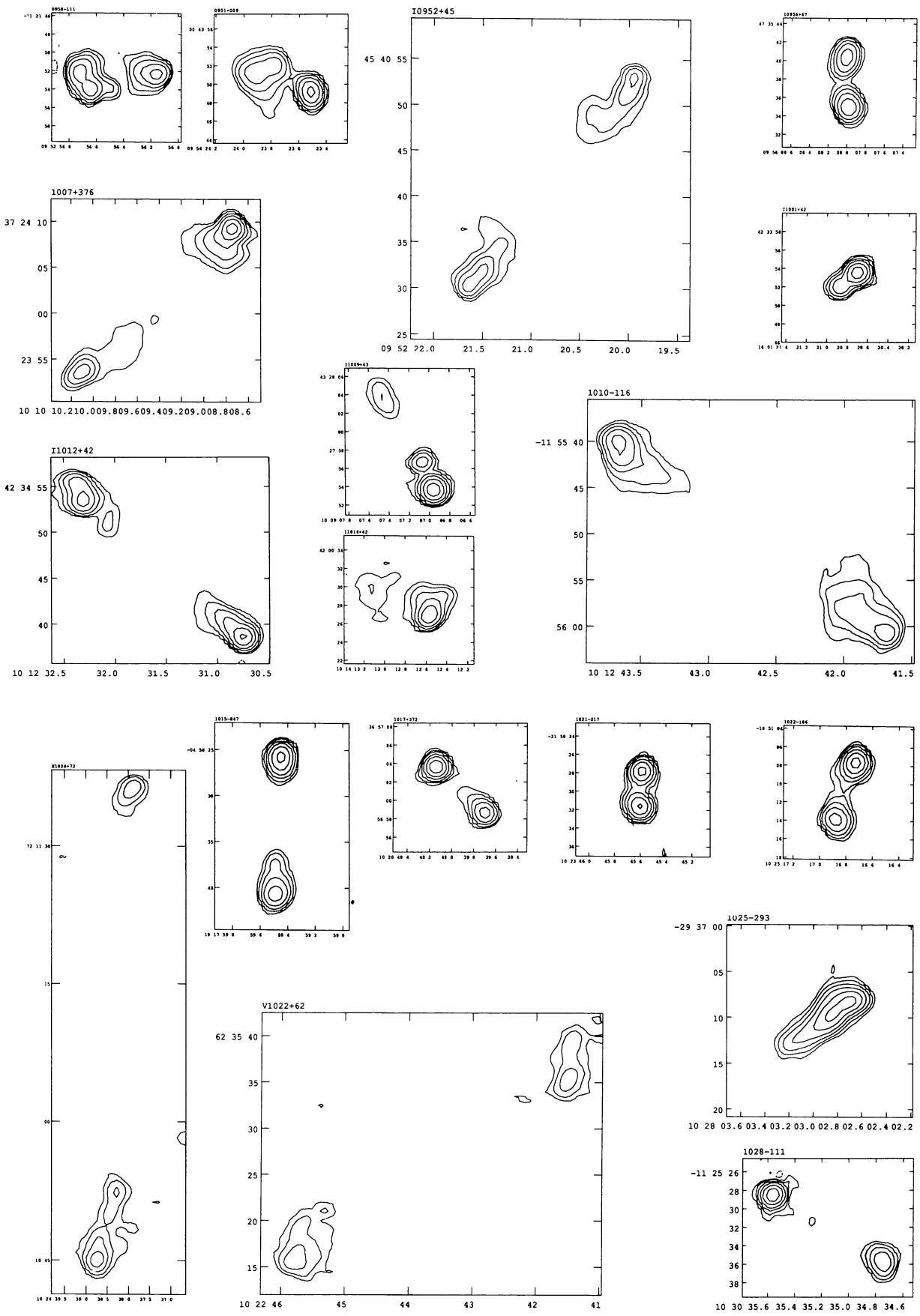

© European Southern Observatory • Provided by the NASA Astrophysics Data System

1994A&AS..108...79R

Appendix B. continued

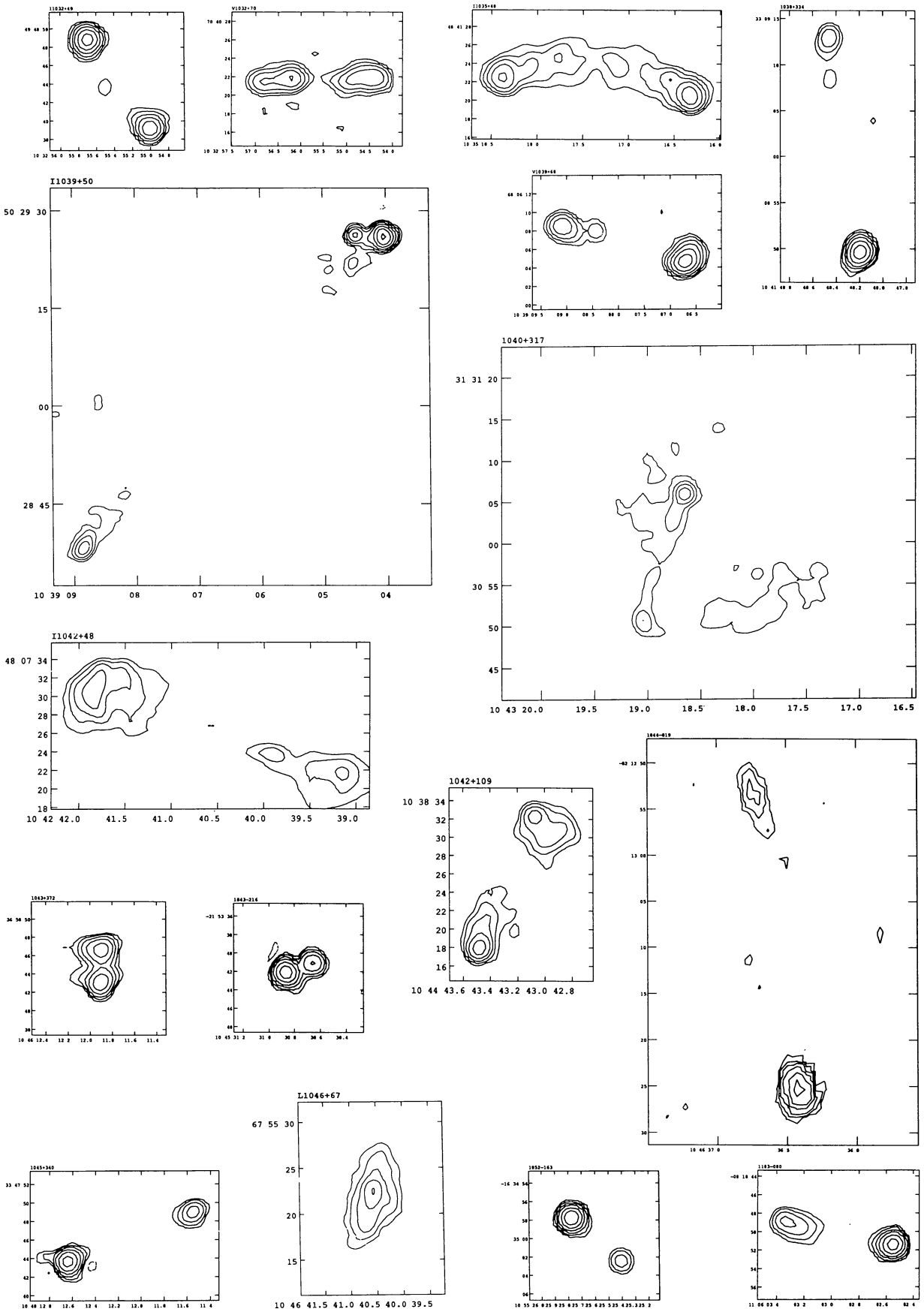

© European Southern Observatory • Provided by the NASA Astrophysics Data System

1994A&AS..108...79R

Appendix B. continued

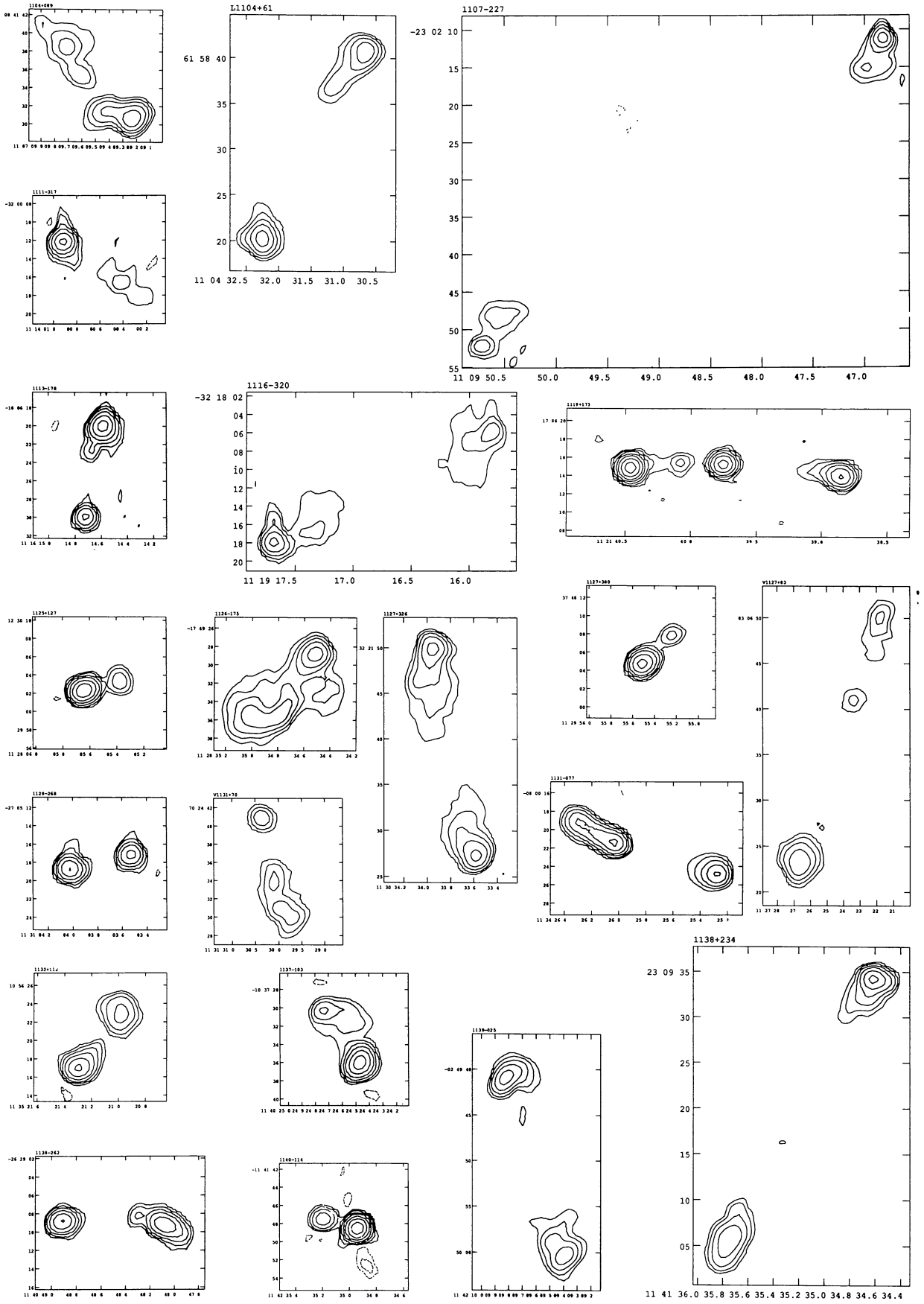

© European Southern Observatory • Provided by the NASA Astrophysics Data System

1994A&AS..108...79R

Appendix B. continued

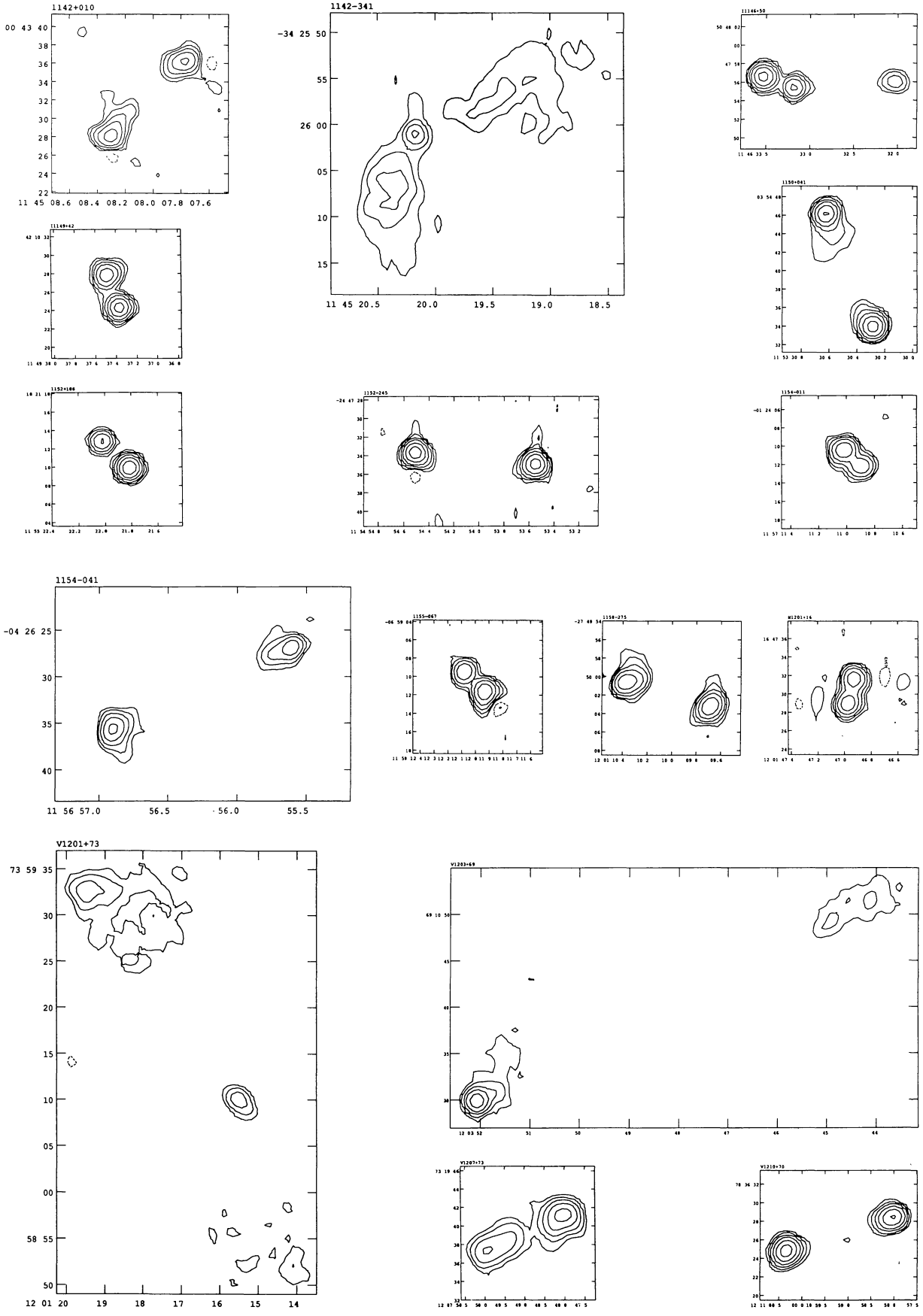

© European Southern Observatory • Provided by the NASA Astrophysics Data System

1994A&AS..108...79R

Appendix B. continued

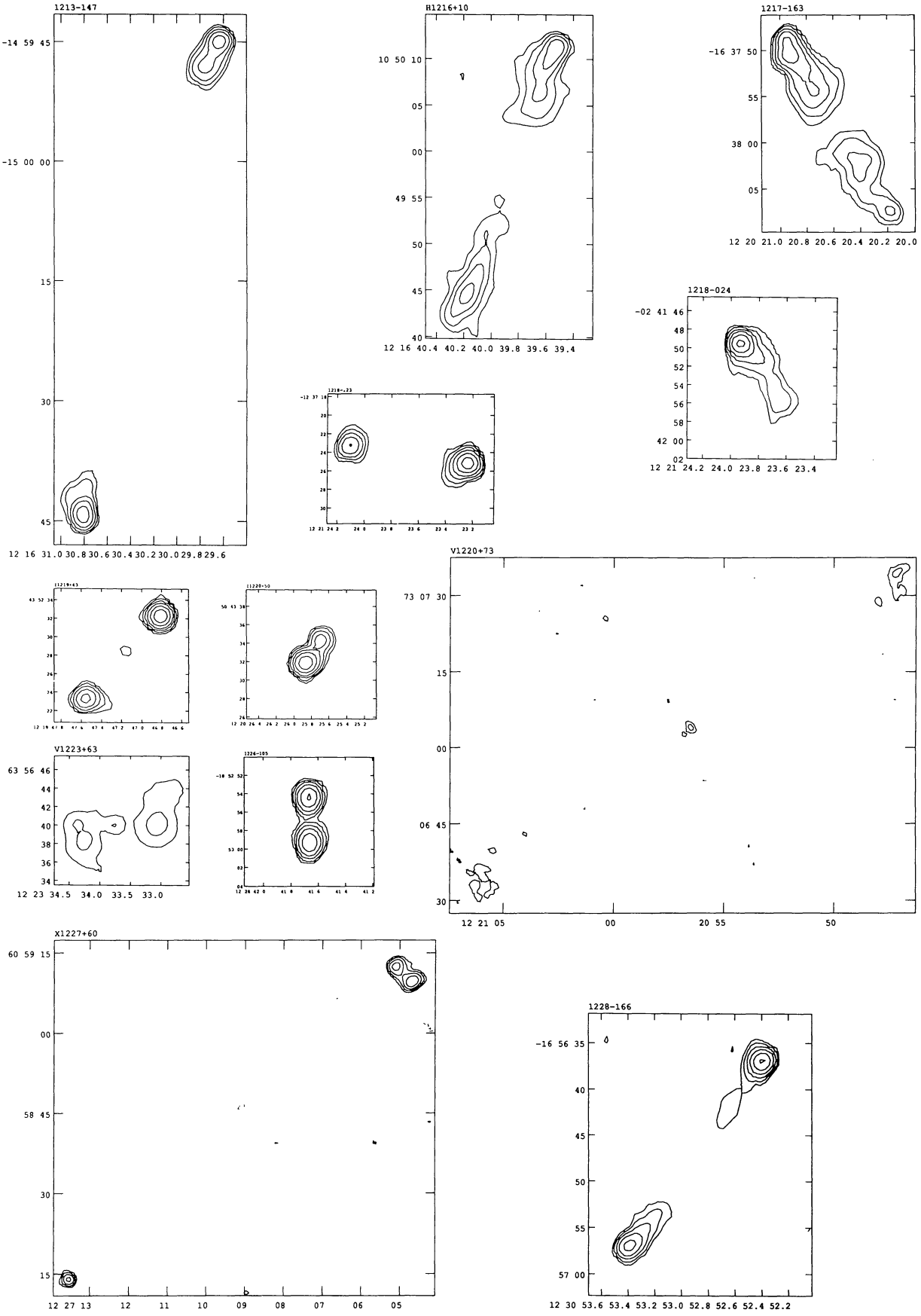

© European Southern Observatory • Provided by the NASA Astrophysics Data System

1994A&AS..108...79R

Appendix B. continued

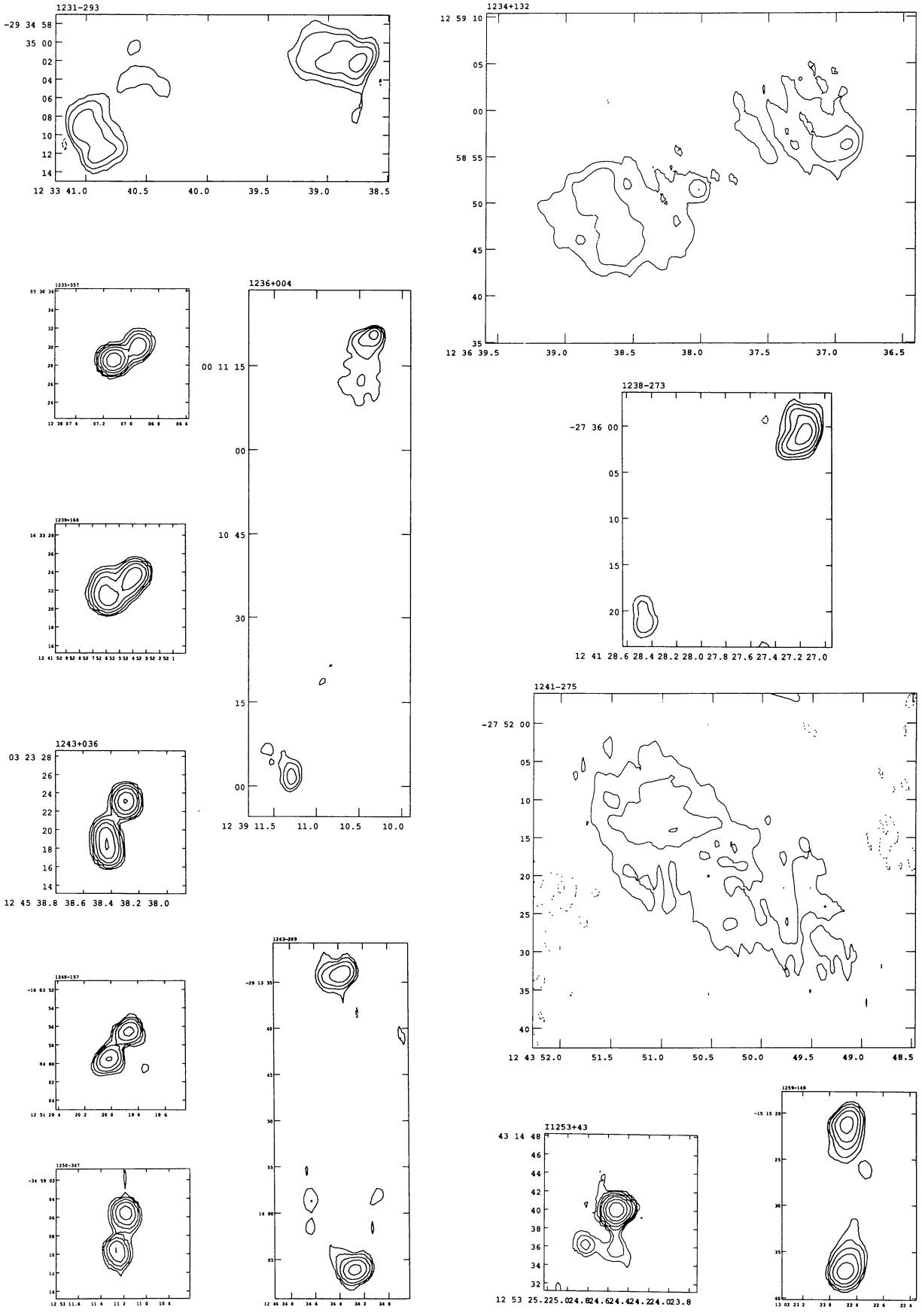

© European Southern Observatory • Provided by the NASA Astrophysics Data System

1994A&AS..108...79R

Appendix B. continued

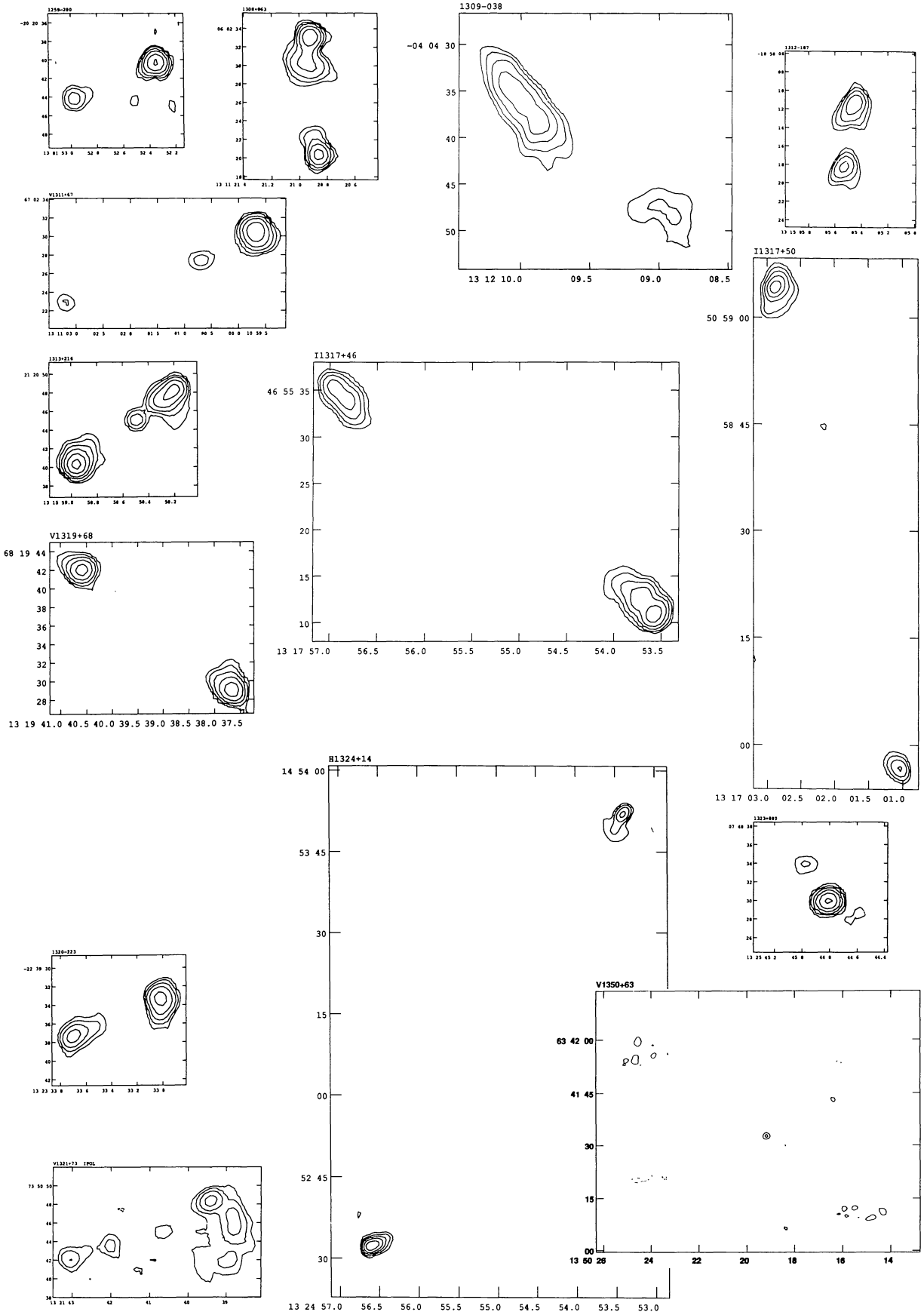

© European Southern Observatory • Provided by the NASA Astrophysics Data System

1994A&AS..108...79R

Appendix B. continued

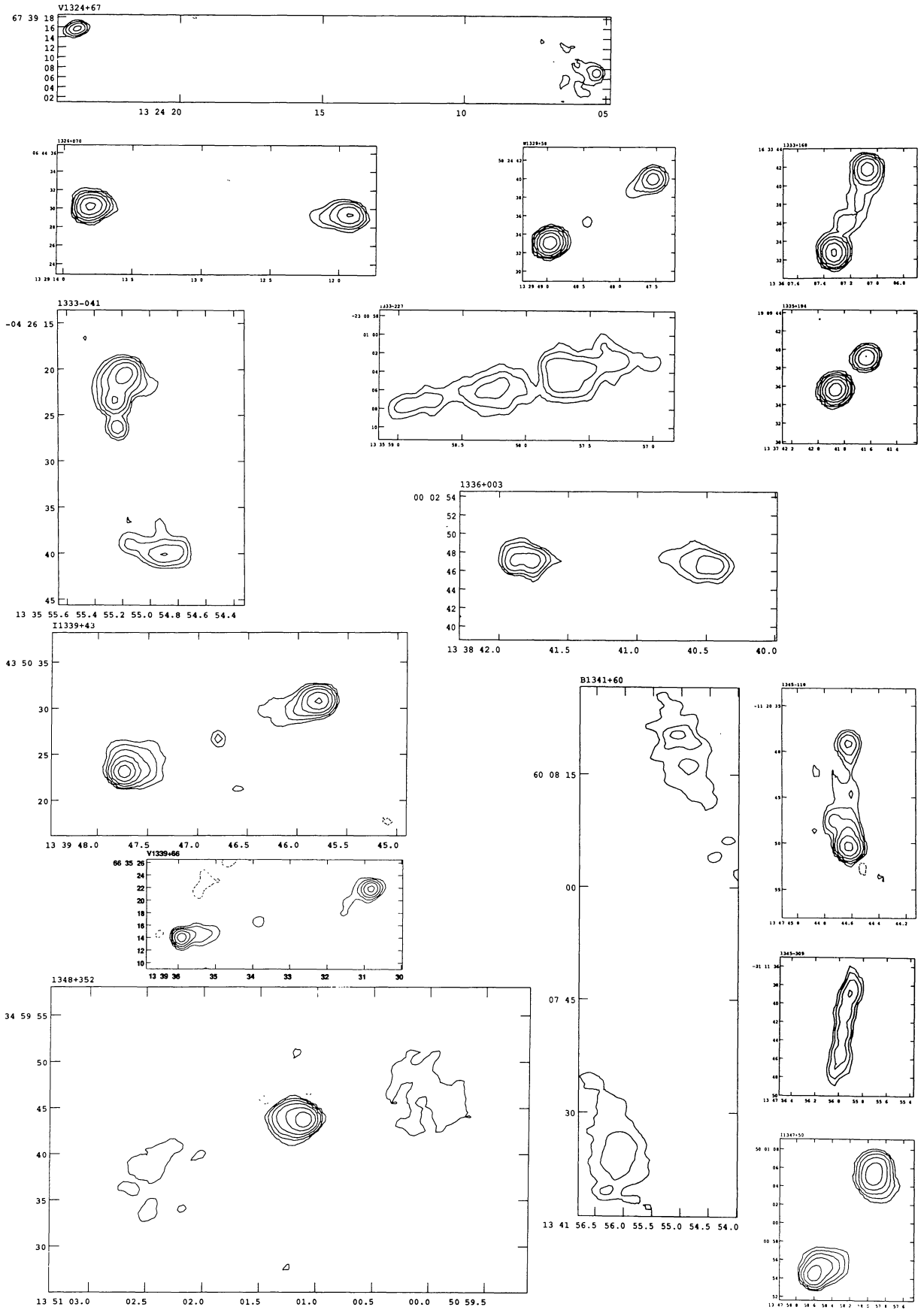

© European Southern Observatory • Provided by the NASA Astrophysics Data System

1994A&AS..108...79R

Appendix B. continued

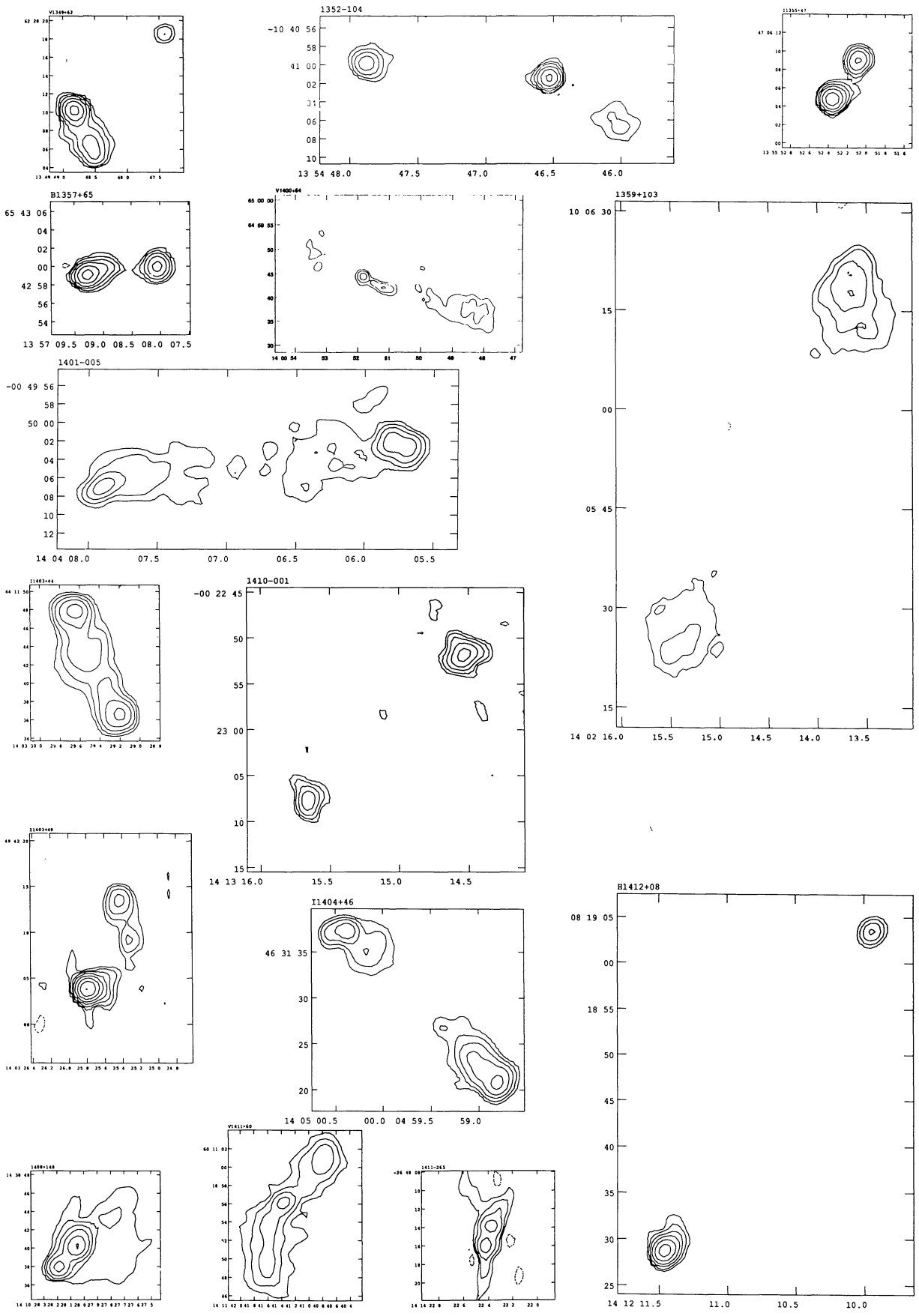

© European Southern Observatory • Provided by the NASA Astrophysics Data System

1994A&AS..108...79R

Appendix B. continued

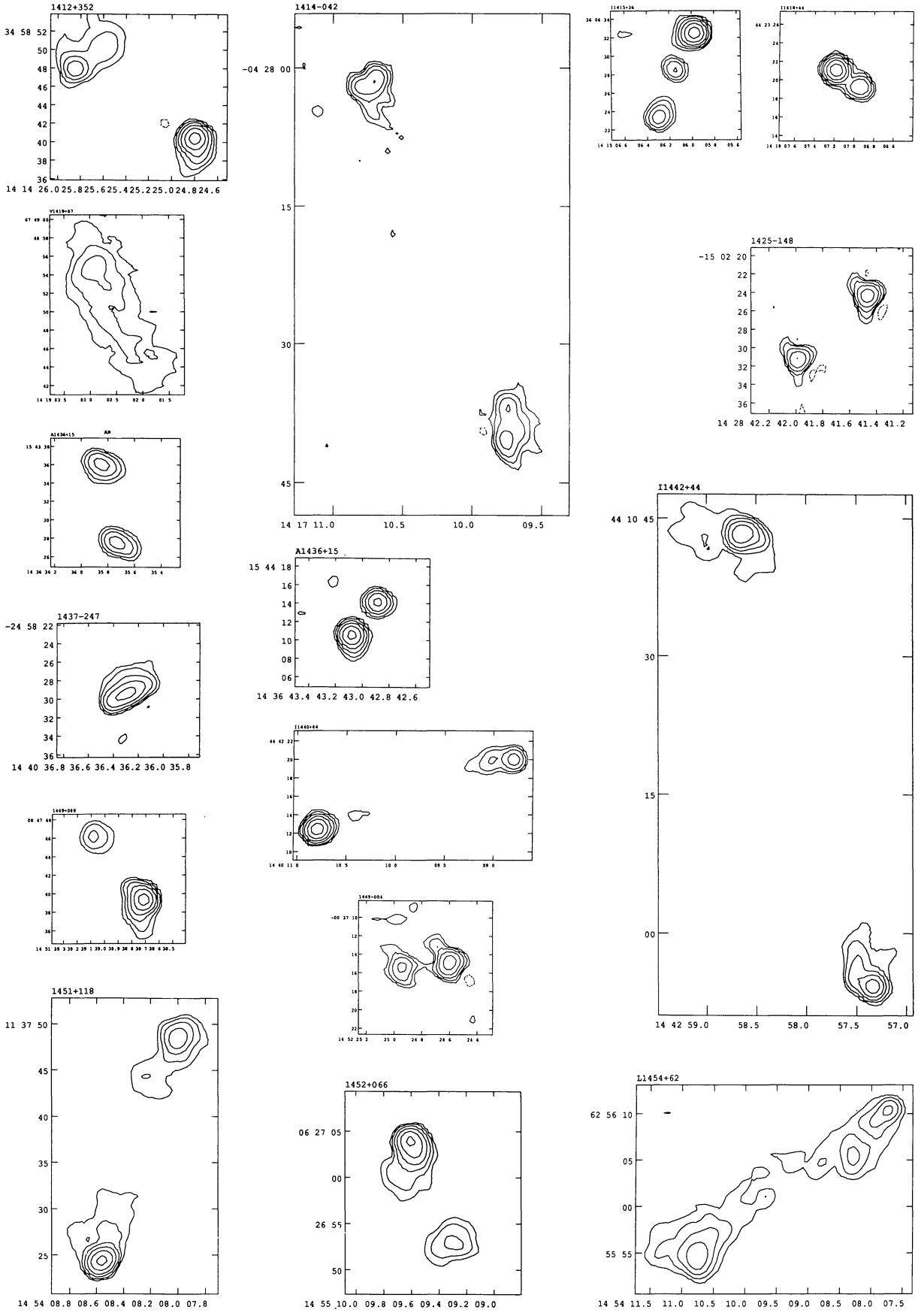

© European Southern Observatory • Provided by the NASA Astrophysics Data System

1994A&AS..108...79R

Appendix B. continued

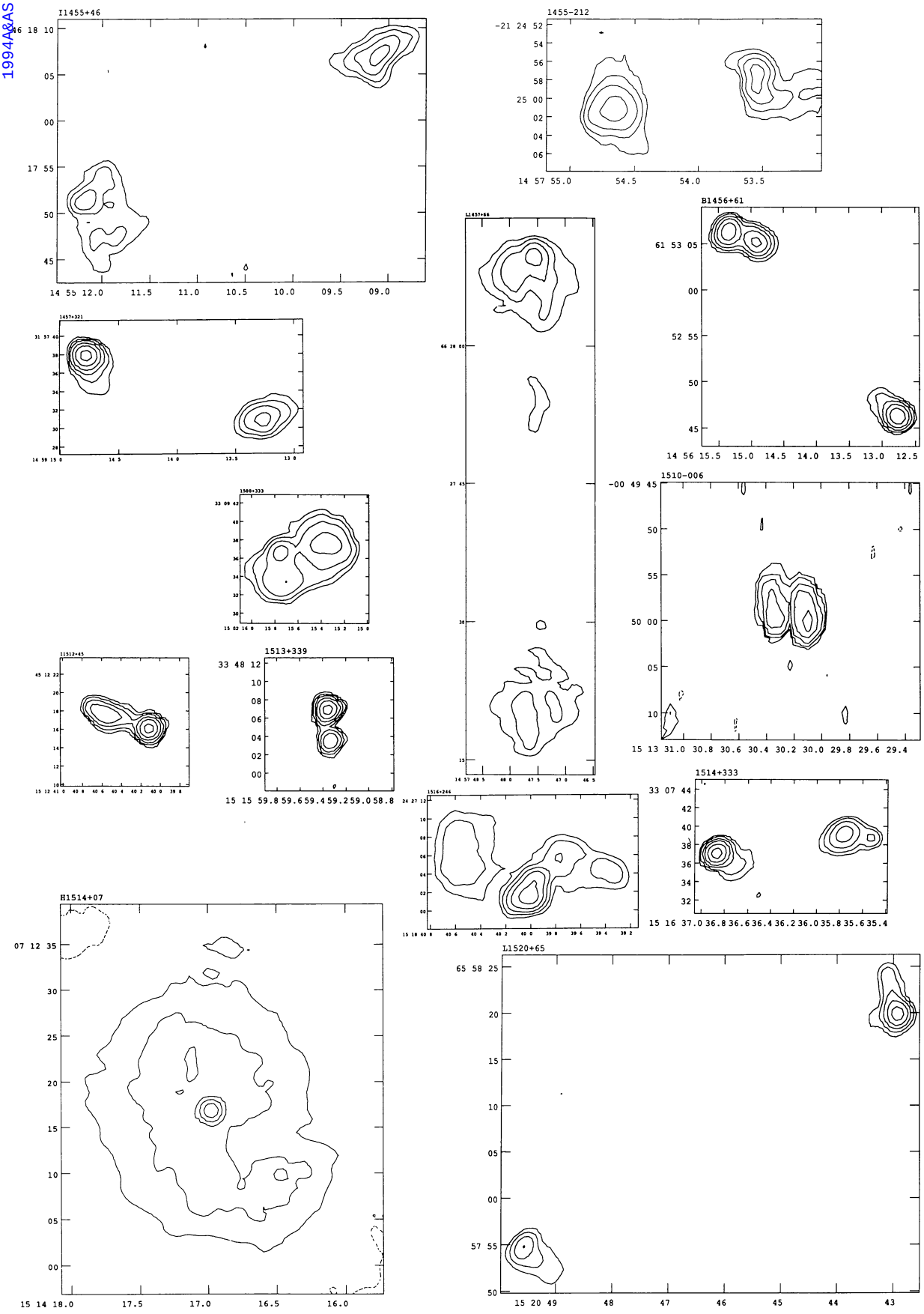

© European Southern Observatory • Provided by the NASA Astrophysics Data System

1994A&AS..108...79R

Appendix B. continued

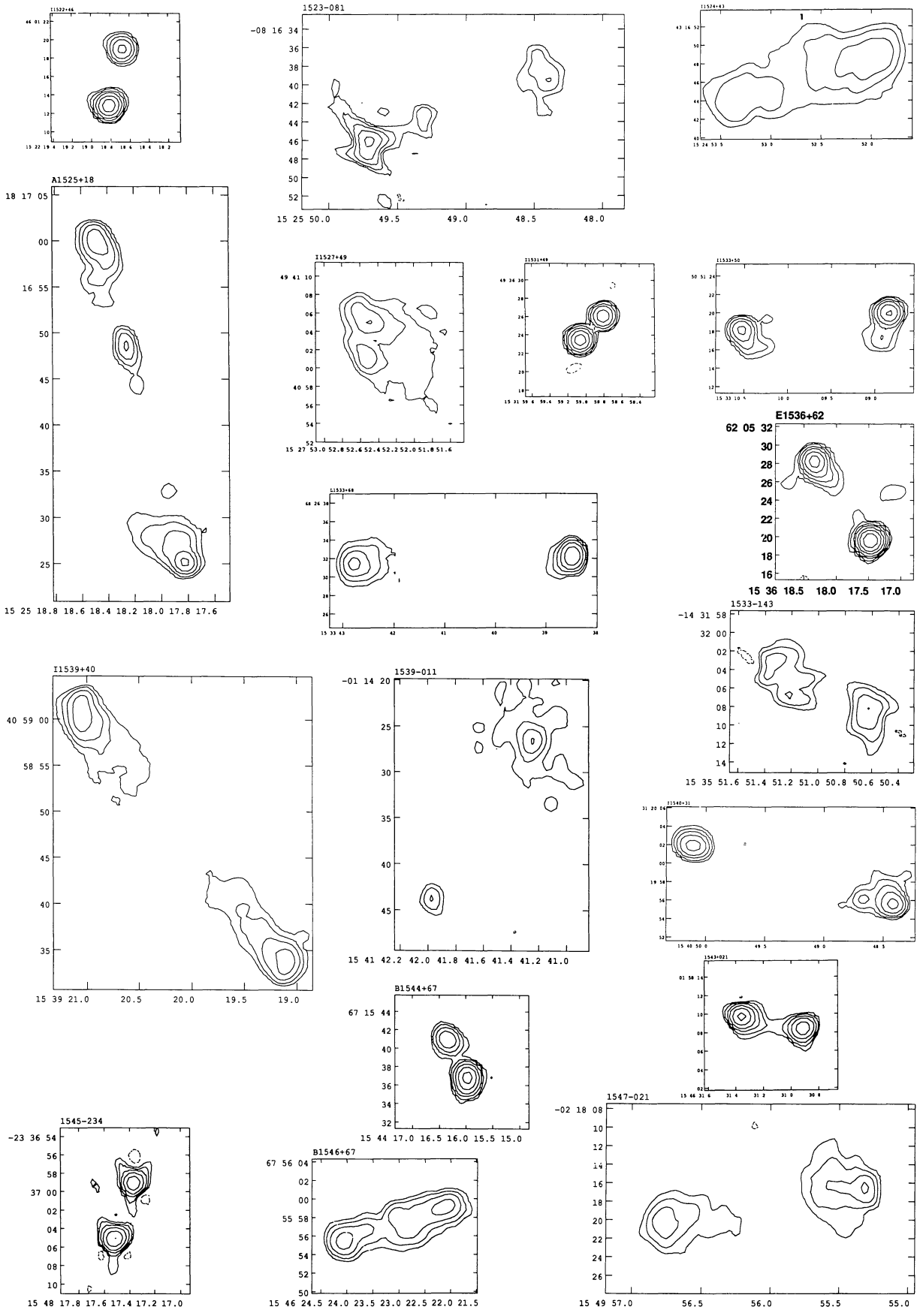

© European Southern Observatory • Provided by the NASA Astrophysics Data System

1994A&AS..108...79R

Appendix B. continued

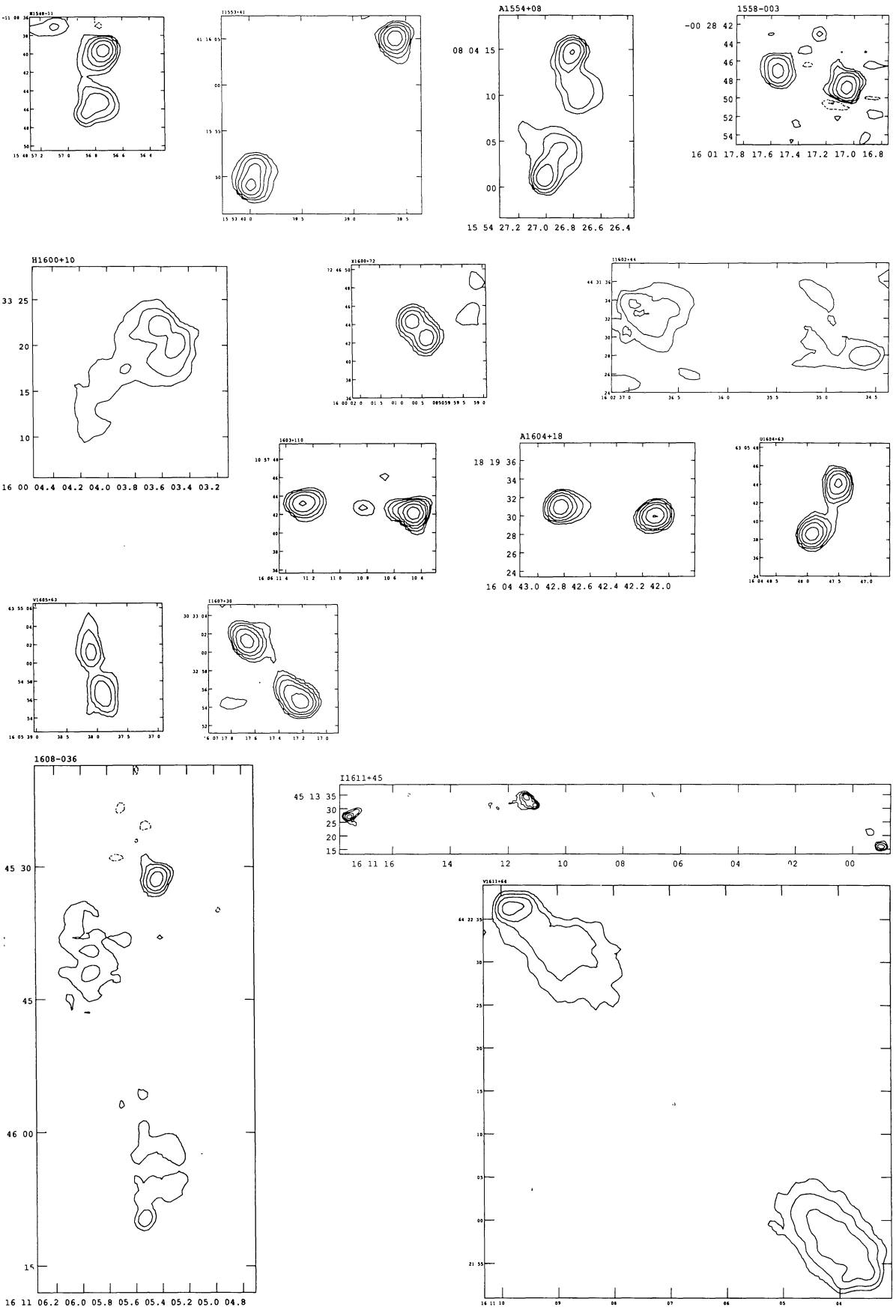

© European Southern Observatory • Provided by the NASA Astrophysics Data System

1994A&AS..108...79R

Appendix B. continued

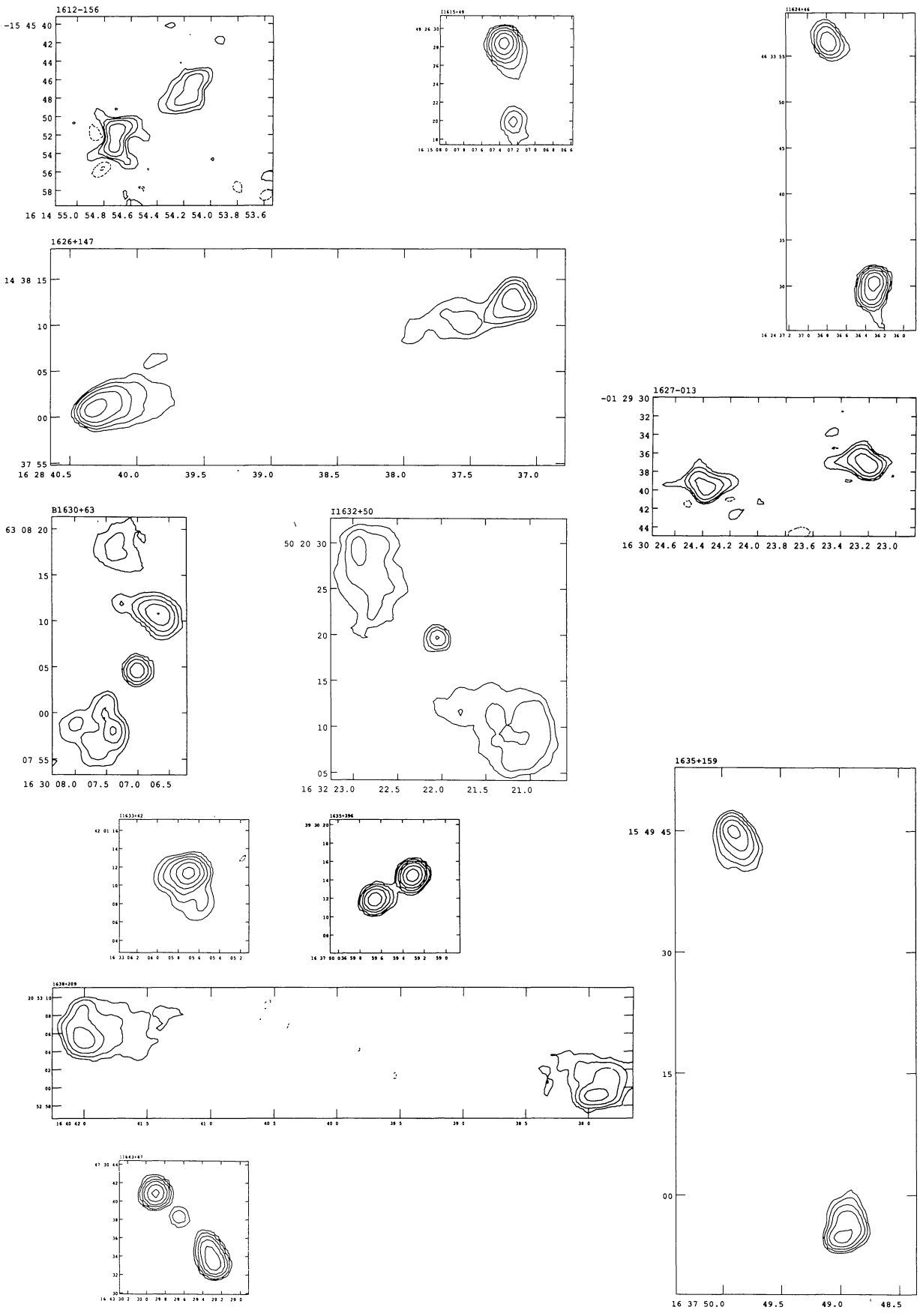

© European Southern Observatory • Provided by the NASA Astrophysics Data System

1994A&AS..108...79R

Appendix B. continued

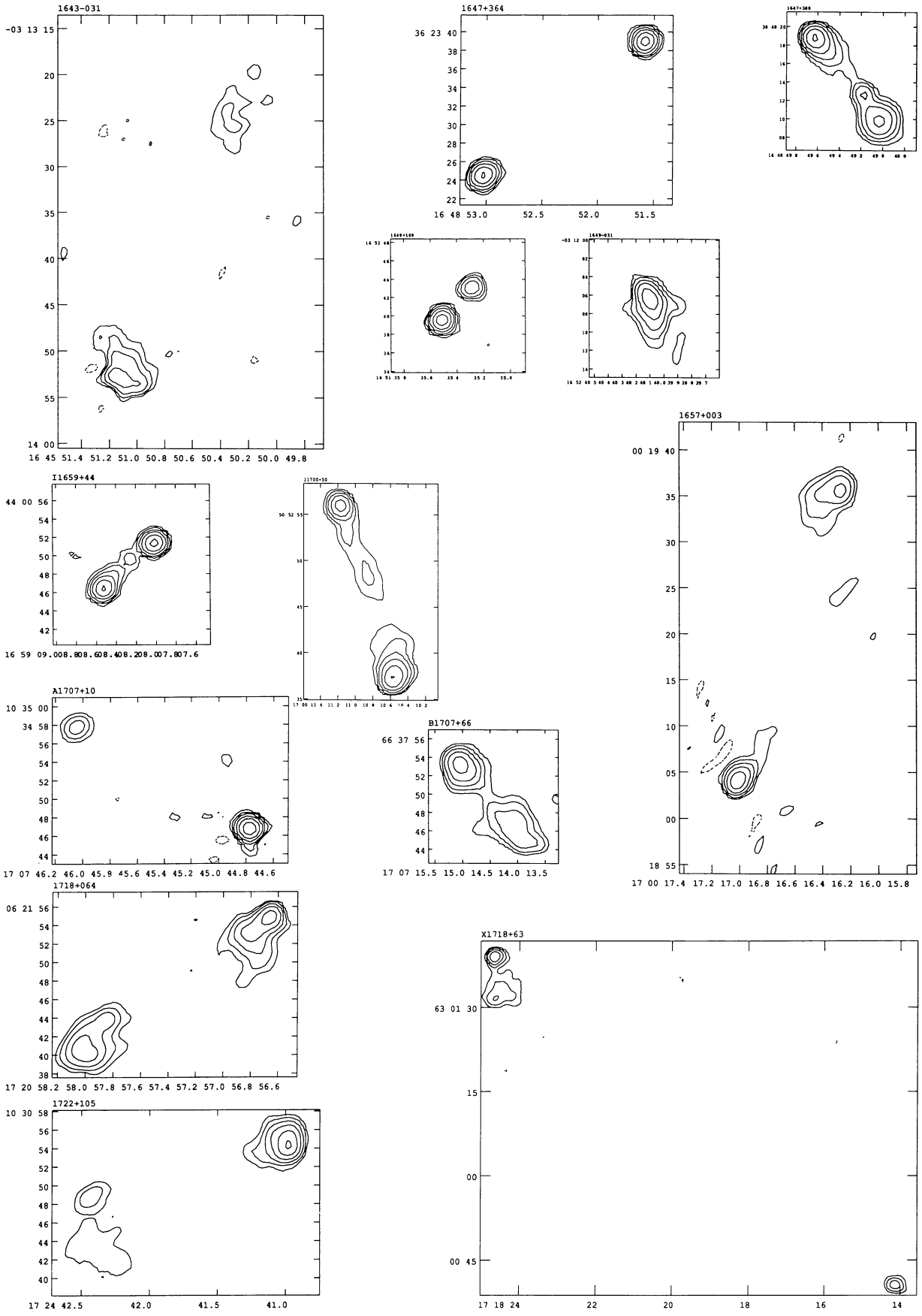

© European Southern Observatory • Provided by the NASA Astrophysics Data System

1994A&AS..108...79R

Appendix B. continued

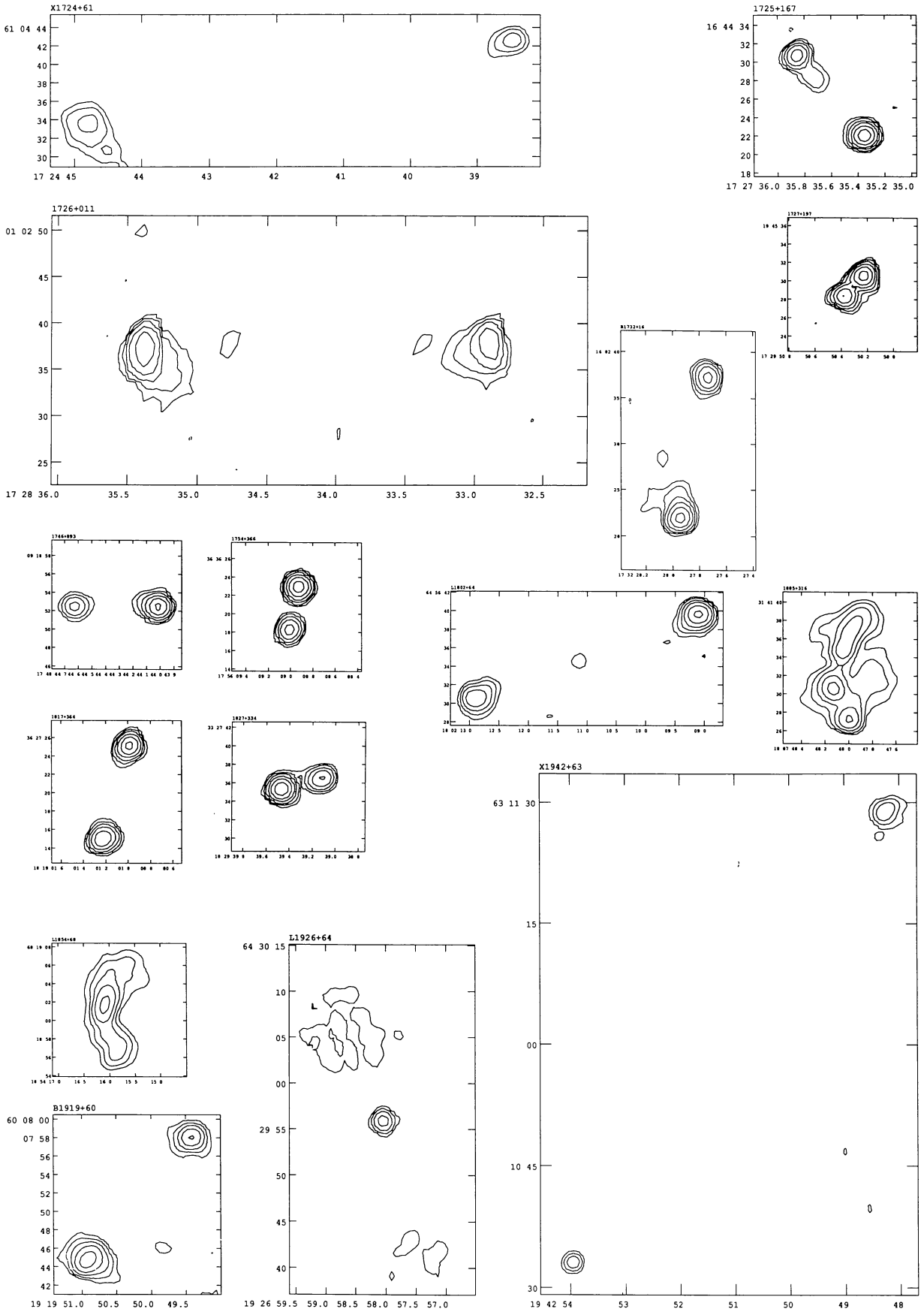

© European Southern Observatory • Provided by the NASA Astrophysics Data System

1994A&AS..108...79R

Appendix B. continued

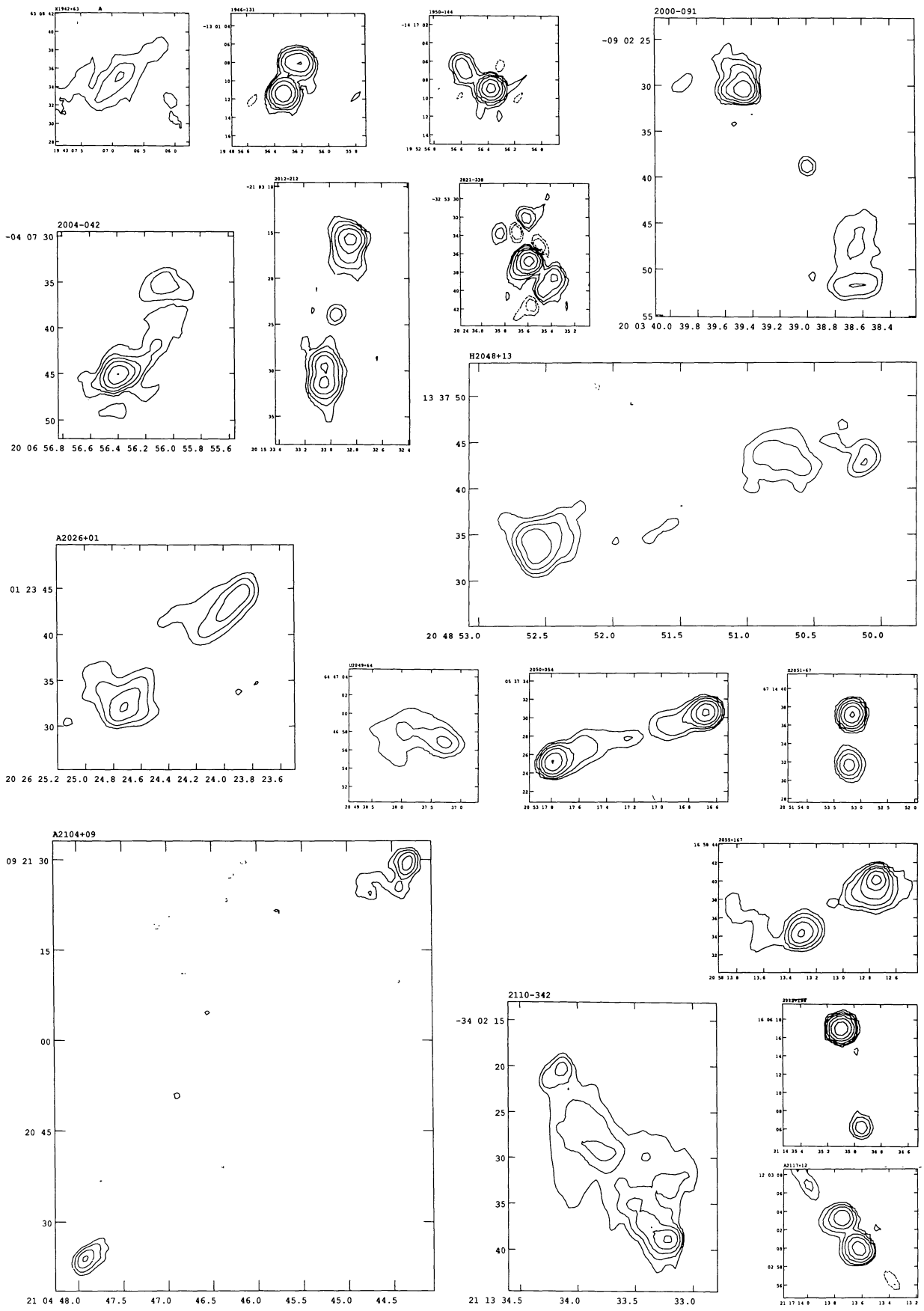

© European Southern Observatory • Provided by the NASA Astrophysics Data System

1994A&AS..108...79R

Appendix B. continued

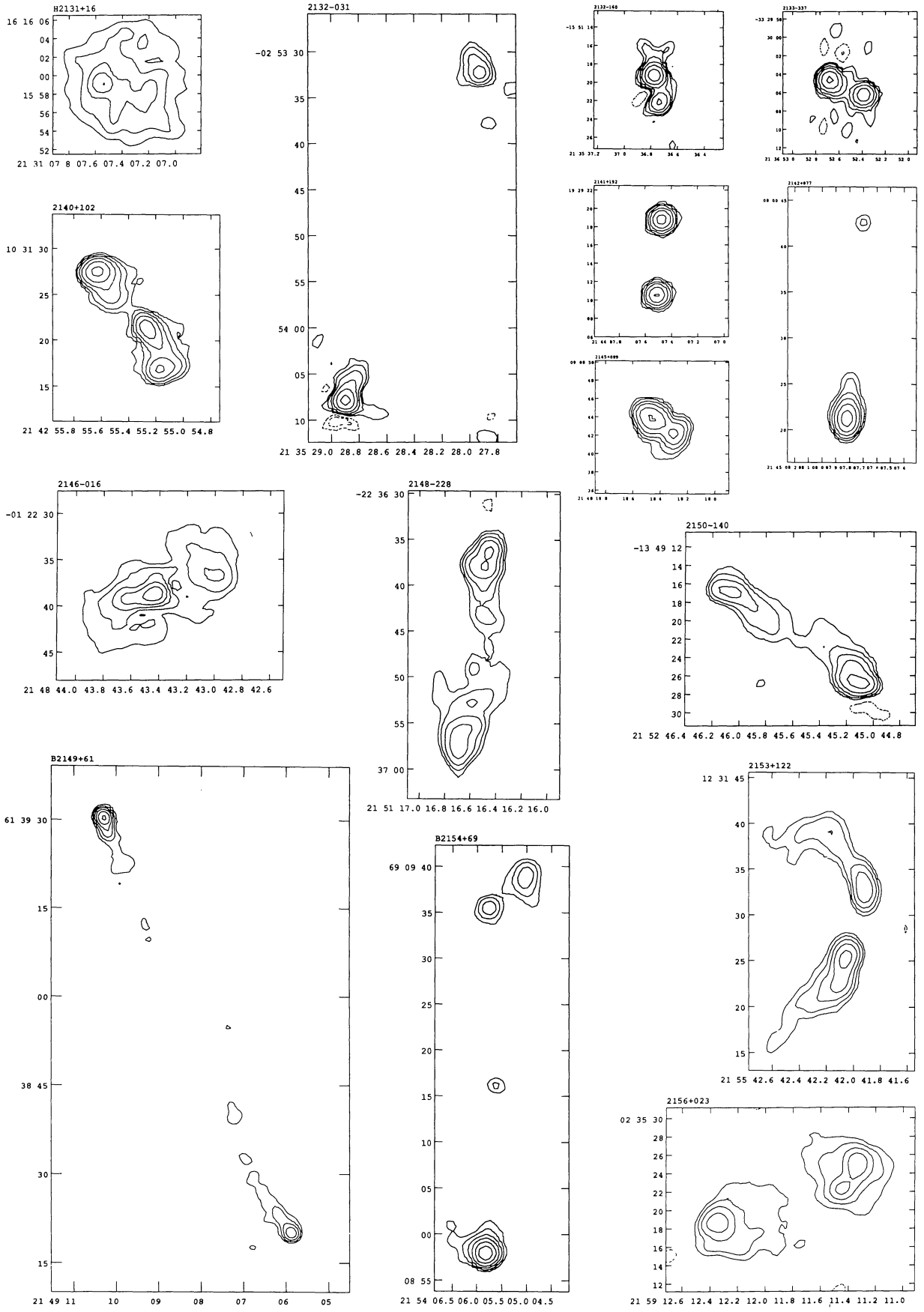

© European Southern Observatory • Provided by the NASA Astrophysics Data System

1994A&AS..108...79R

Appendix B. continued

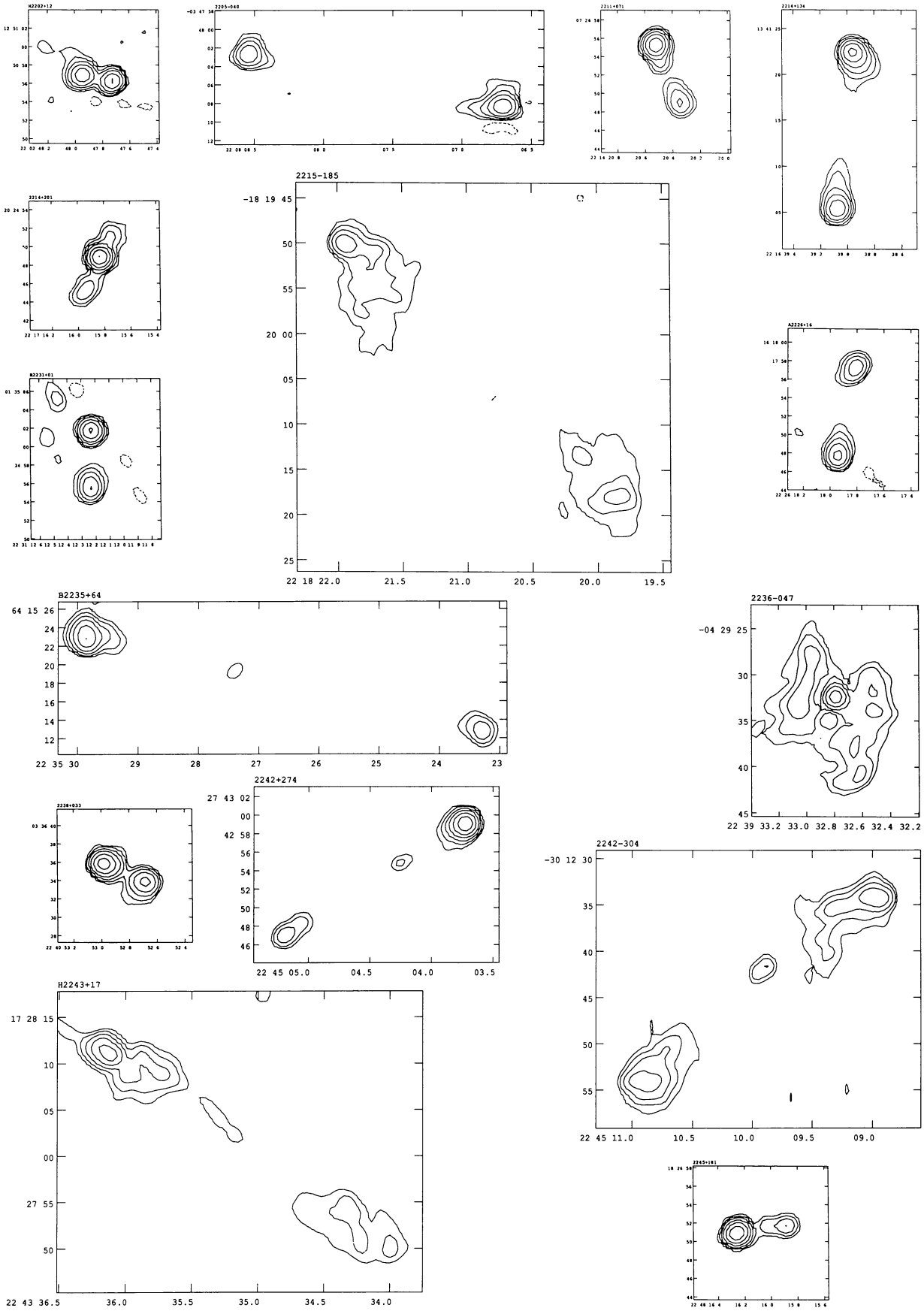

© European Southern Observatory • Provided by the NASA Astrophysics Data System

1994A&AS..108...79R

Appendix B. continued

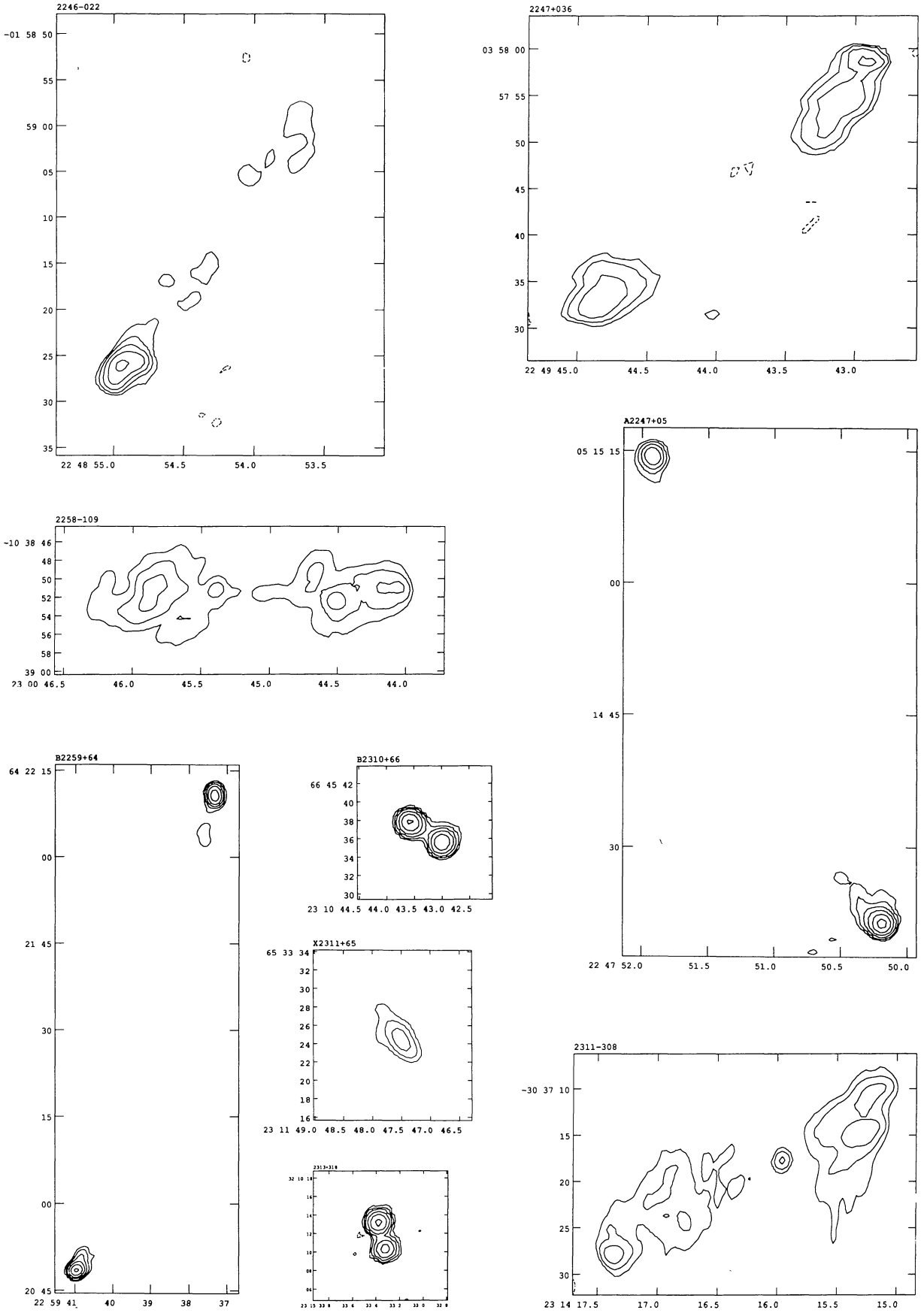

© European Southern Observatory • Provided by the NASA Astrophysics Data System

1994A&AS..108...79R

Appendix B. continued

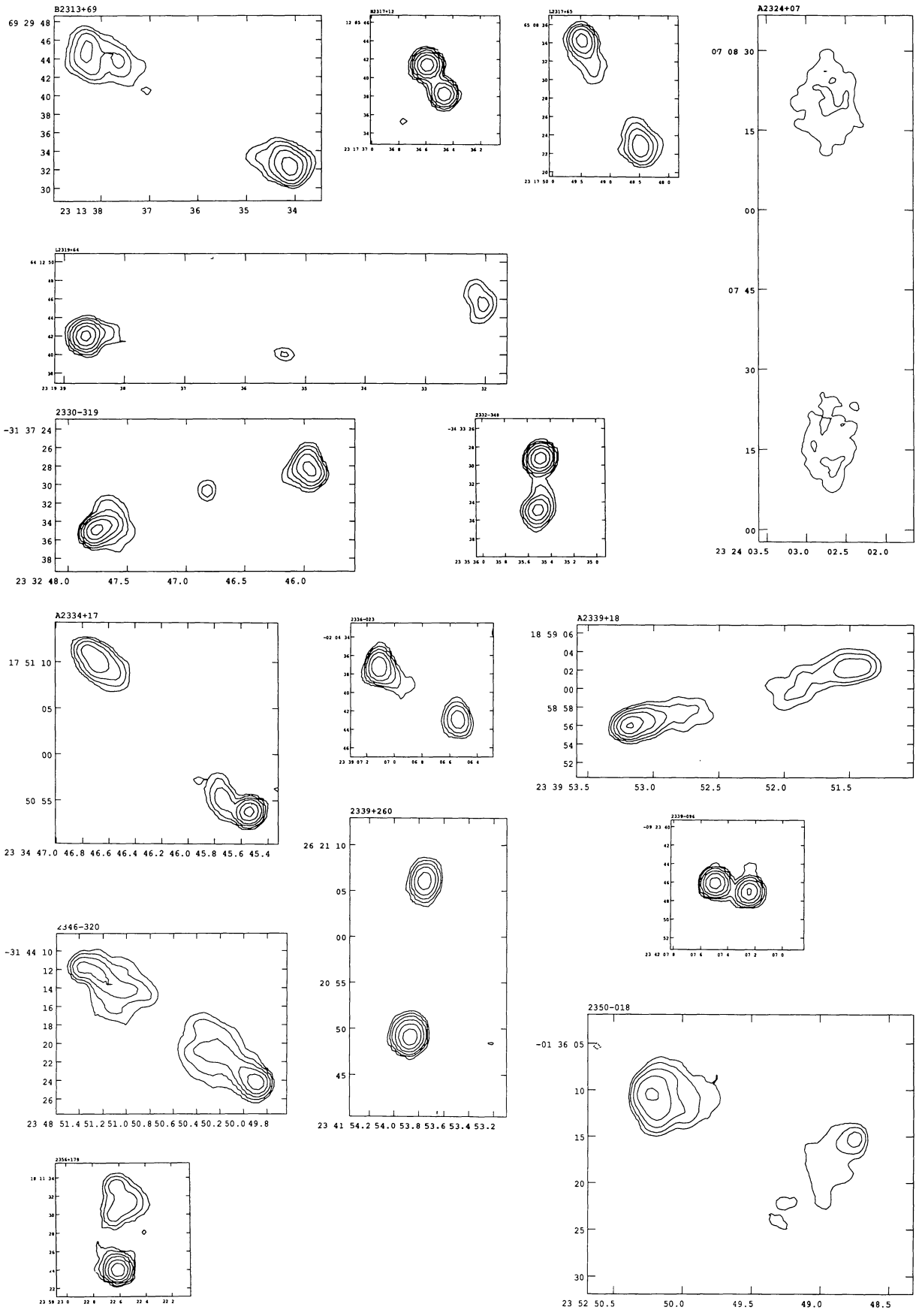

© European Southern Observatory • Provided by the NASA Astrophysics Data System

1994A&AS..108...79R

© European Southern Observatory • Provided by the NASA Astrophysics Data System